Università di Napoli Federico II

Faculty of Agriculture

Doctoral School in
"Improvement and Management of Agro-forestry Resources"

NMR evaluation of the interactions between humic substances and three molecules of agrochemical interest: β-D-glucosidase and alkaline phosphatase enzymes and glyphosate

Tutor
Prof. Alessandro Piccolo

Candidate
Dr. Pierluigi Mazzei

Coordinator
Prof. Guido D'Urso

2008-2011

Acknowledgements

My deepest gratitude goes to Prof. Alessandro Piccolo, who dedicated to a lot of time in discussing topics, experimental procedures and results presented in this thesis. I am also very thankful because of his confidence in my capacity to get acquainted and ever improving my NMR skills.

I am very grateful to my family, that continuously gave me support, tolerated my busy working schedules and encouraged me with optimism.

A kind acknowledgment is also given to the entire Piccolo's Research Group, and especially to the "ever-young" Dr. Riccardo Spaccini who always showed concern on my progress.

I gratefully acknowledge the doctoral fellowship granted by the Istituto di Metodologie Chimiche, CNR.

I am also very grateful to Prof. Hartmut Oschkinat and Dr. Peter Schmieder for their scientific support and kind hospitality when conducting experiments at NMR Facility of the FMP Institute in Berlin.

Last but not least, my special and loving gratitude goes to Dr. Annamaria Sandomenico who always supported and comprehended my decisions and intensions, whatever they were.

Table of contents

Summary

This doctoral thesis reports research work, by liquid-state Nuclear Magnetic Resonance (NMR) technique, on the interactions between humic substances and glyphosate, a widely employed soil herbicide, and two enzymes, β-D-Glucosidase and Alkaline Phosphatase, which are supposed to act in soil as extracellular enzymes. These molecules were examined in their NMR behavior as a function of increasing addition of humic substances. In particular, the following treatments were applied: glyphosate with both a humic and a fulvic acid at pH 5.2 and 7, alkaline phosphatase with two different humic acids (pH 10.4), β-D-Glucosidase with a fulvic acid at pH 5 and 7.2. The three studied molecules interacted with humic substances by forming complexes stabilized by weak forces. These results were first supported by observing signals broadening and/or chemical shift drift in ^{1}H- and ^{31}P-NMR spectra for the molecules in interactions with increasing humic concentrations. The formation of host-guest weakly bound complexes was confirmed by the values of molecular spin relaxation times, their corresponding correlation times, and self-diffusion values. In the case of glyphosate, whose fraction bound to humic matter was also calculated by means of NMR diffusion experiments, the conclusion of the weakly stabilized complex was supported by the application of the saturation transfer difference (STD) NMR experiment. The effect of the interaction between humic matter and enzymes on the catalytic activity of the enzymes was also studied. A progressive inhibition of enzymatic activity was calculated by following the changes of specific substrate in ^{1}H-NMR spectra, with increasing concentration of humic substances in enzyme solutions. A final aim of this thesis was to verify whether the inhibition of enzymatic activity by humic matter observed in the liquid phase occurred also in an heterogeneous phase similar to soil conditions, such as a laboratory synthesized humic-aluminum-montmorillonite aggregate. The preliminary experiments shown here indicate that β-D-Glucosidase simply adsorbed on solid clay-humic particles revealed a significantly lower catalytic activity than that evaluated by NMR in a liquid-state complex with soluble humic matter.

1.

Introduction

1.1 Concept of soils

Soil may be described as an integral part of the earth's ecosystem, situated at the interface between the earth's surface and bedrock (Bridges and Mukhopadhray, 2003). Unlike plants and animals, soil does not have a genetic basis controlling its development, but it is formed through an interaction of factors, such as climate, organisms, relief, parent material and time, thus representing one of the most complex natural systems.

1.2 Soil properties

The physical and chemical state of a soil governs its principal properties. Its composition consists in a *solid phase*, with both mineral and organic compounds, a *liquid phase*, that is the circulating soil solution, and a *gas phase*, constituted mainly by the same atmospheric components but at different concentration. The inorganic fraction of soils is derived from the weathering products of rock parent material, varying in size and composition. Their size distribution forms the texture of soil and it is defined according to the size into three major groups: sand (2 - 0.05 mm), silt (0.05 – 0.002 mm) and clay (< 0.002 mm) (Tan, 1998). The aggregation of mineral particles, promoted by the soil organic matter (SOM), forms particles in which sand, silt an clay fractions are bound together (Tisdall, 2003).

1.3 SOM and humic substances

The soil organic components defined as Soil Organic Matter, is due to the evolution into a higher entropic state of organic compounds resulting from the microbial decomposition of animal and vegetable tissues (Hayes & Swift, 1978).

Humic matter is the most abundant and stable component of SOM and it is believed to be the key factor in several natural processes, like the stabilization, accumulation, and dynamics of organic carbon in soil (Andreux, 1996; Tan *et al*., 2011; Fomba *et al*., 2011). From 70 to 90% of SOM is represented by this stable humus, while the remaining part is constituted by ready decomposable biomolecules and soil microbial biomass (Oades, 1984). Humic substances exhibit a wide chemical heterogeneity that is dependent on climatic, morphological and microbiological features under which the soil develops (Stevenson, 2004; Piccolo *et al*., 2003, Zhang *et al*., 2011). Humic substances intimately interacts with mineral soil components and exert an effect on the general physical, chemical and biological properties of soils, through which they also controlling the fate of of natural and anthropogenic compounds reaching the soil (Piccolo *et al*., 2003).

Humic substances cannot be defined univocally on the basis of their heterogeneous and variable chemical composition or functional groups content. They have been traditionally classified on the operational bases of aqueous solubility at different pH into three major fractions : 1) fulvic acids, soluble under all pH conditions, 2) humic acids, soluble only under alkaline conditions, and 3) humin, insoluble in any pH condition.

1.4 Conformation of Humic Substances

Humic substances have been described traditionally as macromolecular polymers, coiled-down in globular conformations at high concentrations, low pH and high ionic strength, and stretched linear conformations at neutral pH, low ionic strength and low concentration (Ghosh and Schnitzer, 1980; Piccolo, 2002).

However, the macromolecular theory has never been unequivocally demonstrated (Piccolo, 2001; 2002). In fact, the macropolymeric understanding has been gradually abandoned to the sounder and scientifically proved supramolecular structure (Piccolo *et al*., 1996; Piccolo, 2001; Cozzolino *et al*., 2001; Piccolo, 2002; Piccolo *et al*., 2003). According to this, humic molecules, instead of being covalently interlinked into large polymers, are formed to relatively small (< 1000 Da) heterogeneous molecules randomly associated by weak dispersive forces, such as van der Waals, π-π and CH-π interactions, or by intermolecular complexes with polyvalent metals (Wrobel *et al*., 2003), in only apparently large molecular dimensions (Piccolo, 2001), which can be easily disrupted by interaction with natural organic acids (Piccolo, 2001; Piccolo, 2002). The change in the paradigm introduced by this innovative explanation of the chemical nature of humic substances has been supported by an ever increasing number of experimental evidence (Piccolo *et al*., 1996; Conte and Piccolo, 1999; Piccolo *et al*., 1999; Piccolo, 2001; Piccolo *et al*., 2001; Cozzolino *et al*., 2001; Stenson *et al*., 2002; Piccolo & Spiteller, 2003; Stenson *et al*., 2003; Simpson, 2002; Smejkalova & Piccolo, 2008; Piccolo *et al*., 2010; Nebbioso and Piccolo, 2011).

1.5 Host-guest interactions in humic material

Soil humic substances are capable to form complexes or adducts with either natural or anthropogenic molecules distributed in the environment. The supramolecular structure of humic substances is sufficiently flexible and heterogeneous to establish stable associations with other molecules by forming host-guest complexes (Houk *et al*., 2003; Ganin and Vang, 2003; Smeulders *et al*, 2001; Smejkalova and Piccolo 2008 b; Smejkalova *et al*., 2009;). In fact, due to the wide chemical heterogeneity of humic suprastructures, a number of different type of interacting domains are exposed to weak dispersive interactions with guests (Piccolo, 2001; Nebbioso and Piccolo, 2011). In particular, guest ligands may interact with humic matter through their hydrophilic domains forming ionic or hydrogen bonds, and their hydrophobic domains, establishing weak dispersive forces such as van der Waals, π-π, and CH-π interactions. Moreover, humic matter may

be arranged to exhibit hydrophobic cavities to guests where they can be entrapped in stable complexes (Zhang *et al*, 2011).

Nuclear Magnetic Resonance (NMR) spectroscopy represents the most suitable technique to identify the occurrence of these type of interactions. The complexation of humic matter to guest molecules can be revealed by monodimensional ^{1}H experiments. The reduction of Brownian motions of the guest compound, following the increase in molecular size of the humic adduct, implies signal broadening effects because of a less efficient minimization of molecular dipolar couplings. In addition, the change of overall magnetic field experienced by the observed nuclei is univocally shown by a drift of chemical shifts. For instance, hydrophobic interactions may exert an up-shift effect due to the increase of electron density surrounding the observed nucleus, while electron-attractive nuclei involved in hydrogen bonds, can exert a de-shielding effect and a consequent downshift drift.

Moreover, a Saturation Transfer Difference (STD) experiment may be employed to identify the occurrence of weak interactions. Originally introduced by Mayer and Meyer (Mayer and Meyer, 1999) to evaluate the extent of non-covalent protein-ligand interactions by "through-space" polarization transfer, this technique had been previously employed to prove the interactions occurring between humic substances and xenobiotics (Shirzadi *et al.*, 2008; Longstaffe and Simpson, 2011).

Non-covalent association between a small sorbate molecule and the humic sorbent leads to a reduction of the sorbate's translational and rotational motion that is shown by changes in spin-lattice (T_1) and spin-spin (T_2) relaxation times as well as in correlation times (Bortiatynski *et al.*, 1997; Nanny, 1999; Nanny *et al.*, 1997; Dixon *et al.*, 1999).

Finally, experiments by DOSY (Diffusion Ordered SpectroscopY) NMR spectroscopy are used to detect molecular aggregation and provide information on changes of diffusivity when small molecules become involved in non-covalent complexes with humic matter (Smejkalova and Piccolo 2008 b; Smejkalova *et al.*, 2009). Since, according to the Einstein-Stokes description, the diffusivity

of a molecule decreases when the hydrodynamic radius increases (Chapman and Cowling, 1990), by measuring the diffusion coefficient of a molecular system it is possible to obtain quantitative thermodynamic information on intermolecular interactions (Wimmer *et al.*, 2002). In this way, binding constants as well as thermodynamic parameters for host-guest complexes between natural organic matter and different compounds are measurable.

1.6 The herbicide Glyphosate

N-phosphonomethylglycine is the active ingredient of the widely used broad-spectrum and relatively non-selective herbicide, commonly referred to as glyphosate. It is used in the form of an aqueous solution of isopropyl-amine salt under trade names such as Roundup®, Rodeo®, Glyfonox® and Glycel® (Carigny *et al.*, 2004). Introduced by the US Chemical Company Monsanto in the early 1970s, glyphosate represents today up to 60% of the global 'broad-spectrum' herbicide sales, covering a global use of over 70,000 $t.year^{-1}$ of technical acid (Hu *et al.*, 2011). Furthermore, the introduction in 1997 of Roundup Ready® crops, such as cotton, maize, and soybeans, which are made resistant by incorporation of a naturally occurring glyphosate-resistant protein, added popularity to the synthetic herbicide (Borggaard and Gimsing, 2008). Glyphosate high efficiency is due to its potent and specific inhibition of the enzyme 5-enolpyruvylshikimate 3-phosphate (EPSP) synthase (Schonbrunn *et al.*, 2001). In fact, as represented in the following scheme, Glyphosate is capable to compete with phosphoenolpyruvate (PEP), during the shikimate pathway, since it exhibits a large similarity with PEP oxonium ion, thus inhibiting the synthesis of EPSP. This enzyme is a crucial intermediate of the shikimate pathway, that governs the synthesis of aromatic amino acids, as well as almost all other aromatic compounds in higher plants, algae, bacteria and fungi (Bentley and Haslam, 1990; Hayes *et al.*, 1991). Its continuous and worldwide use in agriculture is attributed to its non-toxicity for mammals, since the shikimate pathway is absent in

mammals, which are thus unaffected by glyphosate (Steinrücken and Amrhein, 1980; Busse *et al.*, 2001).

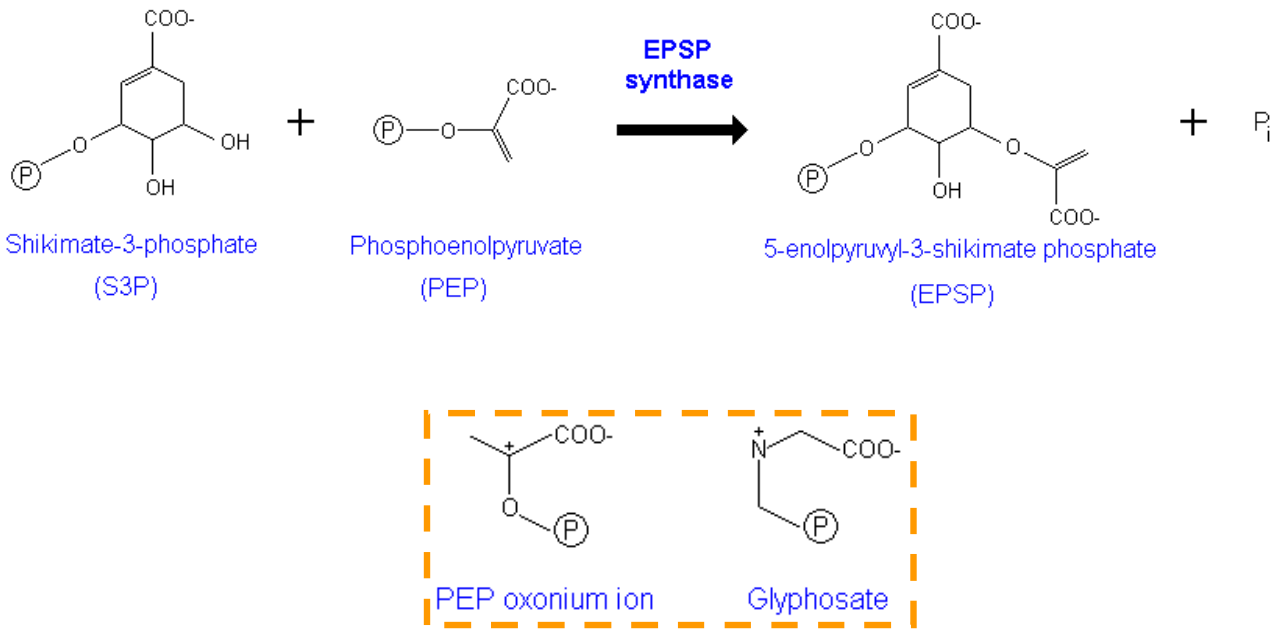

Figure 1.1 Shikimate pathway: EPSP synthase. In the dotted box are compared the glyphosate and the PEP oxonium ion.

Although this herbicide is claimed to decrease the contamination by agro-chemicals in the environment because it implies a reduction in the amount of herbicides applied on non-tolerant crops, and its less persistency and toxicity than other herbicides (Mamy *et al.* 2005), its presence and adsorption in soil may still represents a major threat for a wider environmental pollution (Borggaard and Gimsing, 2008; Vereecken, 2005). Glyphosate microbial persistence is due to the carbon-to-phosphorous bond that is highly resistant to biodegradation (Lipok *et al.* 2011), while its transport in the environment is attributed to its strong interactions with fine organo-mineral soil particles (Piccolo *et al.*, 1994; Albers *et al.*, 2009) and soluble humic fractions (Piccolo *et al.*, 1994; Albers *et al.*, 2009; Piccolo and Celano, 1994, 1996).

1.7 Soil enzymes

Enzymes are high molecular weight (from 10 to 2000 kDa) proteins consisting in chains of amino acids linked together by peptidic bonds. Enzymes catalyze specific chemical reactions in a biological systems, whose rates are greatly enhanced by enzymatic catalysis to sustain life. Since enzymes are selective for their substrates and speed up only a few reactions from among many possibilities, the set of enzymes made in a cell determines which metabolic pathways occur in that system (cell, tissue) (Ritter, 1998). The high specificity that enzymes exhibit for the reactions they catalyze is the main property that makes them so important in metabolic processes. In general, there are four distinct types of specificity: *absolute specificity*, when the enzyme will catalyze only one reaction; *group specificity*, when the enzyme will act only on molecules that have specific functional groups, such as amino, phosphate and methyl groups; (3) *linkage specificity* when the enzyme will act on a particular type of chemical bond regardless of the rest of the molecular structure; (4) *stereochemical specificity* when the enzyme will act on a particular steric or optical isomer (Nelson and Cox, 2004).

A further crucial aspect is the enzymatic inhibition (reversible or irreversible) that interests the decrease of the enzyme reaction rate. It is exerted in different ways: the *competitive* inhibition occurs if an inhibitor competes with the specific substrate; the *uncompetitive* inhibition occurs when the inhibitor interacts with the enzyme-substrate intermediate; the *non-competitive* inhibition is displayed if the inhibitor occurs binds to a non active site in the enzyme. The latter is a special mixed inhibition where the inhibitor has an equal affinity for both the free enzyme and the enzyme-substrate complex (Ritter, 1998).

Plant exudates and bacteria and fungi microorganisms are responsible for the introduction and diffusion of enzymes in soil. Part of enzymes are released as extracellular exo-enzymes, while most of them are released through cytoplasmic exudates or cell debris from either dead or living cells (Burns, 1982). Soil enzymes are believed to be directly involved in the processes of soil organic

matter transformation and mineralization of plant nutrients (Dick *et al.*, 2000). Extracellular enzymes couple the activity of soil microbes in the degradation of complex substrates into low molecular weight compounds which can be even assimilated by plants (Schimel and Bennett, 2004).

1.7.1 Alkaline phosphatase

Alkaline Phosphatase (EC 3.1.3.1), or *Orthophosphoric-monoester phosphohydrolase* (AP), is a common and widespread enzyme in calcareous soils. This enzyme is known to catalyze the hydrolysis of esters and anhydrides of phosphoric acid (Kim and Harold, 1991; Holtz and Kantrowitz, 1999) at the hydrolysis rate of 1.0 µmole of *p*-nitrophenyl phosphate per minute at pH 10.4 and 37°C for one unit of AP.

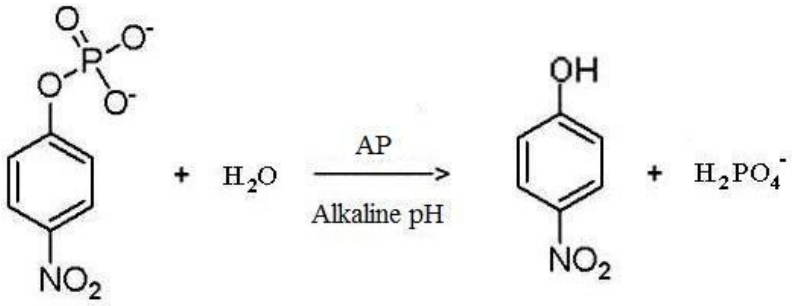

Figure 1.2. Hydrolysis of *p*-Nitrophenylphosphate catalyzed by AP.

Soil extracellular alkaline phosphatases plays an important role in the mineralisation of organo-phosphorus compounds and, thus, in the supply of soluble phosphate for plant growth (Perez-Mateos *et al.*, 1991). AP is mainly introduced in soils by bacteria, fungi and fauna, and, contrary to acid phosphatase, it is not produced by plant roots (Olander and Vitousek, 2000; George *et al.*, 2006). Nevertheless, in most of plants, roots are not able to directly uptake phosphorous bound to organic molecules, although this should be the most available P form in soils. Therefore,

phosphatase enzyme contributes to plant P uptake by converting the organic P forms into inorganic forms which are finally available to plants (Tarafdar and Claassen, 1988; Richardson *et al*., 2005).

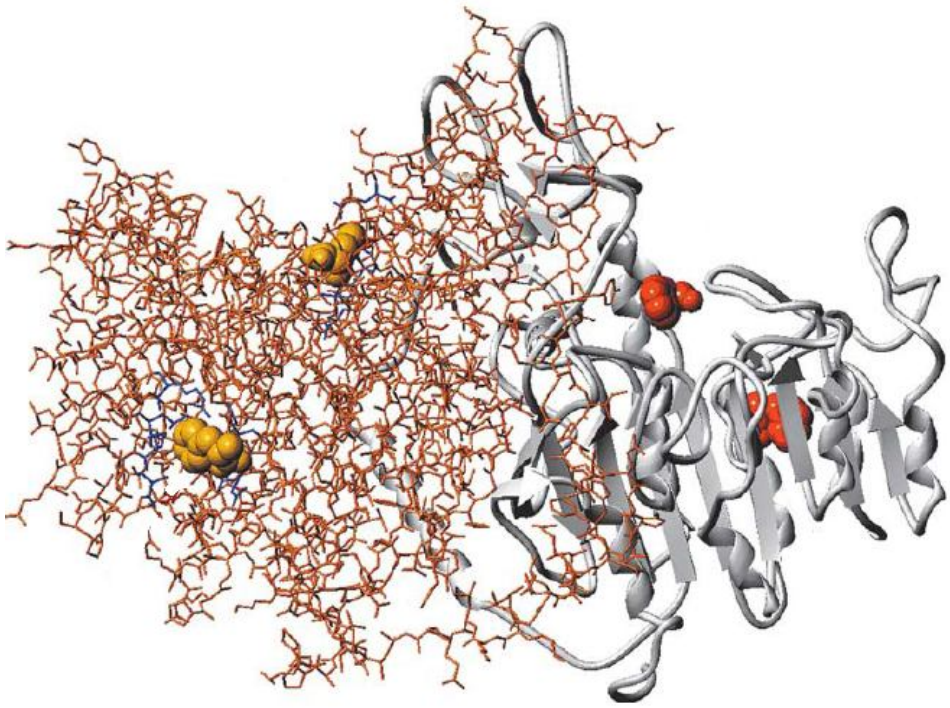

Figure 1.3. Overview of the AP dimer from human placenta (Llinas *et al*., 2005).

1.7.2 β-Glucosidase

β-Glucosidase (EC 3.2.1.21) is abundant in soil and it is important since it takes part in the carbon cycle and is closely related to transformation, composition, and cycling of soil organic matter (Xiao-Chang & Qin, 2006; Busto and Perez-Mateos, 2000). This class of enzymes belongs to the glycoside hydrolase family and operates on substrates hydrolysis by cleaving β,1-4 glycosidic linkages (Bock, 1988). In particular, two β-Glucosidase carboxylic acids are involved in the catalytic active site.

One carboxylate residue functions as a catalytic nucleophile by attacking the anomeric centre of substrate and forming a covalent α-D-glucosyl enzyme intermediate, while the other carboxyl

group acts as an acid/base catalyst by first protonating the glycosidic oxygen and then deprotonating the nucleophilic water molecule (Lawson *et al*. 1998; Rye & Withers, 2000).

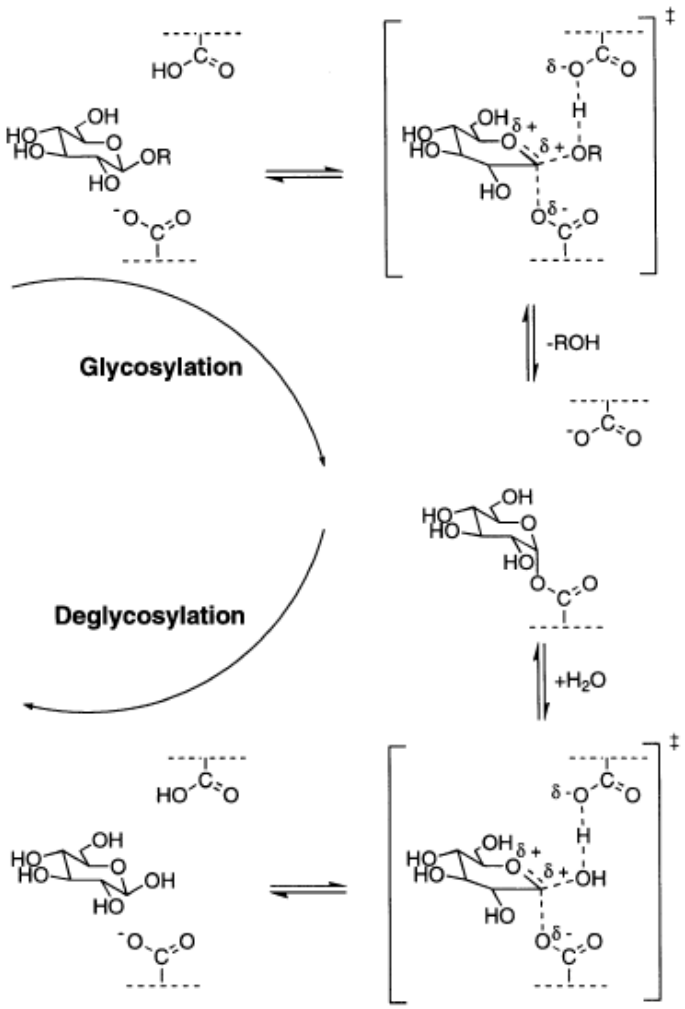

Figure 1.4. Double displacement mechanism for a glucosidase, where R can be either a glucose residue or an alkyl or aryl group (Lawson *et al*. 1998).

Therefore, β-Glucosidase contributes to hydrolyse the β–1-4 glycosylated molecules which are commonly deposited in soils, such as the flavonoid glucosides (Schmidt *et al*., 2011) or the cellulosic materials (Saratchandra & Perrott, 1984). In particular, cellulose degradation in soil is a synergistic process involving other soil enzymes. It is launched by endo-β-1,4-glucanase (EC 3.1.2.4), that breaks cellulose chains into smaller units, and cellobiohydrolase (EC 3.1.2.91), which cleaves the cellobiose dimer (two β-1,4 linked glucose units) starting from the reducing 'ends' of

molecules. Finally, β-Glucosidase completes the hydrolysis process by catalysing the cleavage of cellobiose and releasing two moles of glucose per mole of cellobiose (Turner *et al*., 2002). In plants, β–Glucosidases are involved in crucial processes of growth, such as the degradation of endosperm cell walls during germination or the formation of intermediates in cell wall lignification, as well as in activation of defence compounds, and formation of phytohormones (Schmidt *et al*., 2011).

1.8 Soil enzymes and humic substances

Enzymes in soil interact with other organic and inorganic components and may give rise to stable active associations (Burns, 1986). In the last decades, many works showed that a variety of soil abiotic factors, such as mineral and organic compounds (mainly humus), can regulate both the enzyme stability and the interaction between enzyme and substrates (Sinsabaugh and Moorhead, 1994). In particular, it was verified that a partial inhibition of soil enzymes may arise from the occlusion of active sites and sorption of substrate molecules (Sarkar *et al*., 1989; Quiquampoix *et al*., 2002; Tietjen and Wetzel 2003).

The occurrence of interactions between soil enzymes and other chemical soil components such as clay minerals and humic substances, was repeatedly shown (Burns, 1982; Stevenson, 1982; Busto & Perez-Mateos, 2000; Nannipieri *et al*., 2002). In addition, it has been proved that extracellular enzymes bound to clay or humic matter, are resistant to proteolytic degradation and/or to physical-chemical stresses (Nannipieri *et al*., 1996). Recently, NMR spectroscopy was used to show that enzymes, among other proteins, are encapsulated by humic aggregates, thus suggesting a change in their catalytic activity in soil (Tomaszewski et. al., 2011).

The interactions with soil components of the alkaline phosphatase enzyme and the effect on the catalytic activity were previously studied. Perez-Mateos (1991) verified that, by immobilizing AP on a sterile soil, humic components tended to occupy part of the enzyme active sites, thus preventing the access of the substrate and increasing the activity K_m value. Later, Pilar *et al*. (2003)

showed that AP absorption on soil humates ranged from 58 to 92%, without significantly influencing the catalytic activity of the humate-phosphatase complex.

Recent works were also focused on the formation of complexes between Glucosidase and humic matter. The formation of humic-Glucosidase complexes during composting was shown and it was found that the association took place almost totally during the first stage of composting (Mondini *et al.*, 2004). Later, the isoelectric focusing technique was applied to confirm the occurrence of the humic-Glucosidase adduct and to differentiate soil quality according to different management systems as a function of the humic-glucosidase complexes (Ceccanti *et al*, 2008).

Moreover, a large attention has been paid to assess the activity of both alkaline phosphatase and β-Glucosidase in soils since these enzymes are typically used as indicators of soil quality (Dick, 1997; Turner *et al*., 2002).

1.9 Work Objectives

A thorough understanding of the chemical processes involved in sorption and binding of agro-molecules to soil humic substances, is necessary for a reliable prediction of molecular behaviour in soil and a better comprehension of chemical dynamics related to soil components. Thus, this thesis reports the investigations, conducted by means of Nuclear Magnetic Resonance (NMR) spectroscopy, on the interactions which occur between the humic substances and molecules to be commonly found in soils such as the herbicide Glyphosate and the alkaline phosphatase and β-glucosidase enzymes. NMR spectroscopy was applied to evaluate both the qualitative and quantitative relations occurring between the selected agro-molecules and humic matter.

In the case of Glyphosate, the objectives were to prove the occurrence of interactions between glyphosate and water-soluble humic substances and to quantify the corresponding thermodynamic parameters. In the cases of the two enzymes studied here, the objectives were also to apply NMR spectroscopic techniques to prove the formation of humic-enzyme complexes, and its effect on the enzymes catalytic activity on selected substrates.

2.

Experimental Section

2.1 Humic substances.

Humic substances were isolated as it follows: 1. a humic acid from a Typic Fulvuland soil (Lake Vico, Lazio, Italy), 2. a fulvic acid from an Eutric Regosol (Caserta, Campania, Italy), and, 3. a humic acid from a North Dakota (USA) lignite provided by Mammoth Int. Chemical Company. The adopted extraction was modified from that reported by Stevenson (1994) and consisted by shaking the raw material overnight in a 0.5 M NaOH and 0.1 M $Na_4P_2O_7$ solution under N_2 atmosphere. The suspension was centrifuged at 10000 rpm and the supernatant filtered through glass wool and treated with 6N HCl to pH 1 to allow precipitation of humic acids during one night at 4°C. The precipitated humic acids were separated by centrifugation and purified from coextracted inorganic particles first by three cycles of dissolution in 0.5 M NaOH followed by flocculation in 6 M HCl, and then shaking humic acids twice in a 0.25 M HF/HCl solution for 24 h. The purified humic acids was then dialyzed against distilled water until chloride-free and freeze-dried. The, 30 mg of humic acids were suspended in H_2O, titrated to pH 7 with NaOH 0.1 M by an automatic titrator and freeze dried again. The fulvic acids, which remained in solution after precipitation of humic acids, were purified by adsorbing on a Amberlite XAD8 resin (Thurman and Malcolm, 1981) to eliminate reputed interfering materials such as soluble hydrophilic carbohydrates and proteins, eluting the adsorbate by a 1M NaOH solution. After adjusting the pH of the eluates to 5, the fulvic acids were dialyzed in Spectrapore 3 tubes against distilled water until chloride-free, and freeze-dried. Both humic and fulvic acids were then redissolved in 0.5 M NaOH and passed through a

strong cation-exchange resin (Dowex 50) to further eliminate divalent and trivalent metals, and freeze-dried again. When necessary, the humic substances were characterized for their elemental content by using a Fisons EA 1108 Elemental Analyzer.

2.2 Complexes of Al-humate-montmorillonite (HM)

The thin fraction of montmorillonite (<2 mm, Crook County, WY, USA) was separated by sedimentation after dispersion in water and sodium exchanged by washing three times with 1 M NaCl solution. Excess NaCl was removed by washing in distilled water followed by dialysis until Chloride-free. Then, 0.5 M NaOH was added to mixture of Na-montmorillonite + $AlCl_3$ (6 mmol Al per g of clay) up to reach a suspension pH of 5. After one hour, the organo-mineral complex (HM) was obtained by adding the titrated HA (20 mg per g^{-1} clay) and bringing the pH of suspension to 7 with 0.5 M NaOH. Finally, a vigorous stirring, during complex formation, facilitated penetration of the OH-Al-humate polymers into the interlayers of montmorillonite (Violante *et al.*, 1999). The solid residue was centrifuged (10.000 rpm), washed three times with distilled water and freeze-dried.

2.3 The herbicide Glyphosate

2.3.1 Glyphosate solutions and dissociation forms

Glyphosate (N-phosphonomethylglycine) was provided, in free acid form (99 % pure), by Dr. Ehrenstorfer GmbH (Germany). Glyphosate (GLY) is a weak acid and presents three dissociation constants in aqueous solution due to progressive proton release from carboxyl, phosphonate and ammonium groups at increasing pH (Piccolo and Celano, 1993).

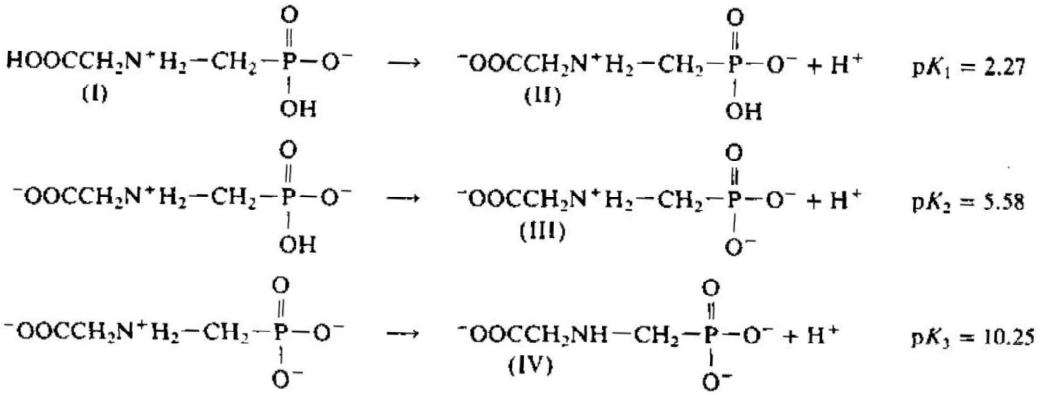

Solutions were prepared by dissolving Glyphosate (1 mg) in 1 mL of either a 0.2 M acetate or a 0.2 M phosphate buffer solutions in deuterated water (99.8% D_2O/H_2O, ARMAR CHEMICALS) at pH of 5.2 and 7, respectively. In the pH range between 5.2 and 7, the equilibrium with the pK_2 acidity constant of 5.58 dictates the concentrations of the dianion (II) and trianion (III) species of GLY. Dianion (II) is slightly more abundant than the trianion (III) at pH 5.2, whereas the latter is largely predominant at pH 7.

2.3.2 Glyphosate-humic solutions

Increasing amounts (0, 5, 10, 15, 20 and 25 mg) of either FA and HA were dissolved into the GLY solutions obtained in the two pH-buffered solutions to carefully avoid any humic precipitation. Control humic solutions were similarly prepared without GLY. All solutions were stirred for 10 minutes to guarantee complete dissolutions of analytes. For the enhanced sensitivity required by STD-NMR experiments, samples were prepared, by dissolving 8.45 mg ($5x10^{-2}$ mmol) of GLY in deuterated buffer solutions at pH 5.2 and 7, also containing 5 mg of either HA and FA.

2.4 Alkaline phosphatase

2.4.1 Enzyme

The alkaline phosphatase enzyme was purchased from Sigma-Aldrich, Italy, as an isolate from Human Placenta (EC 3.1.3.1) Type XXIV (17 units mg^{-1}). The substrate for enzyme activity was 4-nitrophenyl phosphate disodium salt hexahydrate (*p*-NPP) and was also purchased (99.0% pure) from Sigma-Aldrich, Italy. One unit of AP is reported to hydrolyze 1.0 μmole of *p*-nitrophenyl phosphate per minute at pH 10.4 and 37°C. The enzyme exhibits a ribbon-shaped homo-dimeric structure and each monomer consists in 478 residues, 1 catalytic active site and 3 metal ions (2 Zinc and 1 Magnesium atoms) (Le Du *et al.*, 2001).

2.4.2 Solutions of alkaline phosphatase and humic matter

Different amounts of both HA-V and HA-L (0, 0.5, 1, 2, 6 mg mL^{-1}) were dissolved in a 0.2 M carbonate buffer solution prepared with deuterated water (99.8% D_2O/H_2O, ARMAR CHEMICALS) and kept at pH 10.4. The humic solution was sonicated for 10 minutes to completely dissolve humic associations, but maintaining solution temperature below 30 °C. Then, 3.5 mg of the alkaline phosphatase enzyme were added to 700 μL of each humic solution for a final enzyme concentration of 5 mg ml^{-1}, stirred for 10 minutes and left to stabilize for 30 minutes. Each solution was degassed for 2 minutes by a gentle N_2 flux prior to NMR analysis.

2.5 β-D-Glucosidase

2.5.1 Enzyme

A β-D-Glucosidase (GLU) (Grover *et al.*, 1977; Grover and Cushley, 1977) was purchased from Sigma-Aldrich, Italy, as an extract from sweet almonds (2.31 units mg^{-1}). The substrates for enzyme activity were *p*-Nitrophenyl-β-D-glucopyranoside (*p*-NPG, > 98.0% purity) and

2-(Hydroxymethyl)phenyl-β-D-glucopyranoside (Salicin, > 99.0 % purity) and were also purchased from Sigma-Aldrich, Italy.

2.5.2 Solutions of β-D-Glucosidase and humic matter

Different amounts of FA (0, 0.1, 0.2, 0.35, 0.5, 0.6, 0.8, 1, 1.5 mg mL^{-1}) were dissolved into 0.2 M phosphate buffer solutions in deuterated water (99.8% D_2O/H_2O, ARMAR CHEMICALS), at pH of either 5 or 7.2. The FA solution was sonicated for 10 min to complete dissolution, but maintaining solution temperature below 30 °C. Then, 5 mg of GLU were dissolved into 1 mL of each humic solution, stirred for 10 min, and left to stabilize for 30 min before NMR measurements. No precipitations were observed neither during the preparation of samples or when NMR analyses were completed.

2.6 Catalysis experiments

The samples employed to follow the change in activity of alkaline phosphatase catalysis by NMR spectroscopy were prepared by dissolving 1.68 mg of AP in 700 μL (2.4 mg mL^{-1}) of buffered deuterated carbonate solution (pH 10.4) containing different amounts of humic acids (0, 6, 8 and 12 mg mL^{-1}). The enzymatic catalysis was started by adding 3.5 mg of 4-NitroPhenyl Phosphate disodium salt hexahydrate (*p*-NPP) to each sample. This was weakly stirred for 30 seconds, and transferred into a 5mm NMR tube. For the NMR studies of activity of β-D-Glucosidase catalysis, samples were prepared by dissolving 0.6 mg of glucosidase enzyme in 1 mL of buffered phosphate deuterated solution at pH 5 and containing different amounts of FA (0, 0.03, 0.1 and 0.2 mg mL^{-1}). The catalysis was started by adding 10 mg of substrate (either *p*-NPG or Salicin) to the samples containing the FA and glucosidase solution. Thee mixture was weakly stirred for 30 seconds and transferred into 5 mm NMR tubes.

2.7 NMR Experiments

2.7.1 Monodimensional (1D) spectra

A 400 MHz Bruker Avance spectrometer, equipped with a 5 mm Bruker BBI (Broad Band Inverse) probe, working at the ^{31}P and ^{1}H frequencies of 161.81 and 400.13 MHz, respectively, was employed to conduct all liquid-state NMR measurements for Glyphosate (GLY) and β-Glucosidase (GLU) at a temperature of 298±1°K. In the case of the experiments with alkaline phosphatase, a 600 MHz Bruker DRX spectrometer, equipped with a 5 mm Bruker Inverse Quadruple resonance (QXI) probe, working at ^{1}H frequency of 600.19 MHz was employed to conduct all liquid-state NMR measurements at a temperature of 298±1°K.

^{1}H-NMR spectra (32768 time domain points) were acquired with 2 s of thermal equilibrium delay and a 90° pulse length ranging between 7.3 and 14 μs. In the case of GLY, ^{31}P-NMR spectra (32768 time domain points) were acquired by setting 7 s of initial delay and a 90° pulse length ranging between 11.1 and 11.5 μs. An 80 μs length Waltz16 decoupling scheme with around 15.6 dB as power level, under an inverse gated pulse sequence, was employed to decouple phosphorous from proton nuclei. In the case of GLU and AP, ^{1}H experiments accumulated 256 transients, while, for GLY, both ^{1}H and ^{31}P spectra were acquired with 100 scans.

2.7.2 T_1 and T_2 relaxation measurements

An inversion recovery pulse sequence with 20 increments and variable delays included within the range 0.01 to 10 s was adopted to measure both ^{1}H and ^{31}P longitudinal (spin-lattice) relaxation time constants (T_1), while the transverse (spin-spin) relaxation time constants (T_2) were measured using a Carr-Purcell-Meiboom-Gill (CPMG) pulse sequence, using 20 increments and 2 to 2000 spin-echo repetitions, with a constant spin-echo delay of 1.4 and 1.5 ms, in the case of both enzymes and GLY, respectively. A time domain of 32768 points (16384 in the case of GLY) was set for all the relaxometric experiments.

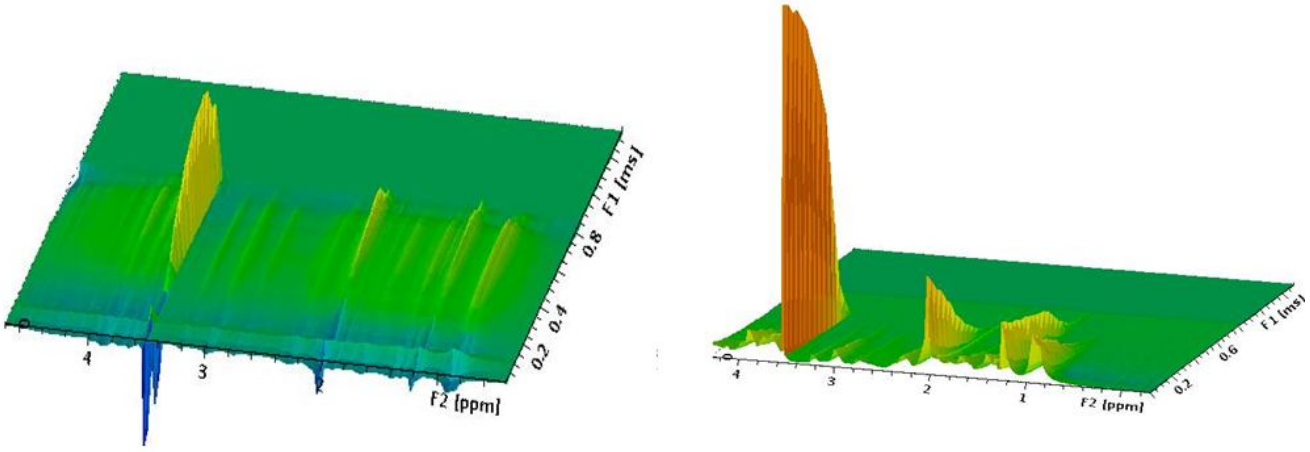

Figure 2.1. 3D visualization of 1D NMR spectra achieved by Inversion recovery (left) and CPMG (right) pulse sequences.

2.7.3 DOSY (Diffusion Ordered SpectroscopY) experiments

^{1}H and ^{31}P DOSY (Diffusion Ordered SpectroscopY) NMR spectra were obtained by choosing a stimulated echo pulse sequence with bipolar gradients, and combined with two spoil gradients and an eddy current delay. This sequence was selected to reduce signals losses due to short spin-spin relaxation times. In the case of GLY, the acquisition was executed by setting, for ^{1}H and ^{31}P nuclei, respectively, 1600 and 2300 μs long sine-shaped gradients (δ), linearly ranging from 0.674 to 32.030 G cm^{-1} in 32 increments, and selecting a delay of 0.09 and 0.25 s (Δ) between the encoding and the decoding gradients. In the case of AP only proton diffusion was measured and optimal δ and Δ were 1600 μs and 0.27 s, respectively.

2.7.4 STD (Saturation Transfer Difference) experiments

STD experiments (2048 scans) were conducted only in the case of GLY. They were executed according to previous indications (Meyers and Peters, 2003). Selective saturation of humic substances was achieved by a train of 50 ms Gauss shaped pulses, truncated at 1%, and separated by a 50 μs delay. A total length of saturation train of 5.005 s was achieved with 100 selective pulses.

The best on-resonance irradiation for humic substances was found at 0.8 ppm, whereas off-resonance irradiation was set at 30 ppm, where no proton signals were visible. Spectra were internally subtracted by phase cycling after each scan. Reference spectra were recorded using the same sequence without irradiation. During STD experiments, the frequency of large molecules (short tumbling rate) was saturated by an on-resonance selective shape pulse irradiation. The ligand interacting with the irradiated molecular aggregate received a partial saturation transfer through the NOE effect and it was NMR detected. A second similar pulse sequence was then applied by an off-resonance irradiation to avoid any saturation of humic matter. Finally, by subtracting the second spectrum from the first one, the difference spectrum showed only signals for protons involved in non-covalent interactions. These protons were affected by the applied saturation irradiation, that determined the polarization transfer among the involved molecules, thus inducing a through-space increase of NOE intensity.

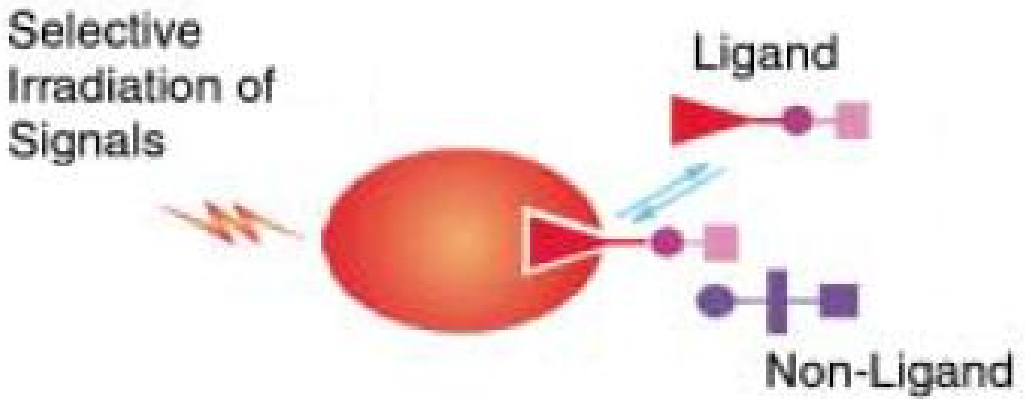

Figure 2.2. During STD experiments, only the interacting ligands can receive by a through-space NOE transfer, the molecular polarization, previously inducted by a selective irradiation (Mayers and Meyers, 1999).

2.7.5 Water suppression

Residual water signal was removed from ^{1}H-NMR spectra by a common pre-saturation technique. A watergate 3-9-19 pulsed train sequence was preferred for DOSY experiments, whereas

an excitation sculpting technique was chosen for STD experiments, using a 2 ms selective rectangular pulse, defined by 1000 points, and truncated to 1%.

2.7.6 NMR Processing

The free induction decays (FID) of both ^{1}H and ^{31}P spectra of GLY were multiplied by 1 and 4 Hz exponential factors, respectively. In the case of both enzymes, no apodization was executed in spectra. No zero filling was applied in any spectra, while baseline correction was invariably executed in all spectra. Spectra were elaborated by both Bruker Topspin (v.1.3) and MestReC (v. 4.9.9.9) NMR processing softwares.

2.7.7 NMR experiments for enzymatic catalysis

2.7.7.1 Alkaline phosphatase

To monitor substrate hydrolysis during catalysis, a sequence of seventeen proton acquisitions, properly inter-delayed, was launched at 25 °C since the beginning of reaction (after 7, 8, 10, 15, 21, 27, 29, 40, 52, 64, 86, 108, 140, 172, 204, 236, 256 min) on each sample as a function of humic concentrations (0, 6, 8 and 12 mg mL^{-1}). ^{1}H-NMR spectra were acquired with 2 s of thermal equilibrium delay, a 12.95 μs 90° pulse length, 32768 time domain points and 32 transients (55 s for each acquisition). The proton frequency axis was calibrated by associating the doublets resonating at to 8.231 and 8.074 ppm, to aromatic *meta* protons of *p*-NPP and *p*-Nitrophenol, respectively. Throughout the catalytic reaction, the area contained in the doublets resonating at 8.231 and 7.95, and corresponding to meta protons of 4-NitroPhenyl Phosphate (S1) and *p*-Nitrophenol (P1), respectively, was integrated. The relative substrate concentration (%) was calculated by dividing the area of S1 by that of P1 and multiplying by 100.

2.7.7.2 β-Glucosidase

A sequence of twelve proton spectra, properly inter-delayed, were acquired on each sample containing GLU and FA (0, 0.03, 0.1 and 0.2 mg mL^{-1}), after 11, 13, 15, 23, 30, 38, 45, 53, 65, 78, 90 and 123 min since the start of substrates catalytic reaction. ^{1}H-NMR spectra were acquired with 2 s of thermal equilibrium delay, an 11 μs 90° pulse length, 32768 time domain points and 32 transients (52 seconds each acquisition). In the case of the Salicin substrate, the proton frequency axis was calibrated by attributing the doublets, resonating at 5.051 and 5.146, to the α anomeric protons of Salicin (S1) and Glucose (P1), respectively. In the case of *p*-NPG, the doublets resonating at 8.1619 and 8.073 ppm were associated to aromatic *meta* protons of *p*-NPG (S2) and *p*-Nitrophenol (P2), respectively. The areas under substrate and products signals were integrated throughout the experiments and the relative substrate concentrations (%) were calculated by dividing the area S by that of P and multiplying by 100.

2.7.8. Viscosity measurements

Possible modifications of NMR measured parameters (T_1, T_2 and DOSY self-diffusion coefficients) may be due to change in viscosity among samples (Smejkalova and Piccolo, 2008a). Thus, dynamic viscosity was measured with a Bohlin Advanced Rheometer (Bohlin Instruments Ltd., Gloucestershire, UK), using a coaxial cylinder geometry with a gap size of 150 μm. All viscosity measurements were performed in triplicate, at 25ºC, and under a constant shear stress of 0.1 Pa.

2.8 Activity of GLU immobilized on Al-humate-montmorillonite (HM) complex

2.8.1 Immobilization

β-D-Glucosidase (100 mg) was dissolved in 0.2 M phosphate buffer solution at pH 5 to obtain a final concentration of 5 mg mL^{-1}. The HM complex (1 g) was placed in a 50 mL centrifuge tube together with 20 mL of the buffer solution containing the GLU enzyme. A control suspension without the enzyme was prepared similarly as control. Control and enzyme suspensions were in triplicates. Each HM suspension was rotary-shaken at 90 rpm for 24 h and the supernatants removed by centrifugation at 2500 rpm for 40 minutes. The residues were washed 4 times with 20 mL of buffer solution. All supernatants were separated by centrifugation and their residual content of GLU enzyme measured by UV-Vis spectrophotometer. At the disappearance of the free enzyme in the supernatant, the centrifuged residue was finally dried by a gentle N_2 flux and stored at 4°C.

2.8.2 GLU measurement by UV spectrophotometer

The supernatants were 20 folds diluted with the buffer solution at pH 5 and analyzed by a Perkin Elmer Lambda 25 UV-VIS spectrophotometer at 278 nm. The enzyme concentration in the supernatants was evaluated against a calibration curve (r^2 = 0.99932) built by measuring solutions containing known GLU concentrations (10, 25, 50, 75, 100, 250, 500 and 1000 μg mL^{-1}).

2.8.3 Catalytic activity of immobilized GLU enzyme

The Salicin substrate was dissolved in a 0.2M phosphate buffer solution at pH 5 to reach a concentration of 2 mg mL^{-1}. The heterogeneous catalysis reaction was started by adding 20 ml of Salicin solution to the dried residue of the GLU enzyme immobilized on the HM complex and to the corresponding control residues without GLU. Three replicates were prepared for all samples and the reaction vessels were subjected to rotary-shaking at 90 rpm. After 0.04, 0.33, 0.66, 1, 2.5, 4, 6.5

and 66 h since the reaction start, 300 μL of solution were collected, to which 30.03 mg of urea were added to stop the reaction and reach a final 2.5 M urea solution. Each sample solution was then passed through a 0.45 μm cellulose-acetate filter and analyzed by HPLC combined with an UV/Vis detector. Concomitantly, a second control sample was prepared by starting the homogeneous catalysis in a liquid phase (LP). In this case, 20 mg of free GLU enzyme were solubilised in 20 mL of 0.2M phosphate buffer solution at pH 5, and the homogeneous catalysis was launched by adding 1812 μg mL^{-1} of Salicin. In order to make the LP results directly comparable to those by LPS, only 1812 μg mL^{-1} (that is exactly 90.6 % of 2000 μg mL^{-1}) of Salicin were added to enzyme solution. In this way, the observed Salicin adsorption on HM was taken in account. This reaction was conducted in duplicate.

2.8.4 Measurement of change of catalysis substrate by HPLC

The HPLC system consisted of a Perkin Elmer 200 LC pump, equipped with a 10 μL sample loop on a 7125 Rheodyne Rotary injector, a Phenomenex Sphereclone 5 ODS column (250 x 4.6 mm, 5 μm beads diameter,) and a Gilson 18 UV/Vis detector. The UV detector was set at 270 nm and the eluent solution was a binary phase of methanol (A) and 0.75 % (v/v) trifluoracetic acid solution in MilliQ grade water (B). The chromatogram was achieved with the following gradient elution: 10% of A for 3 min at 0.5 mL min^{-1}; 25% of A for 4 min at 0.5 mL min^{-1}; 75% of A for 8 min at 0.5 mL min^{-1}; 90% of A for 4 min at 0.5 mL min^{-1}; 100% of A for 1 min at 0.65 mL min^{-1}, for 1 min at 0.85 mL min^{-1}, for 7 min at 1 mL min^{-1}. A Perkin Elmer TotalChrom 6.2.0 software was employed to acquire and elaborate chromatograms. The enzyme substrate hydrolysis was monitored by a quantitative analysis of Salicin (Retention time = 14.1±0.12 min), against a calibration curve (r^2 = 0.99922) by measuring solutions containing known Salicin concentrations (1, 5, 10, 50, 100, 250, 500, 750, 1000, 1500 and 2000 μg mL^{-1}).

3.

Quantitative evaluation of non-covalent interactions between Glyphosate and dissolved humic substances by NMR spectroscopy

Pierluigi Mazzei [1,2], Alessandro Piccolo[1*]

[1] Centro Interdipartimentale per la Risonanza Magnetica Nucleare (CERMANU), Università di Napoli Federico II, Via Università 100, 80055 Portici, Italy

[2] Istituto di Metodologie Chimiche, CNR, Via Salaria Km 29.300, 00016 Monterotondo Stazione, Italy

Corresponding author: tel. +39 081 253 91 60; fax +39 081 253 91 86;

e-mail: alessandro.piccolo@unina.it.

To be submitted to "Environmental Science and Technology"

Keywords: NMR, Glyphosate, Humic substances, relaxometry, diffusion, STD, environment.

Abstract

Interactions of Glyphosate (N-phosphonomethylglycine) herbicide (GLY) with soluble fulvic (FA) and humic acids (HA) at pH 5.2 and 7 were studied by ^{1}H- and ^{31}P-NMR spectroscopy. Increasing concentrations of soluble humic matter determined the broadening and chemical shift drifts of proton and phosphorus GLY signals. This indicated the establishment of weak interactions between the herbicide and the humic supramolecular structures. The extent of interactions were larger for FA and pH 5.2 than for HA and pH 7, thus suggesting the occurrence of hydrogen bondings between GLY carboxyl and phosphonate groups and complementary functions in humic matter. The weak GLY-humic interactions were also inferred by the changes in relaxation and correlation times for both the herbicide ^{1}H and ^{31}P signals. Saturation Transfer Difference (STD) NMR pulse sequences confirmed the non-covalent nature of the GLY-humic interactions. Diffusion ordered NMR spectra (DOSY) allowed to calculate the fraction of Glyphosate bound to humic suprastructures and determine the thermodynamic parameters inherent the formation of GLY-humic complexes, such as the association constants (K_a) at both pHs, and the Gibbs free energies of transfer. These values showed that the most effective non-covalent interactions occurred at pH 5.2 and with fulvic acids. The NMR techniques applied here demonstrated that Glyphosate is capable of a spontaneous and significant binding to soluble humic matter by non-covalent interactions and, thus, be transported through the soil profiles to natural water bodies.

Introduction

N-phosphonomethylglycine is the active ingredient of the popular broad-spectrum and relatively non-selective herbicide, commonly referred to as glyphosate. It is used in the form of an aqueous solution of isopropyl-amine salt under trade names such as Roundup®, Rodeo®, Glyfonox® and Glycel® [1]. Introduced by the US Chemical Company Monsanto in the early 1970s, glyphosate represents today up to 60% of the global 'broad-spectrum' herbicide sales, covering a

global use of over 70,000 t.year^{-1} of technical acid [2]. Furthermore, the introduction in 1997 of Roundup Ready® crops, such as cotton, maize, and soybeans, which are made resistant by incorporation of a naturally occurring glyphosate-resistant protein, added popularity to the synthetic herbicide [3]. Glyphosate high efficiency is due to its potent and specific inhibition of the enzyme 5-enolpyruvylshikimate 3-phosphate (EPSP) synthase [4]. The enzyme is an intermediate of the shikimate pathway, that governs the synthesis of aromatic amino acids, as well as almost all other aromatic compounds in higher plants, algae, bacteria and fungi [5, 6]. Its continuous and worldwide use in agriculture is accounted to its non-toxicity for mammals, since the shikimate pathway is absent in mammals, which are thus unaffected by glyphosate [7, 8].

Although this herbicide is claimed to decrease the environmental contamination by agro-chemicals because it reduces the number of herbicides used on non-tolerant crops, and because it is less persistent and toxic than other herbicides [9], its relatively persistence in soil may still represents a major threat for a wider environmental pollution [10, 3] Glyphosate environmental persistence is due to the carbon-to-phosphorous bond that is highly resistant to biodegradation [11], while its transport in the environment is attributed to its strong interactions with fine organo-mineral soil particles [12, 13] and soluble humus fractions [12-15].

Despite the environmental importance of humic matter, its chemical complexity as supramolecular association of small heterogeneous molecular bioproducts poorly stabilized by weak forces [16], makes difficult to investigate the interactions with herbicides and glyphosate, in particular. In fact, it is the strength of these interactions that controls the transport of agrochemicals through soil profiles to groundwaters but also their bio-availability to microorganisms [17]. Moreover, the thermodynamic evaluation of such interactions strength is further complicated by the difficulty in determining low concentrations of glyphosate, which cannot yet be achieved by straightforward analytical methods [18, 19, 20, 21].

Nuclear Magnetic Resonance (NMR) spectroscopy is a powerful technique for studying both the qualitative and quantitative relations among different organic molecules, and, thus also those

between environmental pollutants and natural organic matter [17, 22, 23]. Despite some earlier works on humus-Glyphosate interactions [14, 15], ^{1}H or ^{31}P liquid-state NMR spectroscopy was never employed to assess the extent of such interactions, while it has been instead applied in human and plant physiological and ecotoxicological studies of glyphosate behaviour [1, 11, 24].

The objective of this work was to apply ^{1}H and ^{31}P NMR techniques to prove the occurrence of interactions between glyphosate and water-soluble humic substances and to reach the corresponding thermodynamic parameters. As by earlier approaches [22, 23, 25], the NMR techniques adopted in this work consisted in: 1. relaxometric measurements to extrapolate nuclear correlation times that indicate the mobility of interacting molecules, 2. Diffusion ordered (DOSY) NMR experiments to obtain self-diffusion values and calculate the complex humic-glyphosate association constants. Moreover, the homo-nuclear protonic saturation transfer difference (STD) pulse sequence [26, 27] was employed here for the first time to identify the occurrence of noncovalent bonds between relative large humic associations, and the small glyphosate ligand.

Materials and Methods

Humic substances. Fulvic acids (FA) and humic acids (HA) were isolated, as previously described [28], from a volcanic soil (Typic Fulvuland, Lazio, Italy) and a North Dakota Leonardite (Mammoth Int. Chem. Co.), respectively. HA were purified of coextracted inorganic particles first by three cycles of dissolution in 0.5 M NaOH followed by flocculation in 6 M HCl, and then shaking humic acids twice in a 0.25 M HF/HCl solution for 24 h. HA were redissolved in 0.5 M NaOH and passed through a strong cation-exchange resin (Dowex 50) to eliminate remaining di- and trivalent metals. The eluate was precipitated at pH 1, dialyzed, and freeze-dried. After homogenization, 30 mg of HA were suspended in H_2O, titrated to pH 7 and freeze dried again. FA were adsorbed on a XAD-8 column to eliminate soluble hydrophilic impurities (carbohydrates and proteins), and then eluted out of column by a 1 M NaOH solution, immediately neutralized,

dialyzed against water, and freeze-dried. Respectively, a total organic carbon content of 23.8 % and 45.9 % was present in FA and HA.

Samples preparations. 1 mg of Glyphosate (GLY) free acid (99 % pure, Dr. Ehrenstorfer, Germany) was dissolved in 1 mL of two deuterated water (99.8% D_2O/H_2O, ARMAR CHEMICALS) solutions, kept at the pH of either 5.2 or 7, and prepared with 0.2 M acetate and 0.2 M phosphate buffer solutions, respectively. Different amounts (0, 5, 10, 15, 20 and 25 mg) of either FA or HA were dissolved into the two GLY solutions, without any humic precipitations at both pHs. Control humic substances solutions were similarly prepared but without GLY addition. All solutions were stirred for 10 minutes to guarantee the complete dissolutions of analytes before NMR analysis.

For most sensitive STD-NMR spectra, the small ligand is required to be stoichiometrically in greater amount than the interacting macromolecule [26, 27]. In the case of humic suprastructures acting as the macromolecule, we assumed an average nominal molecular weight between 5 and 10 kDa, thus signifying a stoichiometric relation between 1:50 and 1:100. Consequently, four different samples were prepared, by dissolving 8.45 mg ($5x10^{-2}$ mmol) of GLY in deuterated solutions at either pH 5.2 or 7 that also contained 5 mg of either HA or FA. All samples under NMR analyses were transferred into stoppered NMR tubes (5mm, 7", 507-HP-7, NORELL) and solutions degassed by N_2 flux for 5 min, followed by a sonication for 15 min.

NMR Experiments. A 400 MHz Bruker Avance spectrometer, equipped with a 5 mm Bruker BBI (Broad Band Inverse) probe, working at ^{31}P and ^{1}H frequencies of 161.81 and 400.13 MHz, respectively, was employed to conduct all liquid-state NMR measurements at a temperature of 298 +/- 1 K. ^{1}H-NMR spectra were acquired with 2 s of thermal equilibrium delay and a 90° pulse length ranging between 7.3 and 8.9 μs. ^{31}P-NMR spectra were acquired setting 7 s of initial delay and a 90° pulse length ranging between 11.1 and 11.5 μs. An 80 μs length Waltz16 decoupling scheme with around 15.6 dB as power level, under an inverse gated pulse sequence, was employed

to decouple phosphorous from proton nuclei. Both ^{31}P and ^{1}H experiments accumulated 100 transients and were acquired with 32768 time domain points.

An inversion recovery pulse sequence with 20 increments and variable delays from 0.01 to 10 s was adopted to measure both ^{1}H and ^{31}P longitudinal (spin-lattice) relaxation time constants (T_1), while the transverse (spin-spin) relaxation time constants (T_2) were measured using a Carr-Purcell-Meiboom-Gill (CPMG) pulse sequence using 20 increments and 2 to 2000 spin-echo repetitions, with a constant 1.5 ms spin-echo delay. A time domain of 16384 points was set for all the relaxometric experiments.

^{1}H and ^{31}P DOSY (Diffusion Ordered SpectroscopY) NMR spectra were obtained by choosing a stimulated echo pulse sequence with bipolar gradients, and combined with two spoil gradients and an eddy current delay. This sequence was selected to reduce signals loss due to short spin-spin relaxation times. The acquisition was executed by setting, for ^{1}H and ^{31}P nuclei, respectively, 1600 and 2300 μs long sine-shaped gradients (δ), that were linearly ranging from 0.674 to 32.030 G cm^{-1} in 32 increments, and selecting a delay of 0.09 and 0.25 s (Δ) between the encoding and the decoding gradients.

STD experiments were conducted according to previous indications [26] and accumulation of 2048 scans. Selective saturation of humic substances was achieved by a train of 50 ms Gauss shaped pulses, truncated at 1%, and separated by a 50 μs delay. A total length of saturation train of 5.005 seconds was achieved with 100 selective pulses. Best on-resonance irradiation for humic substances was found at 0.8 ppm, whereas off-resonance irradiation was set at 30 ppm, where no proton signals were visible. Spectra were internally subtracted by phase cycling after each scan. Reference spectra were recorded using the same sequence without irradiation.

The residual water signal was removed from ^{1}H-NMR spectra by pre-saturation technique, whereas the Watergate 3-9-19 pulsed train sequence was preferred for DOSY experiments, and excitation sculpting was chosen for STD experiments, using a 2 ms selective rectangular pulse, defined by 1000 points, and truncated to 1%. The spectral widths of ^{1}H and ^{31}P NMR spectra were

12 ppm (4.789 kHz) and 100 ppm (16.238 kHz), respectively. The free induction decays (FID) of ^{1}H and ^{31}P spectra were multiplied by 1 and 4 Hz exponential factor, respectively, without zero filling . All spectra were baseline corrected and processed by both Bruker Topspin Software (v.1.3) and MestReC NMR Processing Software (v. 4.9.9.9).

Viscosity measurements. Possible artificial modifications of calculated parameters by change in viscosity [29] was accounted to by measuring dynamic viscosity studies with a Bohlin Advanced Rheometer (Bohlin Instruments Ltd., Gloucestershire, UK) using a coaxial cylinder geometry with a gap size of 150 µm. All measurements were performed in triplicate, at 25ºC, and under a constant shear stress of 0.1 Pa.

Results and Discussion

Chemical shift drifts and signal broadenings. Glyphosate is a weak acid and presents three dissociation constants in aqueous solution due to progressive proton release from carboxyl, phosphonate and ammonium groups at increasing pHs [30]. The equilibrium reported in Figure 1, with a pK_2 acidity constant of 5.58, dictates the concentrations of the dianion (I) and trianion (II) forms of GLY in the pH range between 5.2 and 7. Dianion I is slightly more abundant than the trianion (II) at pH 5.2, whereas the latter is largely predominant at pH 7.

The ^{1}H-NMR spectra of HA and FA at a concentration of 15 mg ml^{-1} are shown in Supplementary Figure S1. The large broadening of ^{1}H signals in these spectra is characteristic of humic molecules in suprastructures whereby a decrease of relaxation times and signals flattening are observed. Nevertheless, HA and FA showed different conformational structures. In fact, alkyl (0.5-2.4 ppm) and hydroxy-alkylic (2.4-4.7 ppm) protons were more intense in FA than in HA spectra, possibly because of a lower hydrophobicity, and, thus, less associated conformation for FA [16].

The ^{1}H and ^{31}P spectra of GLY at different FA concentrations are shown in Figure 2 at both pH 5.2 and 7, while the corresponding spectra of GLY with HA additions are shown in Supplementary

Figure S2. Both humic materials were able to progressively broaden ^{1}H and ^{31}P signals and drift their chemical shifts, though the extent of changes varied with humic type and concentration, being larger for FA and pH 5.2.

The signals resonating between 3.75 and 2.95 ppm and attributed to protons in GLY methylene groups are shown in ^{1}H spectra (Figure 2). The singlet peak (H-1) corresponds to protons next to the carboxyl group, while the doublet (H-2) derives from proton splitting (J = 11.67 Hz) due to geminal coupling with the phosphorous nucleus. An increasing amount of FA added to GLY produced a progressively larger broadening of proton signals at both pHs. Also in the case of ^{31}P spectra, 15 and 25 mg.ml^{-1} of FA addition progressively flattened the 7.75 ppm signal at pH 7, while the P signal even disappeared at pH 5.2 for the largest FA addition. Though a similar behaviour was noted in ^{1}H and ^{31}P spectra of GLY treated with HA (Figure S2), signals broadening was significantly lower than for FA, so that the phosphorous resonance was still neatly visible even at the largest HA concentration.

These observations are attributed to the establishment of weak bonding interactions between the GLY molecule and large humic molecular aggregates. The consequence is a restricted molecular mobility and, thus, tumbling rate, that implies a progressive signals broadening for the involved nuclei. The fact that this effect increased with humic concentration, it may be regarded as a first evidence of weak GLY-humic interactions.

A down-field signal shift was observed at pH 7 in both ^{31}P and ^{1}H spectra at increasing FA concentrations (Figure 2). At 25 mg ml^{-1} of FA, the H-2 signal shifted from 2.93 to 2.98 ppm, while the ^{31}P signal moved from 7 to 7.75 ppm. These shifts of both ^{31}P and H-2 signals further support the occurrence of hydrogen bonds between GLY and the complementary functional groups of FA, that was previously shown by other methods [14]. HA additions (Figure S2) produced similar, though very moderate, down-field shift of the H-1 signal at both pH 5.2 and 7, but no chemical shift drift was observed for the ^{31}P signal.

Saturation transfer difference. A Saturation Transfer Difference (STD) experiment was conducted to confirm the occurrence of weak interactions between GLY and humic matter. The STD pulse sequence was introduced by Mayer and Meyer [31] to evaluate the extent of non-covalent protein-ligand interactions by “through-space” polarization transfer. This technique had been already employed to prove the interactions occurring between humic substances and pesticides [27], since only the pesticide actually interacting with humic matter is NMR visible by STD.

Here, the large-sized humic association [16] was first allowed to interact in solution with the relative small Glyphosate ligand, and then the humic matter frequency was saturated by an on-resonance selective shape pulse irradiation. The ligand interacting with the irradiated molecular aggregate receives a partial saturation transfer through the NOE effect and it is NMR detected. A second similar pulse sequence is then applied by an off-resonance irradiation to avoid any saturation of humic matter. Finally, by subtracting the second spectrum from the first one, the difference spectrum shows only the signals of the proton nuclei involved in humic-GLY interactions. These protons are affected by the applied saturation irradiation that determines the polarization transfer between humic molecules and GLY, thus inducing a through-space increase of NOE intensity. Therefore, the signals intensities for the bound GLY are proportional to its spatial proximity to the interacting humic molecular assembly. Conversely, if the GLY ligand did not interact with the saturated humic aggregate, no signals would result in the final difference spectrum. It is essential that the first on-resonance pulse be irradiated sufficiently away from the ligand signal (as a function of shape pulse length and selectivity), to avoid an undesired ligand selective irradiation, that may result in meaningless difference spectra and overestimation of the binding extent. Contrary to very small molecules, whereby isotropic tumbling average dipolar interactions, these become dominant in stable humic aggregates, thus providing the means for an efficient propagation of spin diffusion, that disturbs the spin population throughout the entire humic supramolecular assembly [27].

Control and difference STD spectra at pH 7 and 5.2 for GLY-humic interactions are shown in Figure 3. The intensities of GLY signals in difference spectra were rather low at pH 7 for both FA

and HA, though slightly more intense signals were obtained with FA. Signals intensities, in difference spectra at pH 5.2, were significantly greater than for pH 7, being those for FA more intense than for HA. The lower the signal intensities in the STD difference spectra, the smaller is the degree of intermolecular non-covalent interactions. Therefore, STD experiments confirmed that GLY was in strict proximity to humic matter at pH 5.2, thus allowing a larger saturation transfer than for pH 7. The STD spectra clearly indicated that GLY had a greater association with hydrophilic FA than with hydrophobic HA. In fact, both H-1 and H-2 protons were visible in STD difference spectra, thus implying the involvement of both carboxyl and phosphate groups in the Glyphosate interactions with humic matter. Hence, these STD findings not only agree with the occurrence of non-covalent binding between GLY and humic matter, as suggested by the observed signal broadenings and down-field shifts, but that hydrogen-bonds are the prevailing interactions, as previously shown [14].

Relaxation times. The T_1 and T_2 relaxation constants of both proton and phosphorous resonances, as obtained by inversion recovery and CPMG experiments, respectively, are reported in Table 1. For protons, both constants became progressively smaller with increasing humic matter as compared to GLY alone. At both pHs, the largest decrease of T_1 and T_2 values were observed with FA additions. In fact, the FA largest concentration (25 mg mL^{-1}) determined a T_1 decrease of 81.45% and 87.84% at pH 5.2 and 7, respectively, whereas the corresponding reduction was only 23.36% and 16.39% with HA (the values are related to averaged H-1 and H-2 relaxation measurements).

In the case of T_2, FA still produced the greatest shortening of spin-spin relaxation time (94.58 % in respect to control) for both proton signals and most significantly at pH 5.2 (Table 1). Conversely, progressive addition of HA not only decreased T_2 values less than FA at the same pH, but the T_2 shortening was more evident for H-1 than for H-2. This suggests a direct involvement of GLY carboxyl group in interactions with complementary groups in HA.

As for ^{31}P, FA decreased both T_1 and T_2 values more than HA at both pHs (Table 1). Moreover, the effect of FA made GLY P spin-lattice relaxation so fast that the consequent signal broadening prevented T_1 to be measured at the largest FA concentration, and T_2 to be calculated even at a FA concentration as low as 10 mg mL^{-1} (Table 1). These observations support the above suggestion, inferred by signal broadening and shift, that the GLY phosphonate group must strongly interact with FA molecules.

Both T_1 and T_2 values in solution are dependent on the correlation time (τ_C), that is defined as the effective average time needed for a molecule to rotate through one radian. Therefore, the larger the τ_C values, the slower is the molecular motion [22]. Correlation times for both H and P nuclei in GLY, as calculated from T_1 and T_2 values [32], increased invariably with humic concentration (Table 1). FA resulted more effective than HA and provided a τ_C increase 3.6 times greater than control for the H-2 signal at pH 5.2. The strong effect of humic matter on GLY tumbling rate could also be inferred by the few τ_C values calculated for the ^{31}P nucleus. In fact, ^{31}P τ_C values significantly increased by adding only 5 mg ml^{-1} of FA at pH 5.2, and from 5 to 15 mg ml^{-1} of FA at pH 7 (Table 1).

Diffusion experiments According to the Einstein-Stokes description, the diffusivity of a molecule decreases when the hydrodynamic radius increases [33] and, thus, the larger the molecular dimension, the smaller is the self-diffusive constant. Moreover, by measuring molecular diffusivity, it is possible to obtain quantitative thermodynamic information on intermolecular interactions [25]. DOSY-NMR spectroscopy is a fast and reliable method to provide information on diffusivity changes when small molecules become involved in non-covalent complexes with humic matter [22, 23].

The ^{1}H 2D-DOSY projections for Glyphosate complexes with increasing amount of FA are shown in Figure 3, whereby slow (large hydrodynamic radius) and fast (small hydrodynamic radius) complexes are found at higher and lower F1 side, respectively. The corresponding self-diffusion

constants for ^{1}H (^{1}H values being the average of H-1 and H-2 self-diffusion) and ^{31}P, as well as for humic matter alone, are reported in Table 2.

The diffusion of Glyphosate progressively decreased with increasing amount of humic matter (Figure 4 and Table 2), being the extent of reduction larger for FA than for HA and much greater at pH 5.2 than at pH 7. This behaviour is explained with the formation of a complex between humic matter and Glyphosate and the consequent progressive enhancement of its hydrodynamic radius. However, while hydrogen bonding interactions are favoured at lower pH and by the more acidic FA, weaker dispersive bonds are the complex stabilizing forces at higher pH and with more hydrophobic HA. Humic matter serves as a host for the Glyphosate guest in the host-guest complex formation, and, thus, both host and guest tend to diffuse at an equal rate and show the same diffusion constant.

The self-diffusion values were used to calculate the fraction of GLY bound (ρ) to humic matter, assuming that a fast exchange occurs between free and humic-bound GLY molecules on the NMR scale [25]:

$$\rho = \frac{D_{\mathrm{GLY,obs}} - D_{\mathrm{GLY,free}}}{D_{\mathrm{complex}} - D_{\mathrm{GLY,free}}}$$

where $D_{GLY,obs}$ is the measured apparent (weight-averaged) diffusion constant of both free and humic-bound GLY, $D_{complex}$ is the diffusion constant of GLY-FA or GLY-HA complexes when GLY is fully bound to humic matter, and $D_{GLY,free}$ is the diffusion constant of GLY molecule in the absence of humic matter. Since GLY does not fully form a complex with humic matter, the value of $D_{complex}$ cannot be not experimentally known. However, being the GLY molecule smaller in size than the humic suprastructures, the $D_{complex}$ for GLY-humic complex should have a value equal to FA or HA diffusion values, as previously assumed [22, 23]. A low signal to noise ratio in ^{31}P spectra prevented calculation of GLY diffusion constants on phosphorous, and the values for the bound GLY fraction was thus achieved only from proton spectra.

The fraction of bound GLY as a function of humic concentration at both pH 5.2 and 7 is shown in Figure 5. As already revealed by relaxometric, STD, and diffusion measurements, soluble humic materials provided the largest interactions with GLY at pH 5.2. While FA interaction with GLY was generally larger extent than for HA at both pHs, the 25 mg ml^{-1} addition of HA and FA at pH 5.2 was able to bind 51.31 and 61,38% of GLY, respectively.

The fraction of bound GLY (ρ) measured by diffusion experiments, was in turn employed to calculate the association constants (K_a) between GLY and both FA and HA. This was achieved by fitting ρ versus HA and FA concentrations [22, 23, 25], according to the following equation derived from the Langmuir adsorption equation [34]:

$$\rho = a\frac{\mathrm{Ka[host]_{free}}}{1+\mathrm{Ka[host]_{free}}}$$

where $[host]_{free}$ is the concentration of the unbound humic matter (expressed as moles of organic carbon) and a is a constant. The optimal a value was empirically found and its best fitting in all cases resulted for a = 1.5. The K_a values are reported in Table 3 and indicate that the largest affinity was again for herbicide interactions with both humic substances at pH 5.2. Furthermore, the K_a constants permitted the calculation of the Gibbs free energy of transfer ($\Delta G = -RT \ln K_a$) of GLY to FA and HA (Table 3). Negative values of the transfer ΔG were found for both humic materials only at pH 5.2, thus showing that, though a decrease in motion implies an entropy reduction, the association of GLY with humic matter at this pH is spontaneous and energetically favourable. Conversely, the association of GLY to HA and FA at pH 7 produced positive $\Delta G°$ values, suggesting that interactions are not spontaneous, in agreement with correlation times and observations by STD spectra.

Conclusions.

Different NMR methods were applied here to accurately quantify the binding to humic substances of the widely employed glyphosate herbicide. Measurements of spin-lattice (T_1) and spin-spin (T_2) relaxation times allowed calculation of nuclear correlation times τ_c for GLY in interaction with different concentrations of humic matter. These data together with "through-space" correlation by Saturation Transfer Difference (STD) NMR experiments confirmed the occurrence of non-covalent complexes between GLY and humic matter. All NMR results indicate that the largest GLY binding was observed at pH 5.2 and with FA.

Chemical shift drifts and resonance broadening in ^{1}H- and ^{31}P-NMR spectra called for a determinant role of hydrogen bond formation in GLY-humic complexes. Especially for FA, both carboxylic and phosphonate groups of Glyphosate appeared responsible for hydrogen bonds with complementary functions in humic matter. The larger extent of GLY-humic interactions at pH 5.2 than at pH 7 is explained with the presence of a dianion form of GLY and a greater degree of protonation in the humic acidic groups. This condition not only provides both interacting molecules with more complementary sites for hydrogen bond formation, but also lowers their reciprocal electronegative repulsion. Diffusion NMR experiments (DOSY) allowed to accurately quantify the fraction of GLY bound to humic materials, and, consequently, the thermodynamic parameters controlling association of the herbicide to both HA and FA, such as the equilibrium constants (K_a) and the free energy of transfer (ΔG).

These findings highlight the importance of weak but spontaneous interaction of Glyphosate to the hydrophilic fulvic fraction of soil organic matter and should be of interest to further investigate transport and/or mobility of the herbicide through the soil profile into groundwaters as favoured by the association to soluble humic matter.

Acknowledgments

P.M. gratefully acknowledges the doctoral fellowship granted by the Istituto di Metodologie Chimiche, CNR.

Supporting information available

^{1}H-NMR spectra of both humic substances, and ^{1}H- and ^{31}P-NMR spectra of glyphosate treated with different concentrations of HA.

Literature Cited

[1] Cartigny B.; Azaroual N.; Imbenotte M.; Mathieu D.; Vermeersch G.; Goulle´ J. P.; Lhermitte M. Determination of glyphosate in biological fluids by ^{1}H and ^{31}P NMR spectroscopy. *Forensic Sci. Int.* **2004,** *143*, 141–145.

[2] Hu Y. S.; Zhao Y. Q.; Sorohan B. Removal of glyphosate from aqueous environment by adsorption using water industrial residual. *Desalination.* **2011**, *271*, 150-156.

[3] Borggaard O. K.; Gimsing A. L. Fate of glyphosate in soil and the possibility of leaching to ground and surface waters: a review. *Pest. Manag. Sci.* **2008**, *64*, 441-456.

[4] Schonbrunn E.; Eschenburg S.; Shuttleworth W. A.; Schloss J. V.; Amrheini N.; Evans J. N. S.; Kabsch W. Interaction of the herbicide glyphosate with its target enzyme 5-enolpyruvylshikimate 3-phosphate synthase in atomic detail. *PNAS*. **2001**, *98 (4)*, 1376–1380.

[5] Hayes W. J.; Wayland J.; Laws E. R. *Handbook of pesticide Toxicology*. Vol 3; San Diego, California. **1991**, pp. 1339–1340.

[6] Bentley R.; Haslam E. The Shikimate Pathway - A Metabolic Tree with Many Branche. *Crit. Rev. Biochem. Mol. Biol.* **1990**, *25*, 307–383.

[7] Steinrücken H. C.; Amrhein N. The herbicide glyphosate is a potent inhibitor of 5-enolpyruvylshikimic acid-3-phosphate synthase. *Biochem. Biophys. Res. Commun.* **1980**, *94 (4)*, 1207-1212.

[8] Busse M. D.; Ratcliff A. W.; Shestak C. J.; Powers R. F. Glyphosate toxicity and the effects of long-term vegetation control on soil microbial communities. *Soil Biol. Biochem.* **2001**, *33*, 1777-1789.

[9] Mamy L.; Barriuso E.; Benoit G. Environmental fate of herbicides trifluralin, metazachlor, metamitron and sulcotrione compared with that of glyphosate, a substitute broad spectrum herbicide for different glyphosate-resistant crops. *Pest. Manag. Sci.* **2005**, *61*, 905-916.

[10] Vereecken H. Mobility and leaching of glyphosate: a review. *Pest. Manag. Sci.* **2005**, *61*, 1139–1151.

[11] Lipok J.; Owsiak T.; Młynarz P.; Forlani G.; Kafarski P. Phosphorus NMR as a tool to study mineralization of Organophosphonates - The ability of *Spirulina spp.* to degrade glyphosate. *Enzyme Microb. Tech.* **2011**, *41*, 286–291.

[12] Piccolo A.; Celano G.; Arienzo M.; Mirabella A. Adsorption and desorption of Glyphosate in some European soils. *J. Environ. Sci Heal B.* **1994**, *B29 (6)*, 1105-1115.

[13] Albers C. N.; Banta G. T.; Hansen P. E.; Jacobsen O. S. The influence of organic matter on sorption and fate of glyphosate in soil – Comparing different soils and humic substances. *Enc. Pol.* **2009**, *157 (10)*, 2865-2870.

[14] Piccolo A.; Celano G. Hydrogen bonding interactions of the herbicide Glyphosate with water soluble humic substances. *Environ. Toxicol. Chem.* **1994**, *13*, 1737-1741.

[15] Piccolo A.; Celano G.; Conte P. Adsorption of Glyphosate by Humic Substances. *J. Agric. Food Chem.* **1996**, *44*, 2442-2446.

[16] Piccolo A. The Supramolecular structure of humic substances. A novel understanding of humus chemistry and implications in soil Science. *Adv. Agron.* **2002**, *75*, 57-134.

[17] Chamignon C.; Haroune N.; Forano C.; Delort A.M.; Besse-Hoggan P.; Combourieu B. Mobility of organic pollutants in soil components. What role can magic angle spinning NMR play? *Eur. J. Soil Sci.* **2008**, *59*, 572–583.

[18] Sun Y.; Wang C.; Wen, Q.; Wang G.; Wang H.; Qu Q.; Hu X. Determination of Glyphosate and Aminomethylphosphonic Acid in Water by LC Using a New Labeling Reagent, 4-Methoxybenzenesulfonyl Fluoride. *Chromatographia* **2010**, *72*, 679–686.

[19] Zelenkova N. F.; Vinokurova N. G.; Leontievskii A. A. Determination of Amine-Containing Phosphonic Acids and Amino Acids as Dansyl Derivatives. *J. Anal. Chem.* **2010**, *65 (11)*, 1143-1147.

[20] Hao C.; Morse D.; Morra F.; Zhao X.; Yang P.; Nunn B. Direct aqueous determination of glyphosate and related compounds by liquid chromatography/tandem mass spectrometry using reversed-phase and weak anion-exchange mixed-mode column. *J. Chromatography A.* **2011**, *1218*, 5638– 5643.

[21] Colombo S. D. M.; Masini J. C. Developing a fluorimetric sequential injection methodology to study adsorption/ desorption of glyphosate on soil and sediment samples. *Microchem. J.* **2011**, *98*, 260–266.

[22] Smejkalova D.; Piccolo A. Host-Guest Interactions between 2,4-Dichlorophenol and Humic Substances As Evaluated by ^{1}H NMR Relaxation and Diffusion Ordered Spectroscopy. *Environ. Sci. Technol.* **2008**, *42*, 8440–8445.

[23] Smejkalova D.; Spaccini R.; Fontaine B.; Piccolo A. Binding of Phenol and Differently Halogenated Phenols to Dissolved Humic Matter As Measured by NMR Spectroscopy. *Environ. Sci. Technol.* **2009**, *43*, 5377–5382.

[24] Ge X.; D'Avignon D.A.; Ackermana J. J. H.; Sammons R. D. Rapid vacuolar sequestration: the horseweed glyphosate resistance mechanism. *Pest. Manag. Sci.* **2010**, *66*, 345–348.

[25] Wimmer R.; Aachmann F. L.; Larsen K. L.; Petersen S. B. NMR diffusion as a novel tool for measuring the association constant between cyclodextrin and guest molecules. *Carbohyd. Res.* **2002**, *337*, 841–849.

[26] Meyer B.; Peters T. NMR Spectroscopy Techniques for Screening and Identifying Ligand Binding to Protein Receptors. *Angew. Chem. Int. Ed*. **2003**, *42 (8)*, 864-890.

[27] Shirzadi A.; Simpson M. J.; Xu Y.; Simpson A.J. Application of Saturation Transfer Double Difference NMR to Elucidate the Mechanistic Interactions of Pesticides with Humic Acid. *Environ. Sci. Technol*. **2008**, *42*, 1084–1090.

[28] Piccolo A.; Spiteller. M. Electrospray ionization mass spectrometry of terrestrial humic substances and their size fractions. *Anal. Bioanal. Chem.* **2003**, *377*, 1047-1059.

[29] Smejkalova D.; Piccolo A. Aggregation and disaggregation of humic supramolecular assemblies by NMR diffusion ordered spectroscopy (DOSY-NMR). *Environ. Sci. Technol.*, **2008**, *42*, 699–706.

[30] Piccolo A.; Celano G.; Modification of infrared spectra of the herbicide glyphosate induced by pH variation. *J. Environ. Sci. Health* **1993**, *B28 (4)*, 447-457.

[31] Mayer M.; Meyer B. Characterization of Ligand Binding by Saturation Transfer Difference NMR Spectroscopy. *Angew. Chem. Int. Ed.* **1999**, *38 (12)*, 1784-1788.

[32] Carper W. R.; Keller C. E. Direct Determination of NMR correlation times from spin-lattice and spin-spin relaxation times. *J. Phys. Chem. A* **1997**, *101*, 3246-3250.

[33] Chapman S.; Cowling T. G. The mathematical theory of non-uniform gases: an account of the kinetic theory of viscosity, thermal conduction, and diffusion in gases. Chapter 6. Elementary theories of the transport phenomena. (3^{th} Ed.). Cambridge **1990**, pp. 97-108.

[34] Langmuir I. The constitution and fundamental properties of solids and liquids. part I. Solids. *J. Am. Chem. Soc.* **1916**, *38*, 2221-2295.

Table 1. ^{1}H and ^{31}P T_1 and T_2 relaxation and correlation times (τ_c) of glyphosate as a function of HA and FA concentration (mg ml^{-1}) at 25 °C at different pHs. H-1 and H-2 are referred to Glyphosate singlet and doublet signals, respectively.

Concentration of Humic Matter	T_1 (s)			T_2 (s)			τ_c (ns)		
	H-1	H-2	P	H-1	H-2	P	H-1	H-2	P
					pH 7				
HA									
0	1.58	1.16	5.67	1.00	0.74	1.24	0.23	0.23	2.68
5	1.46	1.11	5.47	0.84	0.69	1.10	0.28	0.24	2.89
10	1.37	1.04	5.19	0.86	0.69	0.99	0.24	0.22	3.03
15	1.40	1.07	5.59	0.68	0.57	0.79	0.35	0.31	3.69
20	1.32	1.02	4.31	0.49	0.43	0.65	0.50	0.44	3.61
25	1.28	1.00	4.00	0.45	0.39	0.57	0.54	0.47	3.78
FA									
5	0.67	0.48	1.60	0.33	0.34	0.33	0.34	0.20	2.85
10	0.55	0.39	1.32	0.23	0.23	0.17	0.42	0.26	3.77
15	0.45	0.31	1.03	0.17	0.16	0.12	0.47	0.33	4.01
20	0.39	0.27	0.85	0.15	0.11	ND	0.47	0.46	ND
25	0.30	0.21	0.54	0.09	0.08	ND	0.60	0.49	ND
					pH 5.2				
HA									
0	1.46	1.15	5.02	1.12	0.87	0.96	0.17	0.17	2.94
5	1.39	1.12	4.85	0.81	0.67	0.77	0.27	0.26	3.37
10	1.26	1.03	4.45	0.57	0.52	0.69	0.38	0.33	3.42
15	1.19	0.99	3.66	0.58	0.51	0.55	0.35	0.32	3.51
20	1.11	0.93	3.44	0.42	0.38	0.51	0.47	0.42	3.54
25	1.07	0.92	3.23	0.39	0.36	0.45	0.50	0.46	3.75
FA									
5	0.36	0.26	1.59	0.19	0.18	0.18	0.31	0.21	4.03
10	0.26	0.18	0.19	0.12	0.11	ND	0.36	0.24	ND
15	0.22	0.13	0.29	0.09	0.07	ND	0.43	0.34	ND
20	0.21	0.14	0.20	0.08	0.05	ND	0.46	0.50	ND
25	0.19	0.13	ND	0.07	0.04	ND	0.54	0.61	ND

ND: Not determined.

Table 2. Diffusion values (10^{-10} m^2 s^{-1}) for signals of humic protons and ^1H and ^{31}P of Glyphosate progressively added with humic matter (mg mL^{-1}) at 25 °C, at different pH. The values were corrected for solution viscosity.

Concentration of Humic Matter	pH 5.2						pH 7					
	HA	FA	GLY+HA		GLY+FA		HA	FA	GLY+HA		GLY+FA	
	^1H	^1H	^1H	^{31}P	^1H	^{31}P	^1H	^1H	^1H	^{31}P	^1H	^{31}P
0	-	-	5.62	ND	5.62	ND	-	-	5.68	5.67	5.68	5.67
5	1.65	1.83	5.58	ND	5.60	ND	1.51	1.90	5.45	5.64	5.40	5.25
10	1.12	1.77	5.19	ND	5.14	ND	1.47	1.86	5.41	5.54	5.16	ND
15	1.24	1.69	4.47	ND	4.42	ND	1.46	1.83	5.43	5.48	5.07	ND
20	0.94	1.70	3.66	ND	3.54	ND	1.45	1.83	5.42	5.16	4.59	ND
25	1.00	1.64	3.25	ND	3.18	ND	1.34	1.85	5.24	5.22	4.50	ND

ND: Not determined.

Table 3. Binding constants (K_a) and free Gibbs Energy (ΔG) for the association of Glyphosate with FA and HA at 25 °C and at different pH.

pH	K_a (M^{-1})	r^2	Ln K_a	ΔG ($KJmol^{-1}$)
		HA		
5.2	3.414	0.993	1.228	-3.04
7.0	0.046	0.976	-3.079	7.63
		FA		
5.2	6.262	0.995	1.834	-4.55
7.0	0.502	0.963	-0.689	1.71

Figures

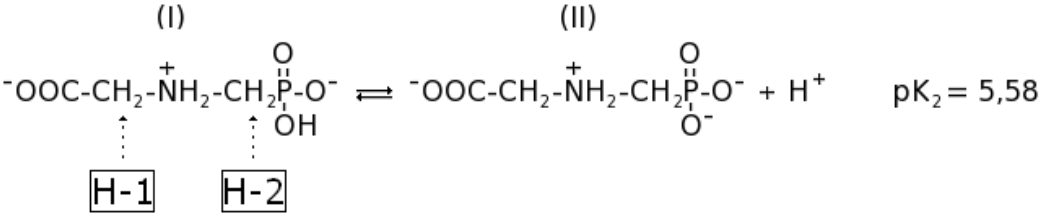

Figure 1. Second dissociation equilibrium of Glyphosate in water with its pK_2 constant.

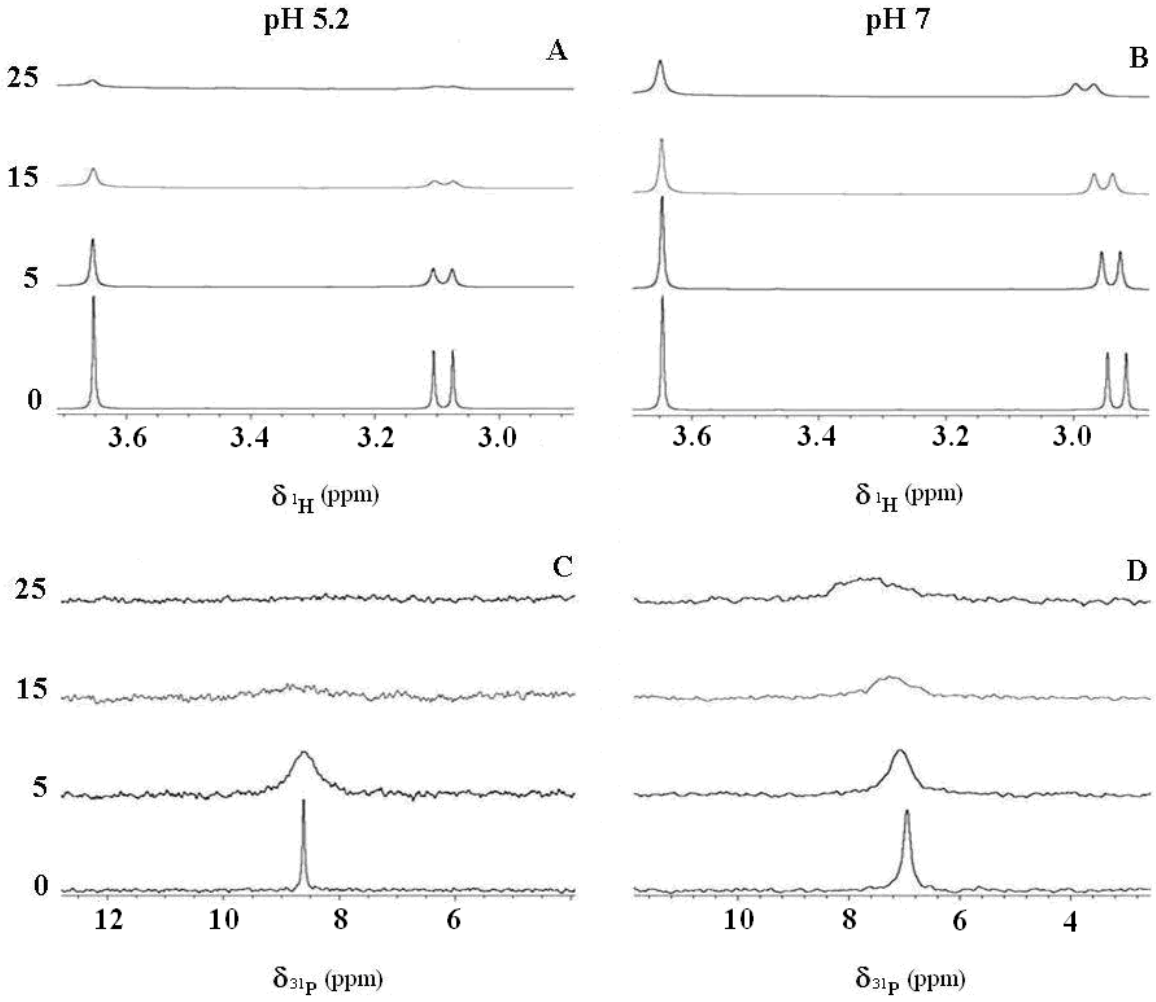

Figure 2. ^{1}H (A and B) and ^{31}P (C and D) spectra of the herbicide Glyphosate as a function of FA concentration (0, 5, 15, 25 mg mL^{-1}) at two different pH.

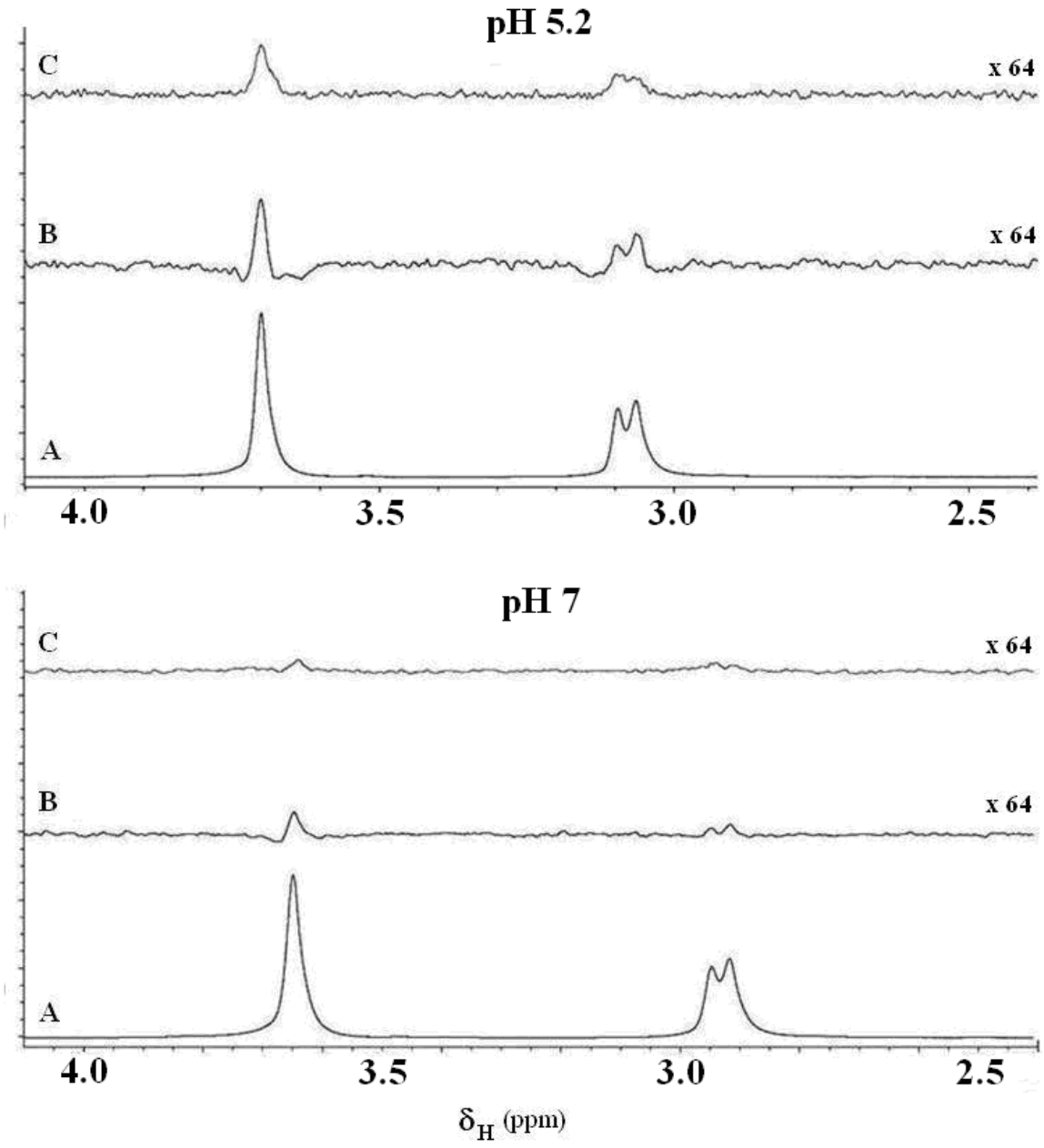

Figure 3. ^{1}H STD (Saturation Transfer Difference) spectra of Glyphosate with humic matter at pH 5.2 and 7. A. Reference STD spectra acquired without irradiation; B. STD difference spectra of sample treated with FA; C. STD difference spectra of sample treated with HA. A vertical expansion (x 64) was applied to difference spectra.

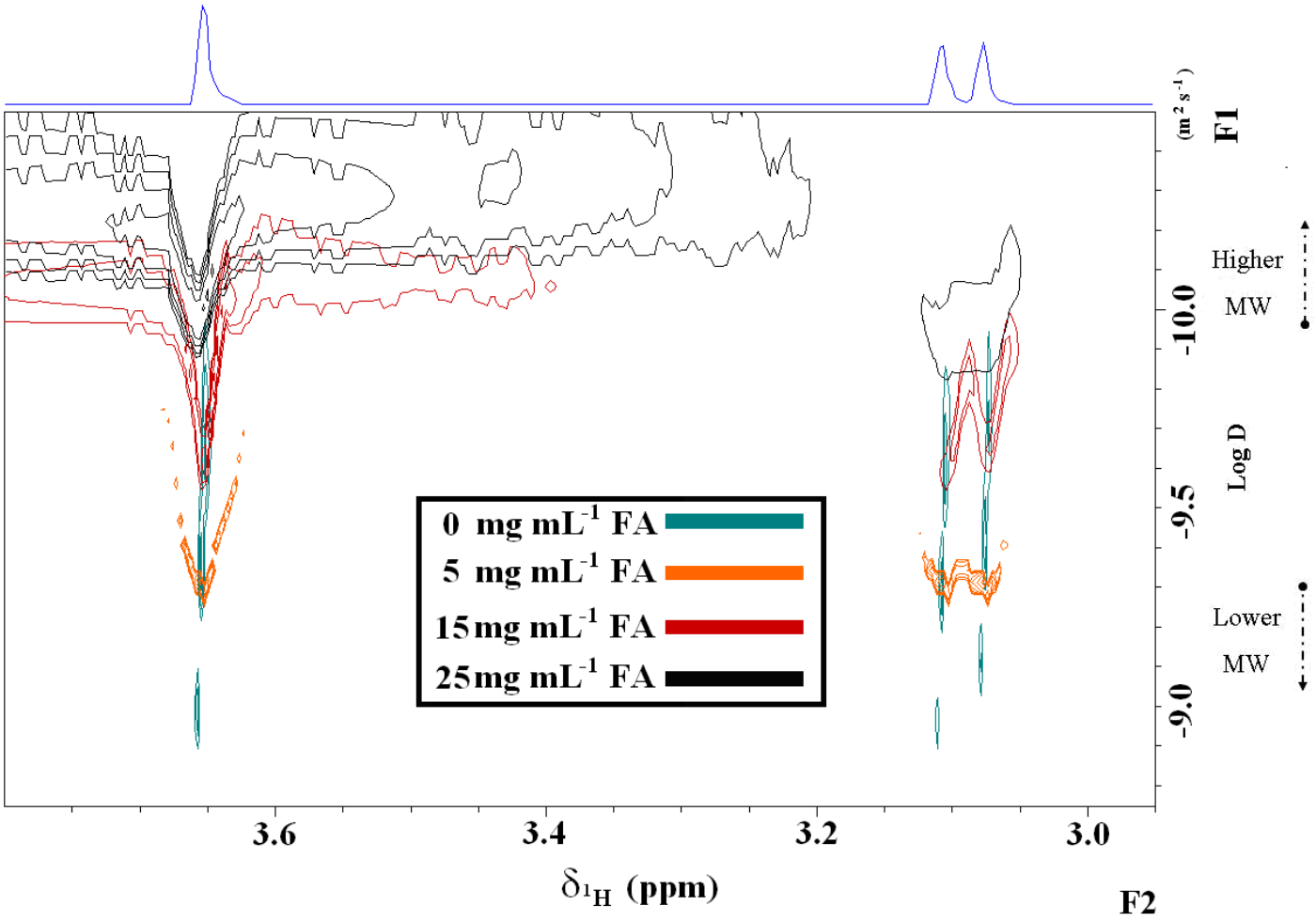

Figure 4. ^{1}H 2D-DOSY projections with diffusions of Glyphosate singlet and doublet signals for different FA concentrations (0, 5, 15, 25 mg mL^{-1}) at pH 5.2.

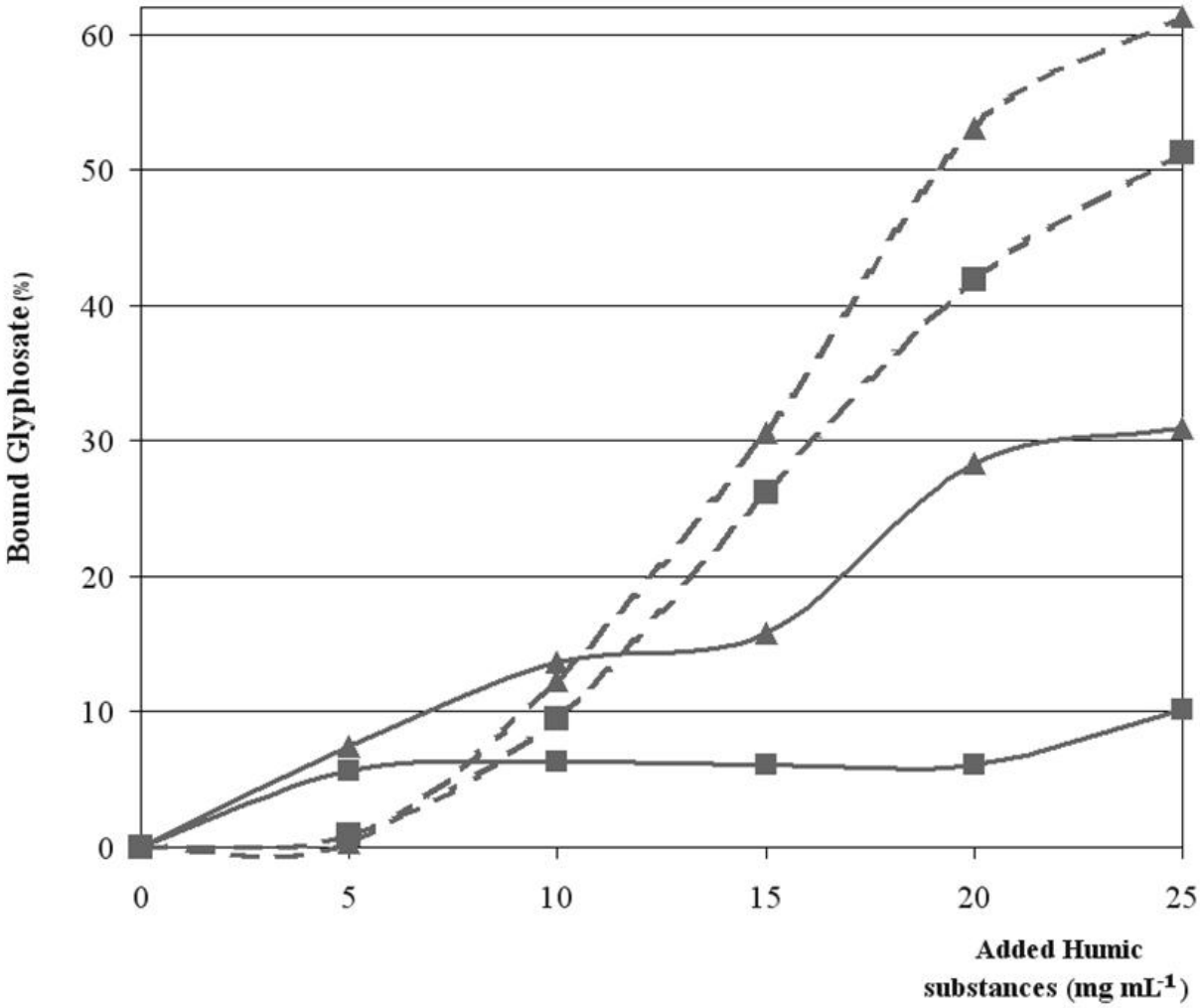

Figure 5. Bound glyphosate (%) for increasing concentrations (0, 5, 10, 15, 20, 25 mg mL^{-1}) of HA (squares) and FA (triangles) at pH 5.2 (dotted line) and 7 (continuous line).

Quantitative evaluation of non-covalent interactions between Glyphosate and dissolved humic substances by NMR spectroscopy

Pierluigi Mazzei and Alessandro Piccolo

SUPPORTING INFORMATION

Pages: 2

SUPPORTING FIGURES

Two Figures

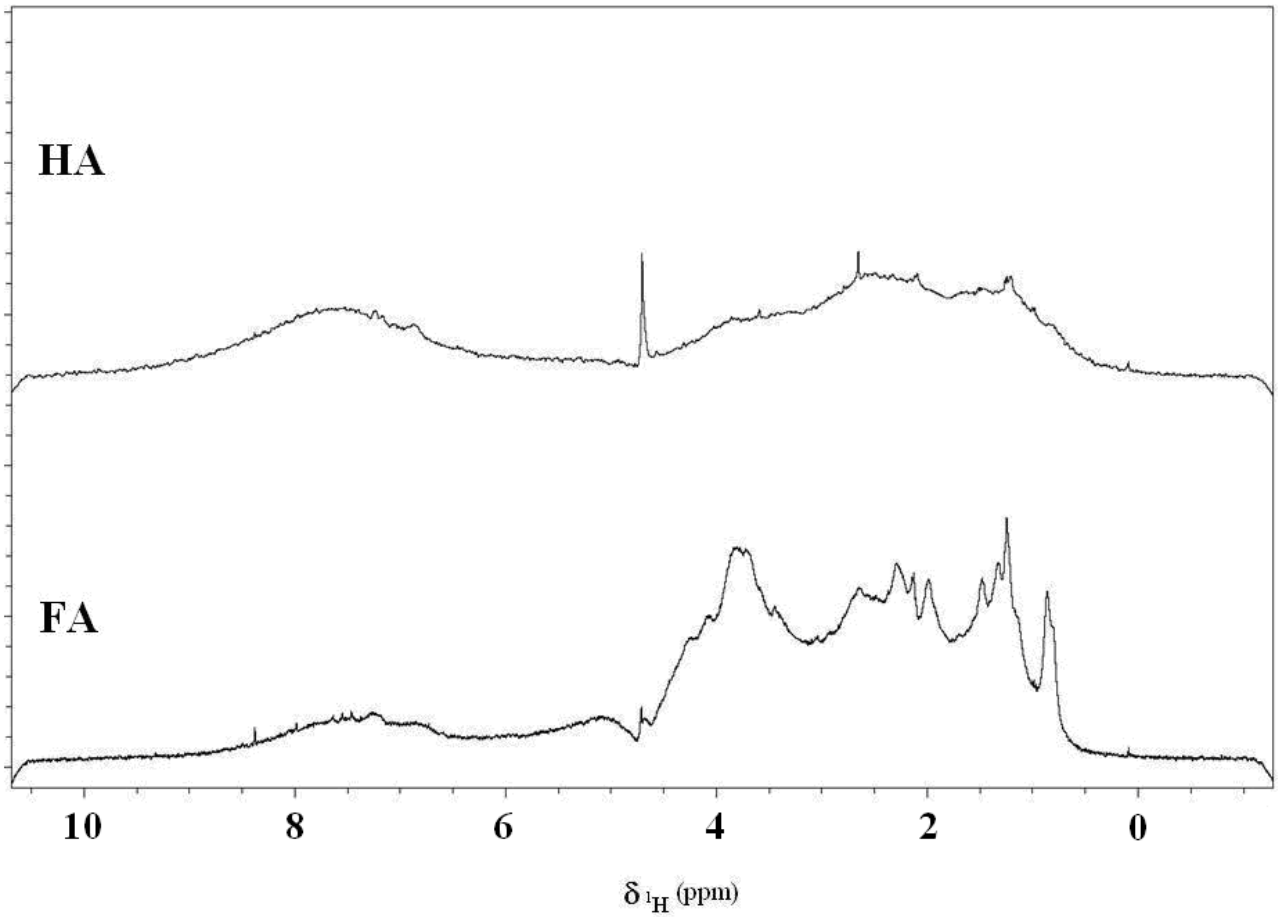

Supplementary Figure S1. Water-suppressed ^{1}H spectra of 15 mg ml^{-1} of HA and FA.

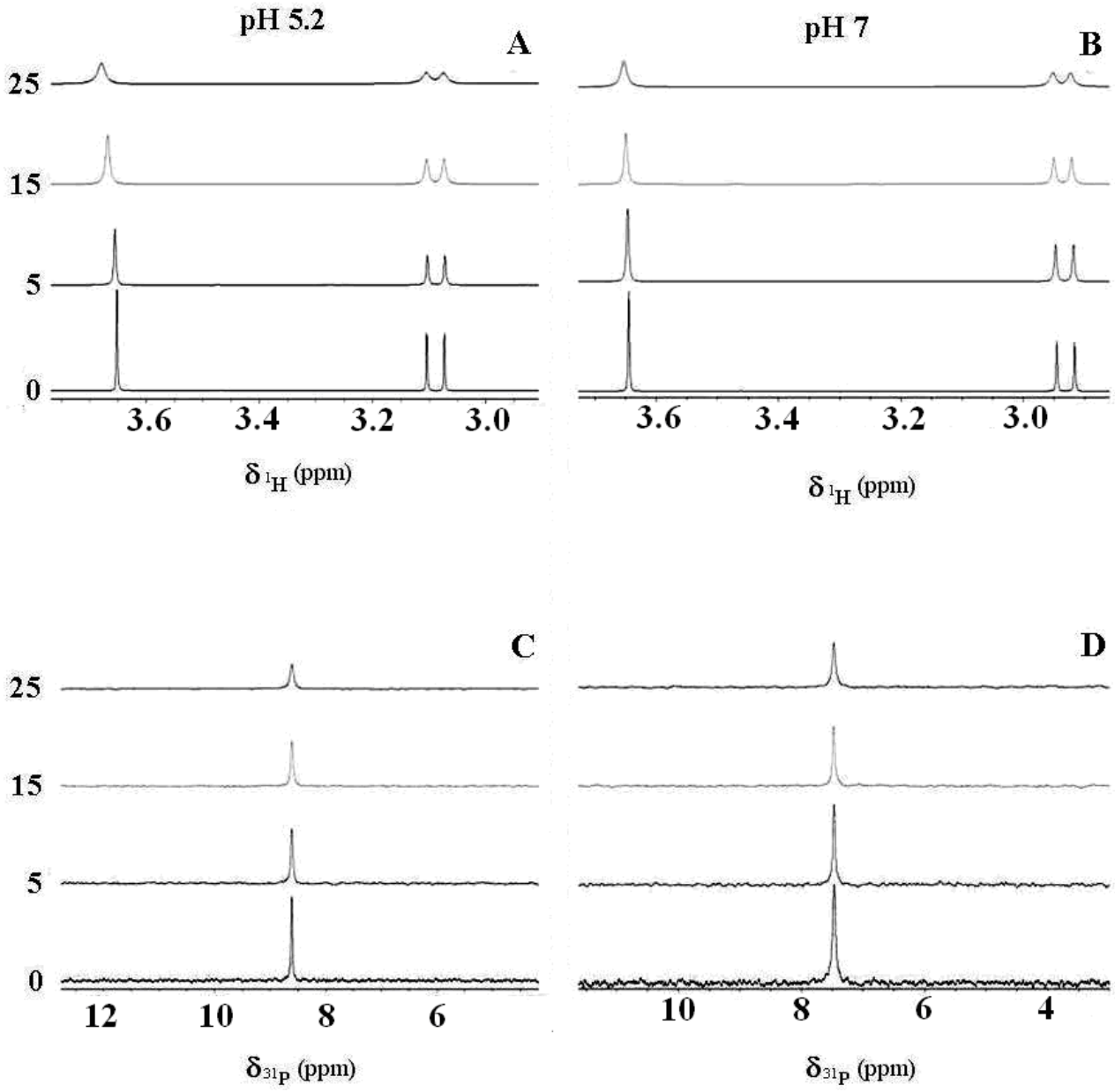

Supplementary Figure S2. ^{1}H (A and B) and ^{31}P (C and D) spectra of the herbicide glyphosate with varying HA concentration (0, 5, 15, 25 mg mL^{-1}) at different pHs.

4.

NMR applications to study the interactions between humic acids and Alkaline Phosphatase and related effects on enzymatic activity

Pierluigi Mazzei [a, b, c], Hartmut Oschkinat[c] & Alessandro Piccolo[a]*

[a] Centro Interdipartimentale per la Risonanza Magnetica Nucleare (CERMANU), Università di Napoli Federico II, Via Università 100, 80055 Portici, Italy.

[b] Istituto di Metodologie Chimiche, CNR, Via Salaria Km 29.300, 00016 Monterotondo Stazione, Italy.

[c] Leibniz-Institut fur Molekulare Pharmakologie, FMP Research Institute, Robert-Rossle-Strasse 10, 13125 Berlin, Germany.

***Corresponding author**

E-mail: alessandro.piccolo@unina.it, alpiccol@unina.it (A. Piccolo).
Tel.: +39 081 2539160
Centro Interdipartimentale per la Risonanza Magnetica Nucleare (CERMANU), Università di Napoli Federico II, Via Università 100, 80055 Portici (NA), Italy.

To be submitted to "Soil Biology and biochemistry"

Key words: Alkaline Phosphatase, Humic Acids, NMR, Relaxometry, DOSY, Enzyme Interactions.

Abstract

NMR spectroscopy was applied here to study the interactions between a model alkaline phosphatase (AP) and two different humic acids from a volcanic soil (HA-V) and a Lignite deposit (HA-L). Signals broadening for the AP enzyme was observed in ^{1}H-NMR spectra with progressive enhancement of humic matter content. To evaluate the humic-enzyme interactions, the AP proton spectra were divided in 22 buckets, and the relaxation (T_1 and T_2) and correlation times (τ_c) were measured for each bucket. The progressive decrease of the enzyme T_1, T_2, and the increase of τ_c values with increasing humic concentrations is explained with the formation of ever larger weakly-bound humic-enzyme complexes, whose translational and rotational motion was increasingly restricted. NMR diffusion experiments also showed that formation of humic-enzyme complexes progressively reduced the diffusive properties of AP, as function of HA concentration. Furthermore, it was found that both correlation times and diffusion values of AP were altered by the hydrophobic HA-L to a larger extent than by the hydrophilic HA-V. The effect of the weakly-bound humic-enzyme complexes on the catalytic activity of alkaline phosphatase was studied by recording ^{1}H-NMR spectra of the hydrolytic products of 4-nitrophenyl phosphate disodium salt hexahydrate (*p*-NPP) as an AP substrate. NMR signals of *p*-NPP were found to decrease during reaction time under AP catalysis, while those of the nitrophenol product concomitantly increased. However, the rate of signals change was significantly slowed down when humic acid concentration was progressively enhanced in the *p*-NPP-AP reaction solution. In agreement with variations of correlation times and diffusion values due to humic-enzyme formation, the catalytic activity of AP was more largely inhibited by HA-L than by HA-V. These NMR results indicate that humic matter interacts weakly with alkaline phosphatase but sufficiently to significantly inhibit its catalytic activity, thereby suggesting that the environmental role of extracellular enzymes may be reduced when coming in contact with natural organic matter.

1. INTRODUCTION

Humic substances (HS) are the major chemical components of soil organic matter (SOM). They result from chemical and biological degradation of vegetable and animal tissues (Stevenson, 1994; Piccolo *et al*., 2003, Zhang *et al*., 2011) and, as the most relevant form of organic carbon in soil and aqueous ecosystems, control the accumulation, transformation and transport of colloidal and ionic species, organic pollutants and nutrients (Tan *et al*., 2011; Fomba *et al*., 2011). HS have beneficial effects on the physical, chemical and biological properties of soil (Nardi *et al*., 2002) and are key factors in the biogeochemistry of carbon and nitrogen cycles (Iakimenko *et al*., 1996). The essential multifunctions of HS in the environment are due to their arrangement in supramolecular associations composed by relatively small heterogeneous molecules, whose conformation is stabilized by weak interactions such as dispersive and hydrogen bonds (Piccolo, 2002; Peuravuori, 2005; Baalousha *et al*., 2006).

Despite intense research, the HS chemical complexity still prevents a full understanding of their interaction with reactive biomolecules released in the environment, such as extracellular enzymes. In fact, soil enzymes are also recognized to be not only directly involved in the main processes of transformation of organic matter in soil, and nutrients cycling and uptake by plants, but also to reflect the biological quality of soil and represent indicators of soil change (Dick *et al*., 2000). Extracellular enzymes enable soil microbes to degrade complex substrates into low molecular weight compounds that can be assimilated for growth (Schimel and Bennett, 2004). A large body of work has shown that a variety of soil abiotic factors, such as mineral and organic compounds (mainly humic molecules), can regulate both the stability of enzymes and their interactions with different substrates (Sinsabaugh and Moorhead, 1994). In particular, it was observed that a partial inhibition of soil enzymes can result from the occlusion and/or steric modification of their active sites by adsorbed substrate molecules (Sarkar *et al*., 1989; Quiquampoix *et al*., 2002; Tietjen and Wetzel 2003).

Alkaline Phosphatase (EC 3.1.3.1), or *Orthophosphoric-monoester phosphohydrolase* (AP), is a common and widespread enzyme in calcareous soils where it catalyzes the hydrolysis of esters and anhydrides of phosphoric acid (Kim and Harold, 1991; Holtz and Kantrowitz, 1999). AP is released in soils by bacteria, fungi and microfauna since, contrary to acid phosphatase, it is not produced by plant roots (Olander and Vitousek, 2000; George *et al*., 2006). Extracellular alkaline phosphatases play an important role in soil by favouring mineralisation of phosphorus contained in organic matter, and it is thus essential to the supply of soluble phosphate for plant uptake (Tarafdar and Claassen, 1988; Perez-Mateos *et al*., 1991; Richardson *et al*., 2005). However, the AP catalytic activity is affected by the interactions with soil organic matter. It was found that, following immobilization of AP on a sterile soil, humic components occupied part of the enzyme active sites, thus limiting substrate bonding and increasing the K_m value (Perez-Mateosk, 1991). Conversely, absorption of AP on soil humates in the range of 58-92%, did not significantly altered its catalytic activity (Pilar *et al*., 2003). Recently, NMR spectroscopy was used to show that enzymes, among other proteins, are encapsulated by humic aggregates, thus suggesting a change in their catalytic activity in soil (Tomaszewski et. al., 2011) .

The aim of this work was to study the type of bonding occurring between the AP enzyme and two different humic acids (HA) and how the HA affect the catalytic activity of the AP enzymes. The interactions and mutual influence of such important soil components were studied by NMR spectroscopy, that represents an additional method for the characterization of the specific alkaline phosphatase used here, that had been previously studied by crystallography (Le Du *et al*., 2001; Llinas *et al*., 2005) and MALDI-TOF-Mass Spectrometry (Eriksson *et al*., 2001).

2. MATERIALS AND METHODS

2.1. Humic substances. Two humic acids (HA) were isolated, as previously described (Piccolo and Celano, 1994), from a volcanic soil (Typic Fulvuland) of the Lake Vico area, Lazio, Italy (HA-V)

and from a North Dakota Leonardite (HA-L) provided by Mammoth Int. Chem. Co., USA. Both HA were purified by subjecting first to three cycles of dissolution in 0.5 M NaOH followed by flocculation in 6 M HCl, and then to shaking twice in a 0.25 M HF/HCl solution for 24 h. The HA were redissolved to pH 7 with minimum amount of 0.5 M NaOH and passed through a strong cation-exchange resin (Dowex 50) to remove di- and trivalent cations. The eluate was precipitated at pH 1, dialyzed, and freeze-dried. After homogenization, 30 mg of HA was suspended in H_2O, titrated to pH 7 with 0.5 M NaOH and freeze dried again.

2.2. Reagents. The alkaline phosphatase enzyme was purchased from Sigma-Aldrich, Italy, as an isolate from Human Placenta Type XXIV (17 units mg^{-1}). The substrate for enzyme activity was 4-nitrophenyl phosphate disodium salt hexahydrate (*p*-NPP) and was also purchased (99.0% pure) from Sigma-Aldrich, Italy.

2.3. Humic-phosphatase adducts and catalytic activity. Different amounts of both HA (0, 0.5, 1, 2, 6 mg mL^{-1}) were dissolved in a 0.2 M carbonate buffer solution prepared with deuterated water (99.8% D_2O/H_2O, ARMAR CHEMICALS) and kept at pH 10.4. The humic solution was sonicated for 10 minutes to completely dissolve humic associations, but maintaining solution temperature below 30 °C. Then, 3.5 mg of the alkaline phosphatase enzyme were added to 700 μL of each humic solution for a final enzyme concentration of 5 mg ml^{-1}, stirred for 10 minutes and left to stabilize for 30 minutes. Each solution was degassed for 2 minutes by a gentle N_2 flux prior to NMR analysis.

Samples to evaluate the catalytic activity of humic-phosphatase adducts were prepared by dissolving 1.68 mg of AP in 700 μL (2.4 mg mL^{-1}) in deuterated carbonate buffer solution at pH 10.4 containing different amounts of HA (0, 6, 8 and 12 mg mL^{-1}), stirred for 10 minutes and left to stabilize for 30 minutes. The enzymatic catalysis was started by adding 3.5 mg of 4-NitroPhenyl Phosphate disodium salt hexahydrate (*p*-NPP) into each humic-phosphatase solution.

All solutions were transferred into stoppered 5 mm NMR tubes for NMR analysis and each sample was prepared in duplicate.

2.4. NMR Experiments. A 600 MHz Bruker DRX spectrometer, equipped with a 5 mm Bruker Inverse Quadruple resonance (QXI) probe, working at ^{1}H frequency of 600.19 MHz was employed to conduct all liquid-state NMR measurements at a temperature of 298 +/- 1 K. ^{1}H-NMR spectra were acquired with 2 s of thermal equilibrium delay, 90° pulse length ranging between 11.75 and 14 μs, 32768 time domain points and 256 transients.

An inversion recovery pulse sequence, with 20 increments and variable delays from 0.02 to 5 s, was adopted to measure ^{1}H longitudinal (spin-lattice) relaxation time constants (T_1). The transverse (spin-spin) relaxation time constants (T_2) were measured using a Carr-Purcell-Meiboom-Gill (CPMG) pulse sequence by using 20 increments and 2 (5.6 ms) to 2000 (5600 ms) spin-echo repetitions, with a constant 1.4 ms spin-echo delay. A time domain of 32768 points was set for all the relaxometric experiments.

^{1}H DOSY (Diffusion Ordered SpectroscopY) NMR spectra were obtained by choosing a stimulated echo pulse sequence with bipolar gradients, and combined with two spoil gradients and an eddy current delay before signal acquisition. This sequence was selected to reduce signals loss due to short spin-spin relaxation times. The acquisition (32768 points) was executed by 1600 μs long sine-shaped gradients (δ), that linearly ranged from 0.674 to 32.030 G cm^{-1} in 32 increments, and selecting a 0.27 s delay (Δ) between the encoding and the decoding gradients. The ^{1}H spectral width was 16.66 ppm (10 kHz) and the residual water signal was removed from ^{1}H-NMR spectra by pre-saturation technique, whereas the Watergate 3-9-19 pulsed train sequence was preferred for DOSY experiments. The proton frequency axis was calibrated by associating to 3.534 ppm the most intense signal included within the 3.5-3.6 ppm interval.

A sequence of 17 protonic acquisitions was launched at 25 °C on each humic-phosphatase solution after the start of catalysis (7, 8, 10, 15, 21, 27, 29, 40, 52, 64, 86, 108, 140, 172, 204, 236, 256 minutes) with the aim to monitor the catalyzed hydrolysis of the *p*-NPP substrate into

p-Nitrophenol. ^{1}H-NMR spectra were acquired with 2 s of thermal equilibrium delay, a 12.95 µs 90° pulse length, 32768 time domain points and 32 transients (55 seconds each acquisition). The proton frequency axis was calibrated by associating the doublets resonating at 8.231 and 8.074 ppm to the aromatic *meta* protons of *p*-NPP and *p*-Nitrophenol, respectively. No zero filling and apodization were applied to free induction decays (FID) excepted for mono-dimensional acquisitions conducted during the catalysis, where 1 Hz multiplication was executed. All spectra were baseline corrected and processed by both Bruker Topspin Software (v.1.3), MestReC NMR Processing Software (v. 4.9.9.9) and Origin (v.6.1). Details on the adopted methods for CPMAS ^{13}C-NMR spectroscopy are given in the Supporting Information.

2.5. Estimation of not hydrolyzed substrate. In spectra recorded after each catalytic time, the area under the doublets resonating at 8.231 and 8.074, corresponding to meta protons of 4-NitroPhenyl Phosphate (S1) and *p*-Nitrophenol (P1), respectively, was integrated. The relative substrate concentration (%) was calculated by dividing the S1 area by that of P1 and multiplying by 100.

2.6. Viscosity measurements. Possible artificial modifications of calculated parameters (T_1, T_2 and DOSY self-diffusion constants) by change in viscosity (Smejkalova and Piccolo, 2008 a) was accounted to by measuring solution dynamic viscosity with a Bohlin Advanced Rheometer (Bohlin Instruments Ltd., Gloucestershire, UK), using a coaxial cylinder geometry with a gap size of 150 µm. All measurements were performed in triplicate, at 25ºC, and under a constant shear stress of 0.1 Pa.

3. RESULTS AND DISCUSSIONS

3.1. Evaluation of humic-enzyme complexes

The structural features of both HA-V and HA-L were shown by liquid-state ^{1}H- and solid-state ^{13}C-NMR spectra (Supporting Information, Figure S1 and S2). More intense signals for

aromatic (107-140 ppm) and phenolic (107-165 ppm) carbons were observed for HA-L than for HA-V in ^{13}C-CPMAS-NMR spectra (Figure S1), in agreement with the intensity of the aromatic regions (5.8-8.5 ppm) of both HA shown in liquid-state ^{1}H-NMR spectra (Figure S2). Conversely, intensities of both O-alkyl (64-90 ppm) and carboxylic (165-190) carbon in CPMAS spectra were higher in HA-V than in HA-L. Likewise, a significant larger amount of signals in the hydroxy-alkylic 3-0-4.5 ppm proton region was found for HA-V than for HA-L (Figure S2). These observations suggest that HA-L was a more hydrophobic material than HA-V, that instead showed a more hydrophilic character.

The AP enzyme is reported to have an average molecular weight of 127 +/- 11 kDa (Eriksson *et al*., 2001). This significant mass size limits its mobility in solution and the molecular dipolar couplings are hardly minimized by Brownian motions, thus favouring very large signals in proton NMR spectra and inhibiting precise signals assignment. The ^{1}H-NMR spectra of the AP enzyme alone and those of AP added 2 and 6 mg mL^{-1} of HA-L and HA-V are reported in Figure 1 and Figure S3, respectively. An increasing signal broadening was observed with progressive addition of humic matter to the AP solution, with HA-L being more effective than HA-V. This behaviour can be explained with a greater rigidity of the enzyme, due to formation of non-covalent complexes with humic components (Bakhmutov , 2004; Smejkalova and Piccolo, 2008 b).

Spin-lattice and spin-spin relaxation times are sensitive NMR parameters to reveal changes in protein flexibility and follow perturbations of the magnetic field on a studied nucleus (Zhang and Forman-Kay, 1995; Tollinger *et al*. 2001; Sapienza and Lee, 2010). The measurement of relaxation times are useful to quantify the overall motion of proteins or parts of proteins when involved in complexes with other molecules (Pickford and Campbell, 2004). In the case of alkaline phosphatase, the changes of T_1 and T_2 relaxation times with increasing amount of humic matter, would help to confirm the formation of non-covalent complexes suggested by signal broadening in ^{1}H-NMR spectra. However, due to severe signal overlapping in proton spectra and lack of previous NMR signal assignment for this specific AP enzyme, spectrum evaluation was conducted by

associating proton intervals to numbered bucket areas. Thus, the spectrum was divided in 22 discrete regions (1-3, aromatic region; 4-15 hydroxy-alkyl region; 16-22 alkyl region) and relaxation times were calculated by integrating the whole area under each bucket (Figure 2).

A progressive decrease of both T_1 and T_2 values for the AP enzyme was observed with increasing concentration of both humic materials. At the largest concentration of both HA-L and HA-V, the AP spin-lattice T_1 relaxation times resulted 33.12% and 32.86% smaller than for control, while the spin-spin T_2 relaxation times showed an average decrease of 53.5% and 43.4%, respectively (Tables 1 and 2). In particular, at such largest humic concentration, the greatest reduction of relaxation times was observed for the buckets of the hydroxy-alkylic and alkylic regions of phosphatase included in both the 3.619-1.757 ppm region (buckets 12 to 18), and the bucket 21. For the aromatic 7.189-6.168 ppm region (buckets 1-3), a similar decrease of T_1 and T_2 for the AP enzyme was shown only for protons resonating in bucket 2 with addition of HA-V, whereas addition of HA-L produced a comparable reduction of relaxation times in bucket 3 (Tables 1 and 2). These results indicate the enzyme regions with the largest affinity to humic matter, since the larger the variation in relaxation times of AP molecular domains, the greater was the involvement of protein protons in interactions with the two HA.

The T_1 and T_2 values for the AP enzyme in solution are dependent on the protein correlation time (τ_C), that is defined as the effective average time needed for a molecule to rotate through one radian. Therefore, the larger the τ_C values, the slower is the molecular motion (Bakhmutov, 2004; Smejkalova and Piccolo, 2008 b). The correlation time for the AP enzyme increased significantly for all buckets with increasing humic concentration, except for buckets 11, 20 and 22 (Table 3, Figure 3). The addition of progressive HA-V amount to the AP enzyme determined a general increasing trend of τ_C values in all spectral buckets, whereas the enhancement of correlation time was significantly more intense in the spectral buckets obtained after AP treatment with HA-L. These findings indicate the formation of humic-phosphatase complexes, whose enhanced dimension retard its molecular mobility, as measured by τ_C, in comparison to the AP enzyme alone. Moreover,

the fact that the correlation time is increased by the most hydrophobic HA over the spectral range of measured buckets, indicates that the humic-phosphatase complexes are preferably stabilized by non-covalent dispersive binding.

Diffusion ordered NMR spectroscopy (DOSY) is a pulsed field gradient technique that enables the measurement of translational diffusion of dissolved molecules. Except for the overall molecular size and shape, the magnitude of diffusion coefficient provides direct information on molecular dynamics, including intermolecular interactions (Brand *et al*., 2005; Cohen *et al*., 2005), aggregation, and conformational changes (Viel *et al*., 2002). Moreover, DOSY processing is a particularly suitable technique for complex samples because it provides a direct correlation of translational diffusion to the chemical shift in the second dimension and hence a prior separation of mixture components is not required (Price *et al*., 2004; Cobas *et al*., 2005).

According to the Einstein-Stock diffusion theory, the larger the hydrodynamic radius of a molecule or molecular complex, the smaller are the diffusive properties. The NMR diffusion experiments conducted to measure the diffusivity of the AP with increasing concentration of humic matter showed a progressive reduction of self-diffusion values (Table 4). These results are consistent with NMR data previously discussed, thus suggesting that the formation of a humic-phosphatase complex increases the overall hydrodynamic volume of the AP enzyme, and progressively reduces its diffusive properties. The DOSY proton projections of AP alone and AP treated with the greatest amount of HA-L and HA-V are shown in Figures 4 and S4, respectively. For both humic materials, the projection of the humic-phosphatase complex resulted in smaller diffusion values than for the AP alone. Moreover, the proton projection for the complex formed between AP and HA-L (Figure 4) revealed a slower diffusion (smaller diffusion values) than for the AP/HA-V complex (Figure S4). In particular, self-diffusion values of the AP enzyme calculated from DOSY spectra decreased by more than 35% for buckets 13-15, 18 and 19, with addition of both humic acids, whereas the signals in buckets 6 and 16 were reduced by the same extent only with HA-L addition (Table 4). This is a further evidence that the interactions of the AP enzyme with

hydrophobic HA-L are of a greater extent than with more hydrophilic HA-V. The importance of weak hydrophobic binding between the AP enzyme and humic matter seems to be justified by the primary structure of the alkaline phosphatase from human placenta used here, that is reported to have a prevalent hydrophobic character due to the abundance of Alanine (10,88%), Leucine (7.95%) and Valine (6.48%) residues for each enzyme homo-monomer (Le Du *et al.*, 2001).

3.2. Modification of enzyme's activity by humic matter

While it is reported that an enzyme–ligand interaction may modify the optimal pH at which the enzyme expresses its greatest catalytic activity (Thibodeau *et al.*, 1985; Ranieri-Raggi *et al.*, 1995) the alkaline phosphatase does not seem to be affected when involved in interactions with soil organic components (Pilar *et al.*, 2003). We thus conducted our catalysis experiments with the commercial alkaline phosphatase used here at the recommended pH of 10.4.

The proton NMR spectra of the *p*-NPP substrate for the AP enzyme at different reaction times are shown in Figure 5. During the enzymatic hydrolysis, NMR signals for aromatic protons in *p*-NPP (H_{S1} and H_{S2}) progressively decreased in intensity with time, whereas those of the *p*-Nitrophenol reaction product (H_{P1} and H_{P2}) concomitantly increased (Holtz and Kantrowitz, 1999). When both HA-L and HA-V were added to the AP enzyme, the disappearance of *p*-NPP signals in NMR spectra due to dephosphorylation induced by AP, was progressively slowed down, as a function of humic concentration in solution (Figure 6). By observing the percentage of residual *p*-NPP calculated from proton spectra at 21 min after the start of the catalysis, it can be noticed that the residual substrate was progressively greater with increasing humic matter in solution (Figure 6). In particular, when the concentration of either HA-L or HA-V reached 12 mg mL^{-1} in the AP enzyme solution, *p*-NPP was still 79.9 and 59.5% of the initial substrate after 21 min, while only 44.6% was the residual *p*-NPP with AP alone.

These results are explained with the inhibition of the enzymatic activity caused the interaction of alkaline phosphatase with humic matter. In fact, we showed that humic molecules formed non-covalent complexes with this AP enzyme in solution, and, by partially or totally adsorbing to the enzyme active sites, they alter its affinity with the substrate (Perez-Mateos, 1991). It has been shown that the AP active sites contain two zinc atoms coordinated by Histidine, Serine and Aspartate residues, while Arginine and Serine residues form adducts with the substrate and stabilize the intermediate enzyme-product complex (Holtz and Kantrowitz, 1999; Kim and Harold, 1991). All these aminoacids, except Histidine, present functional groups, such us –OH for Serine, -COOH for Aspartate, and the guanidinium group for Arginine, which may bind with humic molecules through H-bonds. Furthermore, the aromatic imidazole group of Histidine could also be involved in hydrophobic π–π bonds with complementary aromatic humic molecules. It is thus likely that not only humic molecules may complex zinc ions in the AP active sites with similar acidic functional groups as those of the aminoacids, but that the hydrophobic humic domains are adsorbed on the hydrophobic aminoacidic residues of the enzyme. The result is either the partial or total obstruction of the catalytic active pocket in the enzyme, or a modification of the conformational structure of the protein. Both these effects of the presence of humic molecules in solution are responsible to reduce the catalytic efficiency of alkaline phosphatase or limit the number of AP molecules still capable to catalyze the hydrolysis of a phosphate bond.

4. CONCLUSIONS

Our NMR findings indicate that an alkaline phosphatase enzyme in aqueous solution with increasing concentrations of humic matter becomes involved in ever greater humic-enzyme complexes, which are stabilized by non-covalent interactions, such as van der Waals, H-bonds and π–π bonds. Elaboration of ^{1}H-NMR spectra for the enzyme added with progressive amount of humic matter allowed to follow the changes of relaxation (T_1, T_2) and correlation (τ_C) times as well

as self-diffusivity, which showed an increasing reduction of translational and rotational motion of the loose conformational arrangements of newly-formed humic-enzyme complexes. Most changes of the NMR conformational behaviour of the enzyme was noted with the most hydrophobic humic material.

The modification of the enzyme original conformation by the weakly adsorbed humic molecules had also an impact on the enzymatic catalysis exerted on the hydrolysis of the *p*-NPP substrate. This reaction was monitored with time through NMR spectroscopy and it was found that the reduction of substrate signal intensity was slowed down significantly when humic molecules adsorption modified the enzyme structure. Again, the inhibition of catalytic activity was more pronounced when it was the most hydrophobic humic acid to bind to the enzyme.

Our results suggest, by direct NMR evidence, that extracellular enzymes, which are reputed to play a significant role in the out-of-cell molecular transformations in the environment, may be severely reduced in their activity when interacting with the ubiquitous natural organic matter.

Acknowledgements

This work was conducted in partial fulfilment of the PhD degree in the Doctorate school "Valorizzazione delle risorse agro-forestali". P.M. is grateful to Prof. Hartmut Oschkinat and Dr. Peter Schmieder for scientific support and kind hospitality when conducting experiments at NMR Facility of the Department of Structural Biology, FMP-Institute.

Supplementary data

Supplementary figures and description of method adopted for CPMAS-NMR spectroscopy are reported in Supporting Information, which contain, in particular, ^{1}H- liquid-state and ^{13}C-NMR CPMAS spectra of the two humic acids of this study, as well as ^{1}H- and DOSY-NMR spectra of the AP enzyme treated with HA-V.

References

Baalousha M., Motelica-Heino M., Le Coustumer P. 2006.Conformation and size of humic substances: Effects of major cation concentration and type, pH, salinity, and residence time. Colloids and Surfaces A: Physicochem. Eng. Aspects 272, 48–55.

Bakhmutov, V. I., 2004. Pratical NMR Relaxation for chemists.John Wiley & sons, Ltd.,Chicester, West Sussex, England.

Brand, T., Cabrita, E. J., Berger, S., 2005. Intermolecular interaction as investigated by NOE and diffusion studies. Prog. Nucl. Mag.Reson. Spectrosc. *46*, 159–196.

Carper, W. R., Keller, C. E. 1997. Direct Determination of NMR correlation times from spin-lattice and spin-spin relaxation times. Journal of Physical Chemistry A 101, 3246-3250.

Cobas, J. C., Groves, P., Martín-Pastor, M., De Capua, A., 2005. New applications, processing methods and pulse sequences using diffusion NMR. Curr. Anal. Chem. 1, 289–305.

Cohen, Y., Avram, L., Frish, L., 2005. Diffusion NMR spectroscopy. Angew. Chem., Int. Ed. 44, 520–554.

Dick, W. A., Cheng, L., Wang, P., 2000. Soil acid and alkaline phosphatase activity as pH adjustment indicators. Soil Biology & Biochemistry 32, 1915–1919.

Eriksson, H. J. C., Somsen, G. W., Hinrichs, W. L. J., Frijlink, H. W., De Jong, G. J., 2001. Characterization of human placental alkaline phosphatase by activity and protein assays, capillary electrophoresis and matrix assisted laser desorption / ionization time-of-flight mass spectrometry. Journal of Chromatography B, 755, 311–319.

Fomba, K. W., Galvosas, P., Roland, U., Kaerger, J., Kopinke, F. D., 2011. Mobile Aliphatic Domains in Humic Substances and Their Impact on Contaminant Mobility within the Matrix. Environmental Science and Technologies 45, 5164–5169.

George, T . S., Turner, B. L., Gregory, P. J., Cade-menun, B. J., Richardson, A. E., 2006. Depletion of organic phosphorus from Oxisols in relation to phosphatase activities in the rhizosphere. European Journal of Soil Science 57, 47–57.

Holtz, K. M., Kantrowitz, E. R., 1999. The mechanism of the alkaline phosphatase reaction: insights from NMR, crystallography and site-specific mutagenesis. FEBS Letters 462, 7-11.

Iakimenko, O., Otabbong, E., Sadovnikova, L., Persson, J., Nilsson, I., Orlov, D., Ammosova, Y., 1996. Dynamic transformation of sewage sludge and farmyard manure components. 1. Content of humic substances and mineralisation of organic carbon and nitrogen in incubated soils. Agriculture, Ecosystems and Environment 58, 121-126.

Kim, E. E., Harold, W. W., 1991. Reaction mechanism of alkaline phosphatase based on crustal struictures. Journal of Molecular Biology 218, 449-464.

Le Du, M. H., Stigbrand, T., Taussigi, M. J., Ménez, A., Stura, E. A., 2001. Crystal Structure of Alkaline Phosphatase from Human Placenta at 1.8 Å Resolution. Implication for a substrate. 276 (12), 9158–9165.

Llinas, P., Stura, E. A., Ménez, A., Kiss, Z., Stigbrand, T., Millàn, J. L., Le Du, M. H. 2005. Structural Studies of Human Placental Alkaline Phosphatase in Complex with Functional Ligands. Journal of Molecular Biology 350, 441–451.

Nardi, S., Sessi, E., Pizzeghello, D., Sturaro, A., Rella, R., Parvoli, G., 2002. Biological activity of soil organic matter mobilised by root exudates. Chemosphere 46, 1075–1081.

Olander, L. P., Vitousek, P. M., 2000. Regulation of soil phosphatase and chitinase activity by N and P availability. Biogeochemistry 49, 175–190.

Perez-Mateos, M., Busto, M. D., Rad, J. C., 1991. Stability and Properties of Alkaline Phosphate Immobilized by a Rendzina Soil. Journal of the Science of Food and Agriculture 55, 229-240.

Peuravuori, J. 2005. NMR spectroscopy study of freshwater humic material in light of supramolecular assembly. Environ. Sci. Technol., 39, 5541-5549.

Piccolo, A., Celano, G., 1994. Hydrogen bonding interactions of the herbicide Glyphosate with water soluble humic substances. Environ. Toxicol. Chem. 13, 1737-1741.

Piccolo, A., 2002. The supramolecular structure of humic substances: a novel understanding of humus chemistry and implications in soil science. Advances in Agronomy 75, 57-134.

Piccolo, A., Conte, P., Cozzolino, A., Spaccini. R. 2003. in: D.K. Benbi and R. Nieder (Eds.), Handbook of processes and modelling in soil-plant system. Haworth Press, New York, 2003, pp. 83-120.

Piccolo, A., Spiteller, M., 2003. Electrospray ionization mass spectrometry of terrestrial humic substances and their size fractions. Anal. Bioanal. Chem. 377, 1047-1059.

Pickford, A. R., Campbell, I. D., 2004. NMR Studies of Modular Protein Structures and Their Interactions. Chemical Reviews 104, 3557-3565.

Pilar, M. C., Ortega, N., Perez-Mateos, M., Busto, M. D., 2003. Kinetic behaviour and stability of escherichia coli ATCC27257 alkaline phosphatase immobilised in soil humates. Journal of the Science of Food and Agriculture 83, 232–239.

Price, K. E., Lucas, L. H., Larive, C. K., 2004. Analytical applications of NMR diffusion measurements. Anal. Bioanal. Chem. *378*, 1405–1407

Quiquampoix, H., Servagent-Noinville, S., Baron, M., 2002. Enzyme adsorption on soil mineral surfaces and consequences for the catalytic activity. In: Burns RG, Dick RP (eds) Enzymes in the environment. Marcel Dekker, New York, pp 285–306.

Ranieri-Raggi, M., Ronca, F., Sabbatini A., Raggi, A., 1995. Regulation of skeletal-muscle AMP deaminase: involvement of histidine residues in the pH-dependent inhibition of the rabbit enzyme by ATP. Biochem. J. 309, 845-852.

Richardson, A. E., George, T. S., Hens, M., Simpson, R. J., 2005. Utilization of soil organic phosphorus by higher plants. In: Organic Phosphorus in the Environment (eds B.L. Turner, E. Frossard & D. Baldwin). CABI Publishing, Wallingford, pp. 165–184.

Sapienza, P. J., Lee, A. L., 2010. Using NMR to study fast dynamics in proteins: methods and Applications. Current Opinion in Pharmacology 10, 723–730.

Sarkar, J.M., Leonowicz, A., Bollag, J.M. 1989. Immobilization of enzymes on clays and soils. Soil Biol Biochem 21, 223–230.

Schimel, J.P. , Bennett , J. , 2004. Nitrogen mineralization: challenges of a changing paradigm. Ecology 85, 591–602.

Sinsabaugh, R.L., Moorhead, D.L., 1994. Resource allocation to extracellular enzyme production: a model for nitrogen and phosphorus control of litter decomposition. Soil Biol Biochem 26, 1305–1311.

Smejkalova, D., Piccolo, A., 2008 a. Aggregation and disaggregation of humic supramolecular assemblies by NMR diffusion ordered spectroscopy (DOSY-NMR). Environmental Science and Technologies 42, 699–706.

Smejkalova, D., Piccolo, A., 2008 b. Host-Guest Interactions between 2,4-Dichlorophenol and Humic Substances As Evaluated by ^{1}H NMR Relaxation and Diffusion Ordered Spectroscopy. Environmental Science and Technologies 42, 8440–8445.

Stevenson, F.J., 1994. Humus chemistry, 2nd edn. Wiley, New York.

Tan, W. F., Norde, W., Koopal, L. K., 2011. Humic substance charge determination by titration with a flexible cationic polyelectrolyte. Geochimica et Cosmochimica Acta 75, 5749–5761.

Tarafdar, J. C., Claassen, N., 1988. Organic phosphorus compounds as a phosphorus source for higher plants through the activity of phosphatases produced by plant roots and microorganisms. Biology and Fertility of Soils 5 (4), 308-312.

Tietjen, T., Wetzel, R. G., 2003. Extracellular enzyme-clay mineral complexes: Enzyme adsorption, alteration of enzyme activity, and protection from photodegradation. Aquatic Ecology 37, 331–339.

Thibodeau, E. A., Bowen, W. H., Marquis, R. E, 1985. pH-Dependent Fluoride Inhibition of Peroxidase Activity. J Dent Res 64 (10), 1211-1213.

Tollinger, M., Skrynnikov, N. R., Mulder, F. A. A., Forman-Kay, J. D., Kay, L. E., 2001. Slow Dynamics in Folded and Unfolded States of an SH3 Domain. Journal of American Chemistry Society 123, 11341-11352.

Tomaszewski, J. E., Schwarzenbach, R. P., Sander, M., 2011. Protein Encapsulation by Humic Substances. Environmental Science and Technologies 45, 6003–6010.

Viel, S, Mannina, L., Segre, A. 2002. Detection of a π-π complex by diffusion-order spectroscopy (DOSY). Tetrahedron Lett. *43*, 2515–2519.

Zhang, O., Forman-Kay, J. D. 1995. Structural Characterization of Folded and Unfolded States of an SH3 Domain in Equilibrium in Aqueous Buffer. Biochemistry 34, 6784-6794.

Zhang, Y. , Du, J., Zhang, F., Yu, Y., Zhang, J., 2011. Chemical characterization of humic substances isolated from mangrove swamp sediments: The Qinglan area of Hainan Island, China. Estuarine, Coastal and Shelf Science 93, 220-227.

Table 1. ^{1}H spin-lattice relaxation times T_1 (s) and standard deviations (%) of enzyme Alkaline Phosphatase as a function of HA-L and HA-V concentration (mg mL^{-1}).

Bucket Number	No HA	HA-L				HA-V			
		0.5	1	2	6	0.5	1	2	6
1	1,033 (0,003)	0,83 (0,052)	ND -	0,604 (0,053)	0,583 (0,059)	1,025 (0,038)	0,845 (0,05)	0,837 (0,033)	0,786 (0,035)
2	1,05 (0,014)	0,751 (0,061)	0,74 0,037)	0,649 (0,051)	0,615 (0,049)	1,046 (0,037)	0,925 (0,049)	0,751 (0,066)	0,718 (0,025)
3	1,037 (0,01)	0,739 (0,045)	ND -	0,454 (0,044)	0,468 (0,042)	0,892 (0,055)	0,786 (0,069)	0,727 (0,067)	0,683 (0,025)
4	1,383 (0,02)	1,171 (0,037)	0,802 (0,028)	0,55 (0,017)	0,449 (0,006)	1,349 (0,042)	1,201 (6,236)	1,114 (0,021)	1,006 (0,011)
5	1,249 (0,022)	1,037 (0,006)	0,848 (0,042)	0,796 (0,015)	0,759 0,024)	1,196 0,021)	1,167 0,023)	0,992 0,029)	0,936 0,018)
6	1,213 (0,009)	1,088 (0,014)	0,92 (0,024)	0,831 (0,027)	0,781 (0,026)	1,12 (0,018)	0,975 (0,034)	0,869 (0,013)	0,814 (0,013)
7	1,153 (0,006)	1,056 (0,018)	0,896 (0,006)	0,823 (0,022)	0,768 (0,005)	1,095 (0,037)	0,957 (0,03)	0,917 (0,014)	0,881 (0,013)
8	1,109 (0,006)	1,024 (0,019)	0,903 (0,019)	0,743 (0,024)	0,705 (0,045)	1,054 (0,067)	0,963 (0,011)	0,871 (0,021)	0,803 (0,017)
9	1,156 (0,011)	1,136 (0,02)	0,983 (0,004)	0,821 (0,027)	0,796 (0,009)	1,099 (0,028)	1,03 (0,028)	0,953 (0,025)	0,891 (0,011)
10	1,248 (0,027)	1,197 (0,028)	1,037 (0,017)	0,823 (0,054)	0,816 (0,007)	1,159 (0,018)	1,084 (0,03)	0,925 (0,021)	0,819 (0,011)
11	1,192 (0)	1,082 (0,03)	0,951 (0,027)	0,827 (0,026)	0,785 0,014)	1,132 0,066)	1,049 0,019)	0,863 0,015)	0,782 0,016)
12	1,411 (0,013)	1,258 (0,036)	1,139 (0,031)	0,872 (0,035)	0,683 (0,029)	1,293 (0,03)	1,202 (0,027)	0,974 (0,028)	0,812 (0,016)
13	0,874 (0,018)	0,739 (0,016)	0,612 (0,014)	0,502 (0,013)	0,475 (0,023)	0,826 (0,038)	0,703 (0,037)	0,488 (0,018)	0,426 (0,031)
14	0,863 (0,012)	0,727 (0,027)	0,641 (0,011)	0,539 (0,014)	0,477 (0,017)	0,815 (0,049)	0,741 (0,017)	0,594 (0,018)	0,408 (0,007)
15	0,927 (0,008)	0,823 (0,009)	0,696 (0,01)	0,612 (0,029)	0,545 (0,008)	0,883 (0,024)	0,792 (0,004)	0,58 (0,013)	0,464 (0,012)
16	0,834 (0,024)	0,792 (0,011)	0,686 (0,024)	0,583 (0,006)	0,507 (0,02)	0,835 (0,022)	0,777 (0,022)	0,66 (0,01)	0,54 (0,006)
17	1,106 (0,007)	1,048 (0,004)	0,869 (0,018)	0,743 (0,027)	0,613 (0,02)	1,013 (0,051)	0,975 (0,03)	0,716 (0,017)	0,608 (0,012)
18	0,849 (0,028)	0,763 (0,007)	0,637 (0,02)	0,534 (0,024)	0,447 (0,019)	0,787 (0,016)	0,751 (0,004)	0,534 (0,014)	0,441 (0,005)
19	0,809 (0,023)	0,777 (0,064)	0,649 (0,016)	0,602 (0,027)	0,593 (0,026)	0,749 (0,015)	0,723 (0,022)	0,605 (0,026)	0,523 (0,005)
20	0,793 (0,018)	0,752 (0,051)	0,637 (0,016)	0,598 (0,036)	0,527 (0,016)	0,727 (0,022)	0,706 (0,024)	0,515 (0,019)	0,435 (0,009)
21	0,819 (0,004)	0,764 (0,014)	0,679 (0,003)	0,549 (0,024)	0,526 (0,018)	0,749 (0,017)	0,733 (0,017)	0,521 (0,011)	0,343 (0,007)
22	0,788 (0,01)	0,743 (0,019)	0,65 (0,042)	0,568 (0,038)	0,546 (0,016)	0,73 (0,003)	0,711 (0,029)	0,618 (0,011)	0,577 (0,008)

ND: Not determined.

Table 2. ^{1}H spin-spin relaxation times T_1 (s) and standard deviations (%) of enzyme Alkaline Phosphatase as a function of HA-L and HA-V concentration (mg mL^{-1}).

Bucket Number	No HA	HA-L				HA-V			
		0.5	1	2	6	0.5	1	2	6
1	179,2	118,8	69,8	46,2	43	169	138,6	131,6	123
	(4,5)	(3,1)	(1)	(1,1)	(1)	(2,8)	(4,8)	(3,5)	(7)
2	41,6	26,1	23,6	21,4	19	39,3	32,2	26,7	25
	(0,6)	(1,3)	(0,8)	(1)	(0,7)	(2,1)	(2,3)	(2)	(1,5)
3	52,2	35,9	27,7	19,8	18,9	45,3	39,2	36,7	32,1
	(3,1)	(1,8)	(1,3)	(0,4)	(0,7)	(1,6)	(2,3)	(0,7)	(1,7)
4	32,6	26	16,5	10,8	8,3	31	27,7	25,5	22,5
	(2,3)	(0,4)	(1)	(0,5)	(0,1)	(0,3)	(0,7)	(0,5)	(0,4)
5	34,4	25	17,5	16,9	15,4	32,1	30,8	26,4	24,5
	(1,7)	(0,3)	(0,3)	(0,3)	(0,1)	(0,4)	(0,3)	(0,7)	(0,3)
6	47,8	34,5	29,5	27,8	26	43	36,1	31,1	27,8
	(0,7)	(0,8)	(0,6)	(0,8)	(0,4)	(0,4)	(0,4)	(0,5)	(0,4)
7	33,7	26,2	21,1	20,2	19,1	31,2	27,6	25,9	24,8
	(0,7)	(0,3)	(0,2)	(0,2)	(0,7)	(0,2)	(0,7)	(0,1)	(0,5)
8	47,8	39,6	30,7	25,6	23,9	44,3	39,8	36,1	32,8
	(0,4)	(0,7)	(0,6)	(0,2)	(0,4)	(0,3)	(0,4)	(0,2)	(0,1)
9	54,4	47,5	45	36	32,8	51,3	47,9	43,3	39,1
	(0,5)	(0,9)	(1,1)	(0,6)	(0,4)	(1,1)	(0,6)	(0,4)	(0,3)
10	47,9	42,2	39,4	28,2	24,4	44,3	40	33,5	29,9
	(1)	(0,4)	(0,4)	(0,8)	(0,4)	(0,7)	(0,1)	(2)	(0,5)
11	58,5	50,3	46	39,9	35,2	54,4	49,3	39	34,1
	(0,5)	(1)	(1,1)	(0,4)	(0,5)	(0,4)	(1,3)	(0,4)	(0,4)
12	55,1	46	36,7	25,8	19,4	48,7	43,7	33,7	27
	(0,6)	(1,3)	(0,7)	(0,4)	(0,5)	(0,8)	(0,8)	(0,6)	(0,4)
13	40,6	31,8	24,8	15,3	13,6	37,4	30,2	19,7	16,1
	(0,1)	(0,4)	(0,7)	(0,6)	(0,5)	(0,4)	(0,9)	(0,3)	(0,6)
14	48,5	39,7	34,3	24,4	19	44	38,3	29,9	19,4
	(0,5)	(0,9)	(0,4)	(0,6)	(0,6)	(0,2)	(1,2)	(0,3)	(0,3)
15	36,3	29,8	23,7	19,4	15,8	33,2	28	21,8	15,1
	(0,3)	(0,9)	(0,3)	(0,5)	(0,6)	(0,7)	(0,7)	(0,4)	(0,3)
16	50,9	41,5	33,4	26,1	20,4	48	42,6	33,8	26,4
	(0,3)	(0,4	(0,3)	(1)	(0,5)	(1,3)	(0,7)	(0,2)	(0,1)
17	61,5	54,9	43,2	33,6	25,6	54,3	50,2	32,7	26,9
	(0,3)	(0,6)	(0,2)	(0,7)	(0,6)	(0,2)	(1,3)	(0,2)	(0,5)
18	28	23,1	17,5	14,3	12	25,4	23,6	17,2	13,7
	(0,6)	(0,4)	(0,2)	(0,3)	(0,8)	(0,4)	(0,7)	(0,5)	(0,2)
19	34,5	29,5	23,6	19,4	17,2	29	26,2	21,8	17,5
	(0,2)	(0,7)	(0,3)	(0,4)	(0,5)	(0,7)	(0,4)	(0,4)	(0,3)
20	37,6	32,2	29,9	29,8	26	35,8	32,6	26,6	25,1
	(0,6)	(0,9)	(0,6)	(0,5)	(0,7)	(0,6)	(0,8)	(0,1)	(0,3)
21	55	51,8	43,4	33,3	28,8	36,2	33,6	20,8	12,1
	(0,7)	(0,4)	(0,5)	(0,6)	(1)	(1,2)	(0,9)	(0,3)	(0,2)
22	47,4	43,4	37,8	33,4	32,1	41,9	39,8	35,7	31,6
	(0,5)	(0,4)	(0,8)	(0,2)	(0,2)	(0,3)	(0,4)	(0,6)	(0,3)

ND: Not determined.

Table 3. ^{1}H correlation times τ_C (ns) of enzyme Alkaline Phosphatase as a function of HA-L and HA-V concentrations (mg mL^{-1}) and the variations (%) of AP/HA correlation times than AP alone.

Bucket Number	No HA	HA-L				HA-V			
		0.5	1	2	6	0.5	1	2	6
1	0,62	0,71	ND	1,01	1,03	0,65	0,65	0,67	0,67
		(14,1)	-	(61,9)	(65)	(3,7)	(4,1)	(7,2)	(7,5)
2	1,55	1,62	1,68	1,66	1,7	1,58	1,62	1,61	1,62
		(4,5)	(7,8)	(6,6)	(9,2)	(1,8)	(4,5)	(3,7)	(4,4)
3	1,44	1,46	ND	1,51	1,54	1,44	1,45	1,44	1,47
		(1)	-	(4,4)	(7)	(-0,3)	(0,2)	(-0,1)	(2)
4	1,89	1,94	2,01	2,05	2,11	1,91	1,91	1,92	1,94
		(2,6)	(6,3)	(8,3)	(11,7)	(1,1)	(0,9)	(1,2)	(2,3)
5	1,77	1,87	2,01	1,98	2,02	1,79	1,81	1,8	1,81
		(5,6)	(13,1)	(11,7)	(14)	(1)	(1,7)	(1,3)	(2,1)
6	1,56	1,68	1,67	1,65	1,65	1,57	1,59	1,61	1,63
		(7,9)	(7,5)	(5,9)	(6)	(0,9)	(2,1)	(3,4)	(5,1)
7	1,73	1,85	1,89	1,86	1,85	1,75	1,74	1,76	1,76
		(6,9)	(9,3)	(7,4)	(6,7)	(1)	(0,5)	(1,3)	(1,5)
8	1,51	1,56	1,64	1,63	1,64	1,52	1,53	1,53	1,54
		(3,5)	(8,3)	(7,7)	(8,5)	(0,8)	(1,3)	(1,2)	(1,7)
9	1,47	1,53	1,48	1,5	1,53	1,47	1,48	1,49	1,5
		(3,7)	(0,9)	(2,2)	(4,2)	(0,2)	(0,4)	(1,1)	(2,1)
10	1,57	1,62	1,57	1,63	1,72	1,57	1,59	1,6	1,6
		(3)	(0,4)	(4,1)	(9,5)	(0,2)	(1,4)	(2)	(1,8)
11	1,45	1,48	1,46	1,46	1,49	1,46	1,47	1,49	1,51
		(1,6)	(0,4)	(0,5)	(2,7)	(0,6)	(1,3)	(2,4)	(3,6)
12	1,56	1,6	1,67	1,72	1,75	1,58	1,6	1,63	1,65
		(2,3)	(7)	(10,5)	(12,4)	(1,2)	(2,5)	(4,3)	(5,8)
13	1,48	1,51	1,54	1,71	1,75	1,49	1,51	1,54	1,58
		(2,3)	(4,3)	(15,5)	(18,4)	(0,8)	(2,4)	(4,5)	(6,8)
14	1,2	1,21	1,23	1,33	1,36	1,22	1,25	1,27	1,3
		(1,6)	(2,8)	(11,3)	(13,5)	(2,2)	(4,6)	(6,1)	(9,1)
15	1,56	1,6	1,64	1,68	1,74	1,58	1,61	1,58	1,66
		(2,7)	(4,9)	(7,8)	(11,3)	(1,3)	(3,5)	(1,4)	(6,6)
16	1,14	1,24	1,29	1,34	1,36	1,18	1,21	1,26	1,29
		(8,8)	(13)	(17,2)	(19,1)	(3,4)	(6,2)	(10,2)	(12,8)
17	1,2	1,24	1,28	1,33	1,36	1,23	1,25	1,33	1,34
		(3,4)	(6,2)	(10,8)	(13)	(2,1)	(4,4)	(10,4)	(11,6)
18	1,65	1,71	1,77	1,8	1,79	1,67	1,69	1,67	1,69
		(3,2)	(7,2)	(8,5)	(8,5)	(0,9)	(1,9)	(1)	(2,4)
19	1,52	1,57	1,6	1,67	1,74	1,56	1,6	1,6	1,65
		(3,8)	(5,4)	(10,2)	(14,6)	(3,2)	(5,5)	(5,6)	(8,6)
20	1,47	1,51	1,47	1,45	1,45	1,45	1,48	1,43	1,39
		(3,2)	(0,3)	(-1,4)	(-1,1)	(-1,1)	(0,9)	(-2,4)	(-5,3)
21	1,34	1,08	1,11	1,14	1,21	1,46	1,48	1,55	1,62
		(-0,5)	(2,7)	(5,8)	(12,1)	(9)	(10,8)	(15,7)	(20,7)
22	1,15	1,39	1,39	1,38	1,38	1,18	1,2	1,18	1,21
		(0,8)	(0,9)	(0,6)	(0,6)	(2,6)	(4,1)	(2,4)	(5,4)

ND: Not determined.

Table 4. ^{1}H Diffusion values (10^{-10} m^2 s^{-1}) and standard deviations (%) of Alkaline Phosphatase as a function of HA-V and HA-L (mg mL^{-1}) concentrations.

Bucket Number	No HA	HA-L				HA-V			
		0.5	1	2	6	0.5	1	2	6
2	1,179 (0,003)	0,91 (0,002)	0,823 (0,007)	1,032 (0,018)	0,754 (0,018)	0,922 (0,002)	ND -	0,803 (0,011)	0,758 (0,019)
3	ND -	0,948 (0,016)	0,948 (0,01)	0,868 (0,018)	0,741 (0,016)	0,937 (0,011)	0,809 (0,015)	0,819 (0,005)	0,791 (0,01)
4	1,157 (0,016)	0,968 (0,009)	0,992 (0,015)	0,901 (0,016)	0,776 (0,017)	0,952 (0,007)	0,851 (0,011)	0,808 (0,004)	0,763 (0,017)
5	1,088 (0,007)	0,905 (0,016)	0,905 (0,02)	0,827 (0,025)	0,719 (0,012)	0,871 (0,011)	0,785 (0,011)	0,718 (0,005)	0,693 (0,011)
6	0,888 (0,006)	0,836 (0,012)	0,842 (0,007)	0,779 (0,028)	0,761 (0,009)	0,816 (0,01)	0,792 (0,016)	0,647 (0,015)	0,623 (0,011)
7	1,108 (0,007)	1,049 (0,008)	0,954 (0,032)	0,846 (0,021)	0,747 (0,008)	0,95 (0,013)	0,811 (0,013)	0,823 (0,021)	0,843 (0,011)
8	1,127 (0,01)	1,014 (0,018)	0,837 (0,02)	0,726 (0,005)	0,637 (0,021)	0,847 (0,019)	0,701 (0,012)	0,748 (0,016)	0,785 (0,02)
9	1,105 (0,011)	0,974 (0,022)	0,936 (0,028)	0,81 (0,02)	0,664 (0,022)	0,91 (0,012)	0,787 (0,022)	0,782 (0,014)	0,749 (0,022)
10	1,074 (0,031)	0,89 (0,018)	0,766 (0,033)	0,635 (0,021)	0,455 (0,019)	0,785 (0,025)	0,59 (0,015)	0,708 (0,015)	0,746 (0,019)
11	0,839 (0,01)	0,832 (0,024)	0,613 (0,016)	0,741 (0,023)	0,633 (0,019)	0,721 (0,011)	0,656 (0,018)	0,657 (0,012)	0,622 (0,015)
12	0,8 (0,027)	0,74 (0,013)	0,726 (0,009)	0,69 (0,021)	0,672 (0,012)	0,737 (0,013)	0,721 (0,014)	0,585 (0,02)	0,603 (0,031)
13	0,768 (0,018)	0,734 (0,005)	0,735 (0,022)	0,683 (0,017)	0,667 (0,019)	0,728 (0,01)	0,715 (0,015)	0,577 (0,008)	0,602 (0,036)
14	0,799 (0,018)	0,764 (0,012)	0,774 (0,022)	0,724 (0,045)	0,696 (0,028)	0,768 (0,009)	0,742 (0,015)	0,616 (0,021)	0,643 (0,031)
15	0,839 (0,017)	0,787 (0,01)	0,814 (0,019)	0,741 (0,022)	0,675 (0,021)	0,791 (0,017)	0,746 (0,007)	0,64 (0,012)	0,7 (0,017)
16	0,864 (0,013)	0,793 (0,026)	0,82 (0,01)	0,713 (0,012)	0,621 (0,003)	0,785 (0,008)	0,715 (0,009)	0,647 (0,011)	ND -
17	0,908 (0,02)	ND -	0,906 (0,036)	0,767 (0,046)	0,627 (0,02)	0,836 (0,001)	ND -	0,693 (0,017)	ND -

ND: Not determined.

Table 5. Residual amount of *p*-NPP (%) and standard deviation (%) resulting from AP hydrolysis (25 °C, pH 10.4) at increasing HA-V and HA-L concentrations (mg mL^{-1}) as a function of the elapsed reaction time (minutes).

Bucket Number	No HA	HA-L			HA-V		
		6	8	12	6	8	12
7	68,7	76,5	78,2	84,2	72,9	75,6	80,9
	(0,1)	(0,3)	(0,3)	(1,2)	(0,1)	(0,2)	(0,4)
8	65	72,8	77,8	82,6	66,8	70,1	77,6
	(0,4)	(0,3)	(0,2)	(0,5)	(0,3)	(0,1)	(0,2)
10	58,5	69,5	75,3	81,8	62,7	64,3	74,3
	(0,1)	(1,7)	(0,1)	(1)	(0,1)	(0,2)	(1,3)
15	53,2	61,5	72,2	80,3	54	58,6	66,7
	(0,3)	(1)	(0,3)	(1)	(0,2)	(0,2)	(0,4)
21	44,6	54,7	69,5	79,5	46,9	51,7	59,9
	(0,2)	(0,3)	(0,3)	(0,9)	(0,1)	(0,2)	(0,3)
27	39	48,9	66,7	77,6	40,9	45,3	53,6
	(0,3)	(1,3)	(0,4)	(0,8)	(0,8)	(0,4)	(1)
29	33	44,7	65,6	73,1	36,6	40,8	48,4
	(0,2)	(0,6)	(0,3)	(0,8)	(0,2)	(0,2)	(0,4)
40	24,7	38	60,8	70,8	28,4	29,4	39,3
	(0,3)	(0,1)	(0,3)	(0,7)	(0,4)	(0,1)	(0,2)
52	20,1	31,8	56,6	68,1	21,1	23,9	32,6
	(0,3)	(0,9)	(0,6)	(0,9)	(0,3)	(0,2)	(0,5)
64	13,4	28,9	53,6	65,9	16	18,5	26,1
	(0,1)	(0,8)	(0,2)	(0,6)	(0,2)	(0,1)	(0,2)
86	9,9	24,9	48,1	62,2	9,8	12,3	18,5
	(0,2)	(0,3)	(0,5)	(0,7)	(0,2)	(0,2)	(0,2)
108	5,3	21,8	43,9	59,1	6,7	9,6	14,1
	(0,1)	(0,2)	(0,3)	(0,8)	(0,1)	(0,2)	(0,2)
140	2,1	18,1	39,5	55,1	4,3	6,4	10,8
	(0)	(0,3)	(0,4)	(0,8)	(0,1)	(0,1)	(0,2)
172	1,1	15,8	35,7	52	3,6	5,3	8,4
	0	(0,2)	(0,4)	(1,1)	(0,1)	(0,1)	(0,2)
204	0	14,9	31,7	48,8	3	5	6,7
	0	(0,3)	(0,4)	(0,8)	(0,1)	(0,1)	(0,1)
236	0	13,4	29,5	46,1	2,4	4,6	5,6
	0	(0,1)	(0,5)	(0,9)	(0,1)	(0,2)	(0,2)
256	0	12,5	28,1	44,7	2	4,3	4,8
	0	(0,2)	(0,4)	(0,7)	(0,1)	(0,2)	(0,1)

Figures

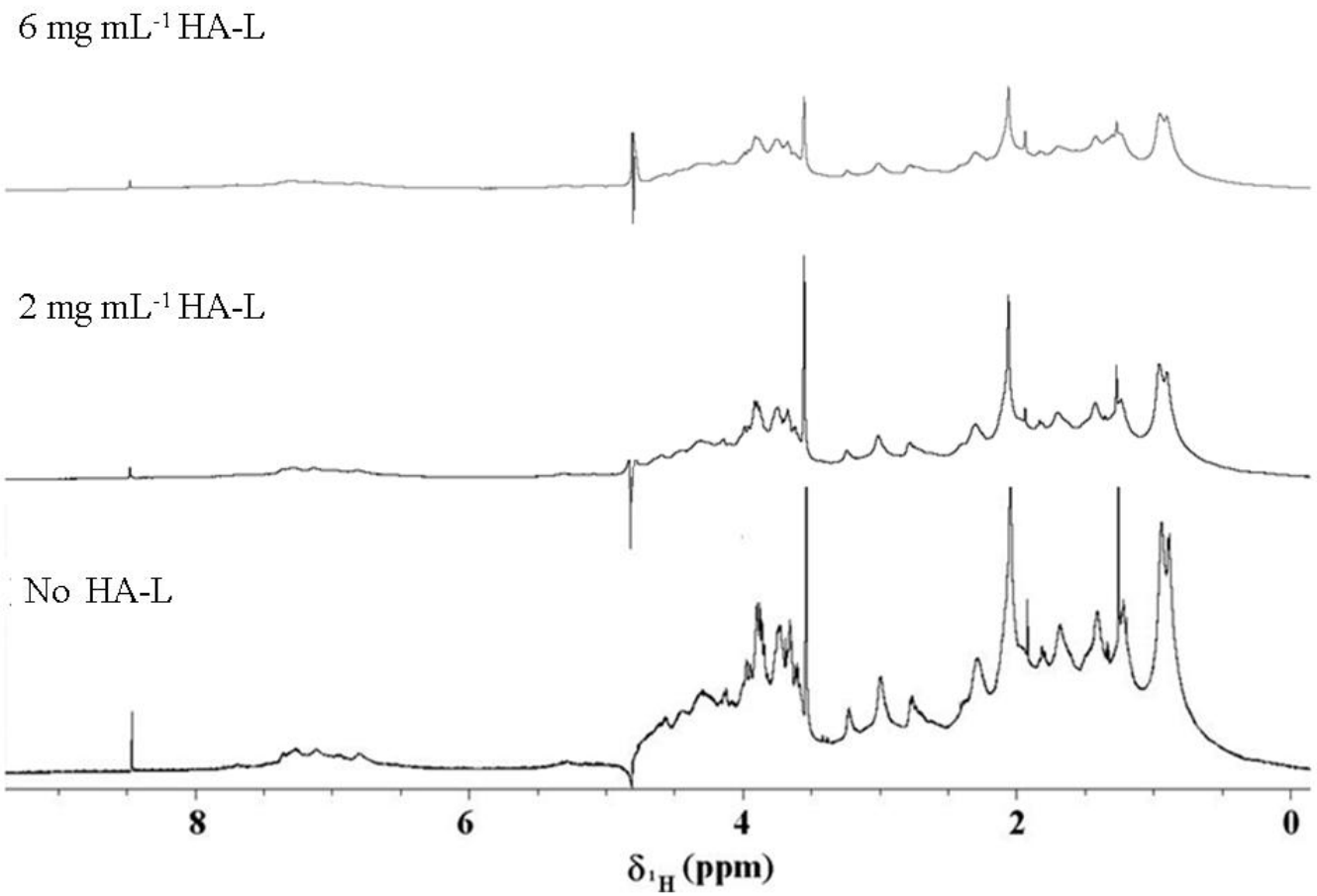

Figure 1. ^{1}H spectra of the AP enzyme solution at pH 10.4 with increasing HA-L concentrations.

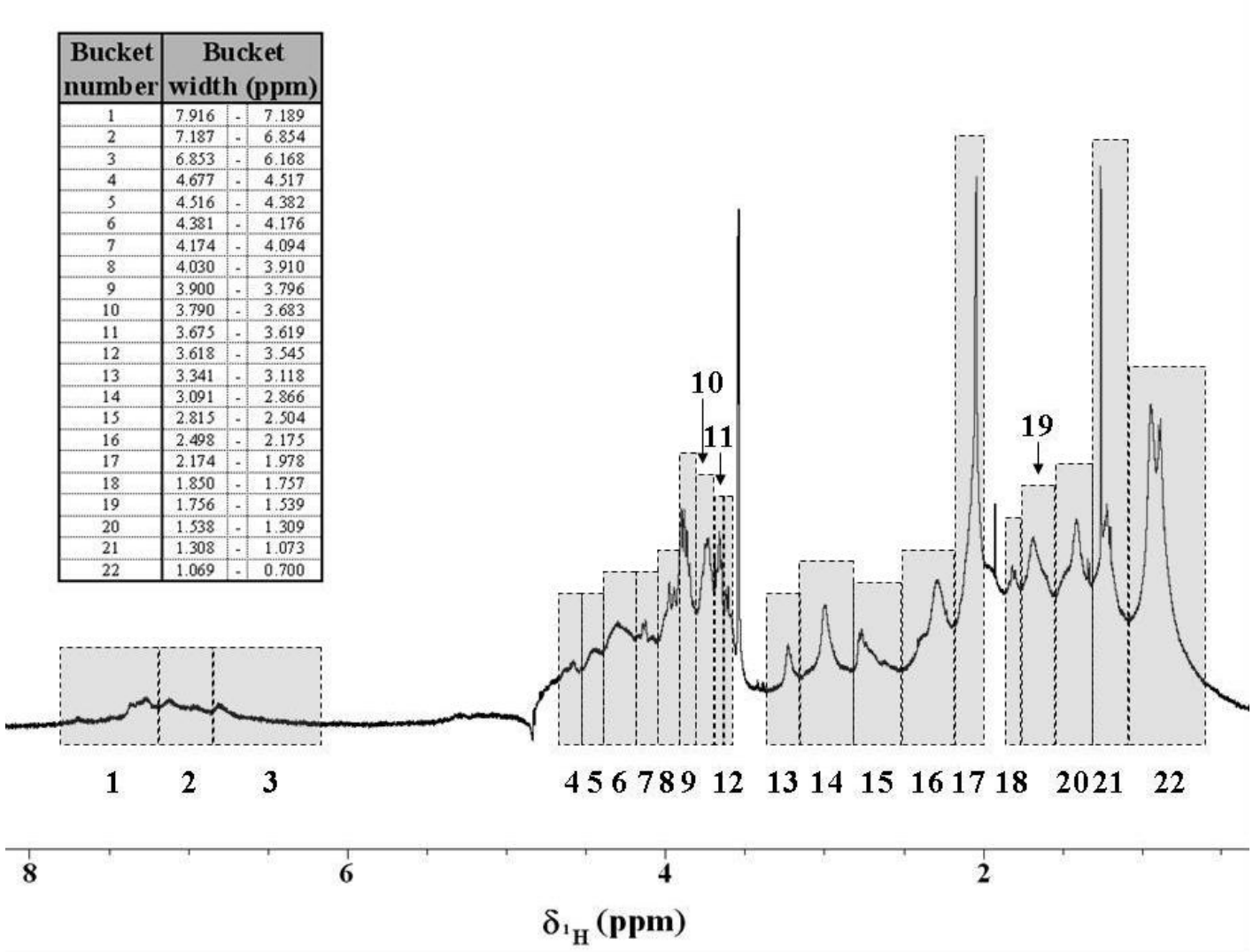

Figure 2. Bucket partition for the ^{1}H spectrum of alkaline phosphatase. On the left hand-side of figure, the bucket number and its region limit (ppm) are highlighted.

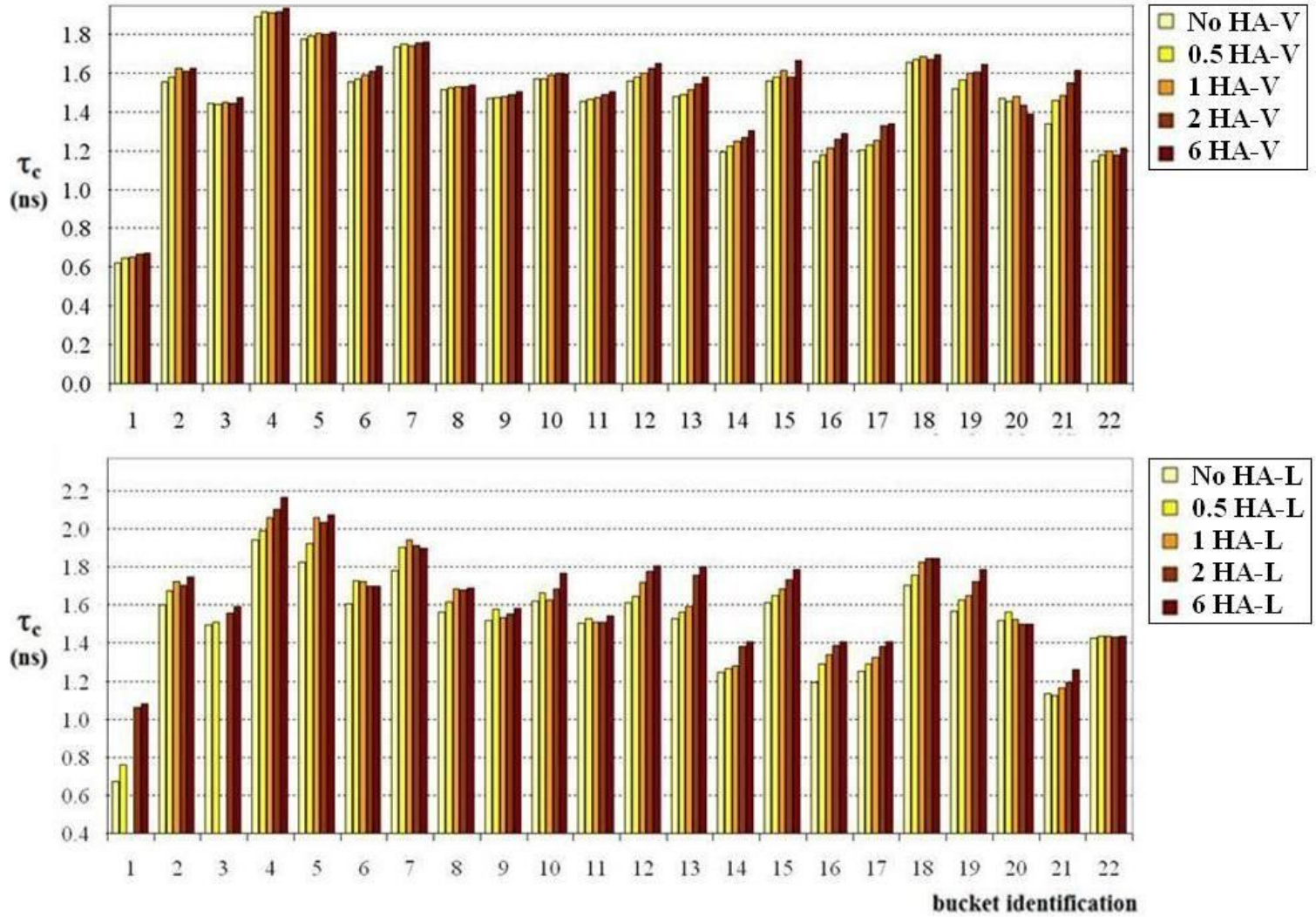

Figure 3. The ^{1}H correlation times (ns) for selected spectral bucket number, as a function of increasing concentration (0, 0.5, 1, 2 and 6 mg mL^{-1}) of HA in the AP solution.

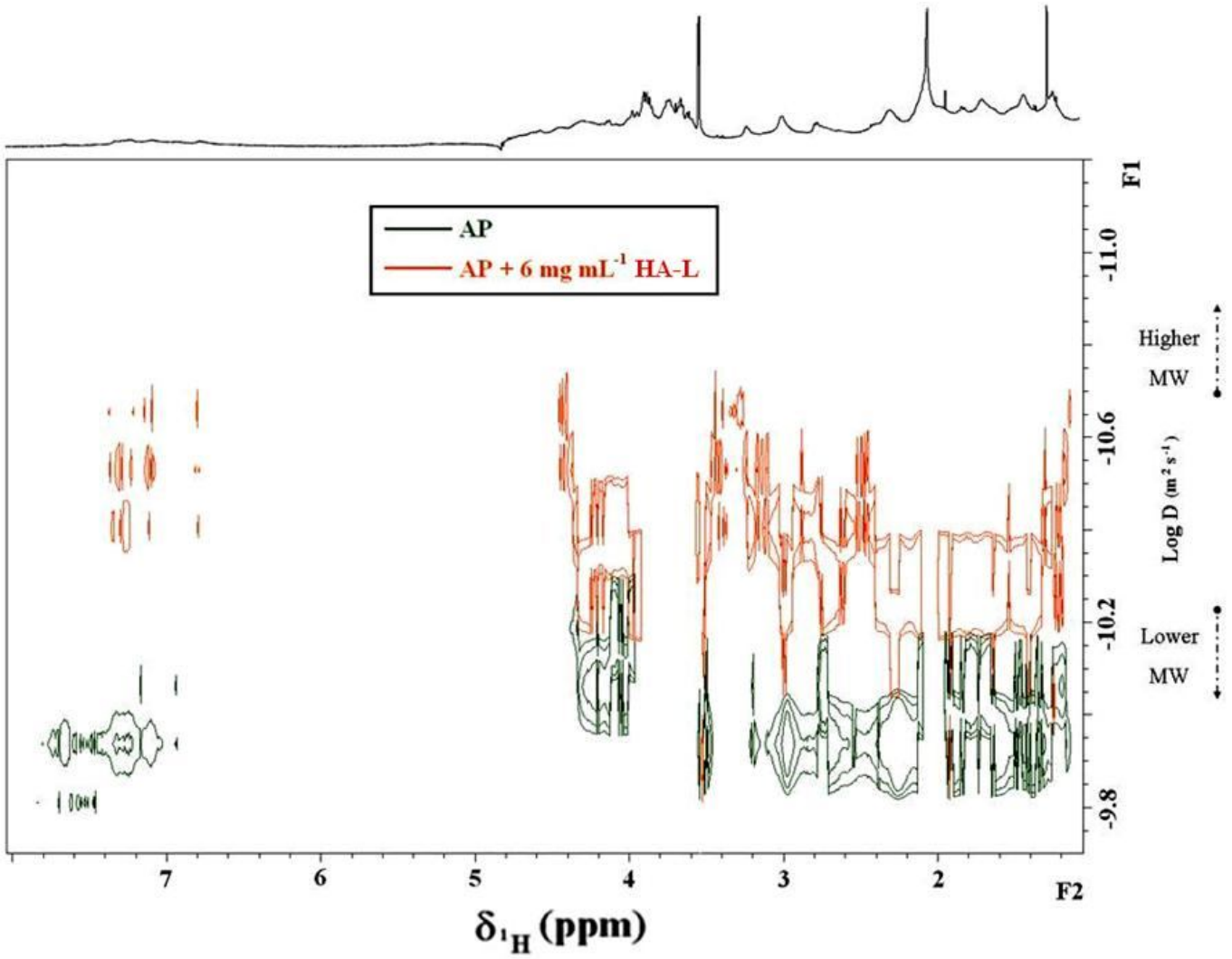

Figure 4. Proton projections of ^{1}H DOSY spectra of an alkaline phosphatase solution without and with 6 mg mL^{-1} of HA-L.

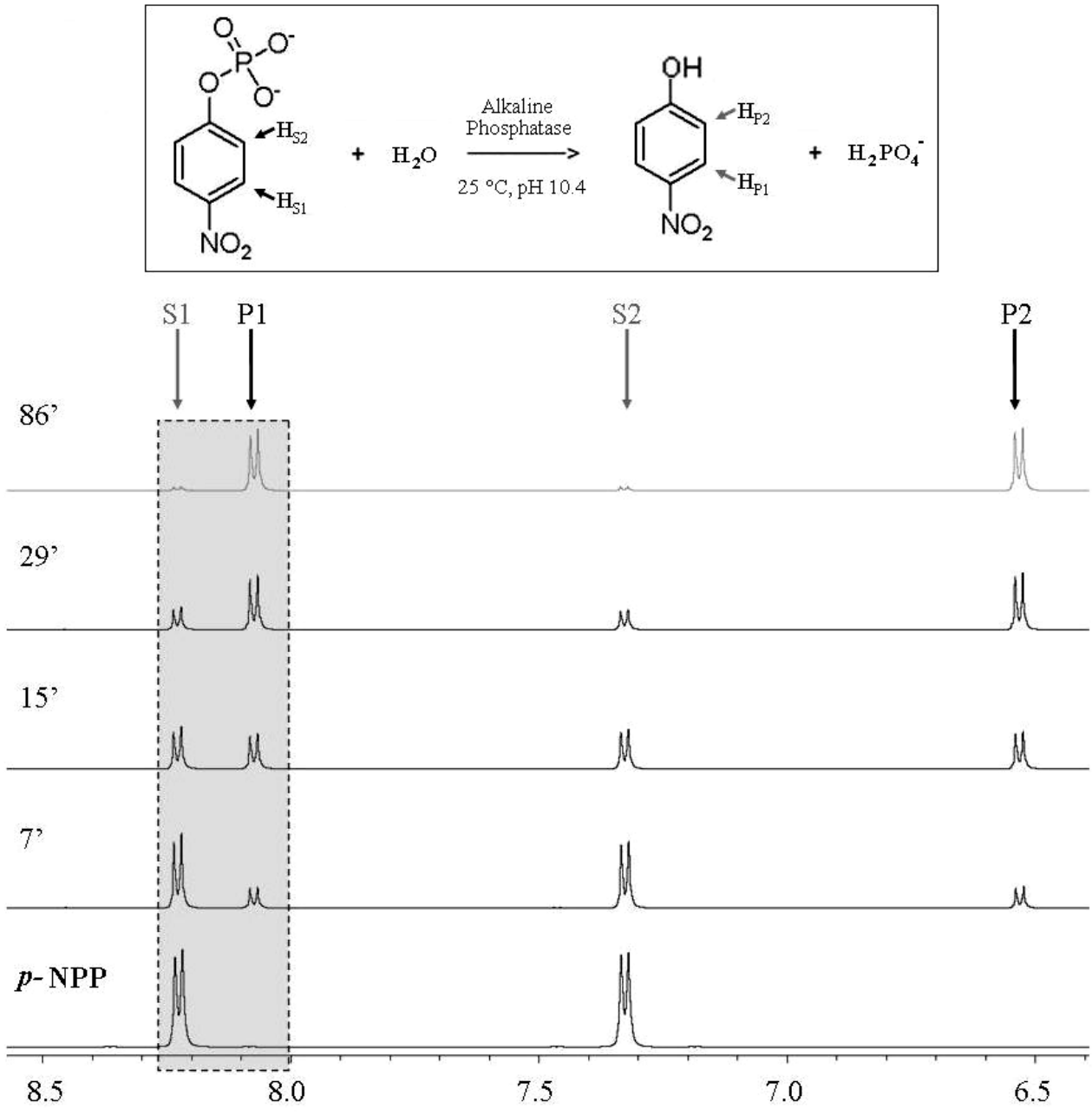

Figure 5. Aromatic region of ^{1}H spectra of *p*-NPP (S) alone and subjected to hydrolysis by the AP enzyme as a function of reaction time (7, 15, 29 and 86 min).

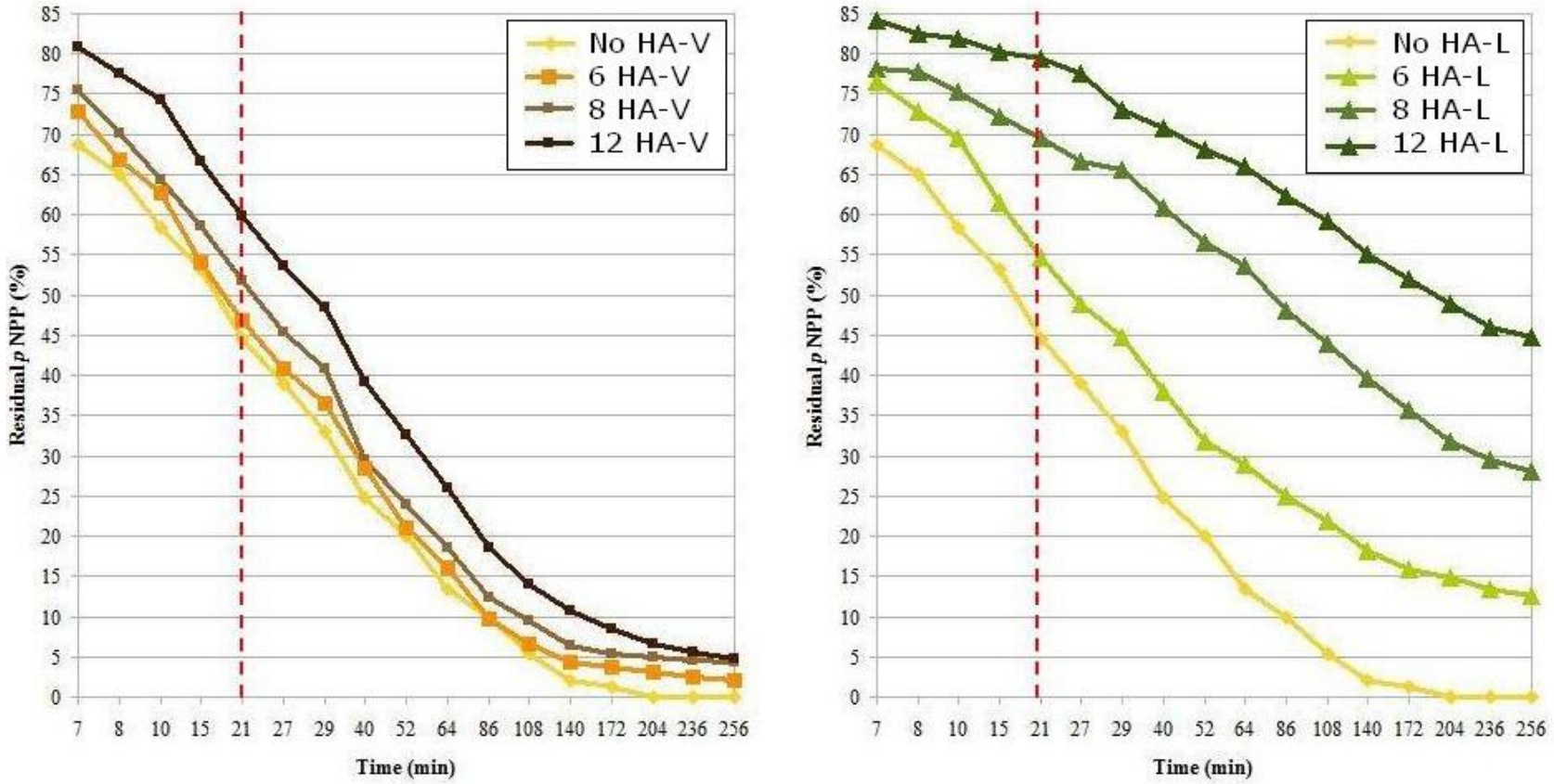

Figure 6. Residual *p*-NPP amount (%) as a function of both time (min) after the onset of the catalysis by alkaline phosphatase and HA concentration (mg mL^{-1}). The red dotted line highlights the extent of substrate hydrolysis after 21 min from the start of the catalysis.

NMR applications to study the interactions between humic acids and Alkaline Phosphatase and related effects on enzymatic activity

Pierluigi Mazzei, Hartmut Oschkinat & Alessandro Piccolo*

SUPPORTING INFORMATION

Pages: 5

SUPPORTING MATERIALS AND METHODS

CPMAS ^{13}C-NMR spectroscopy. Cross polarization magic angle spinning (CPMAS) ^{13}C-NMR spectra of humic materials were acquired with a Bruker AVANCE™ 300, equipped with a 4 mm Wide Bore MAS probe operating at a ^{13}C resonating frequency of 75.475 MHz. Samples (100-200 mg) were packed in 4 mm zirconia rotors with Kel-F caps and spun at 13±1 kHz. A ^{1}H ramp sequence was used during a contact time of 1 ms to account for possible inhomogeneity of the Hartmann-Hahn condition. 2000 scans with 3782 data points were collected over an acquisition time of 25 ms, and a recycle delay of 2 s. The Bruker Topspin 1.3 software was used to acquire and elaborate the spectra. All the free induction decays (FID) were transformed by applying a 4 k zero filling and a line broadening of 15 Hz.

SUPPORTING FIGURES

Four Figures

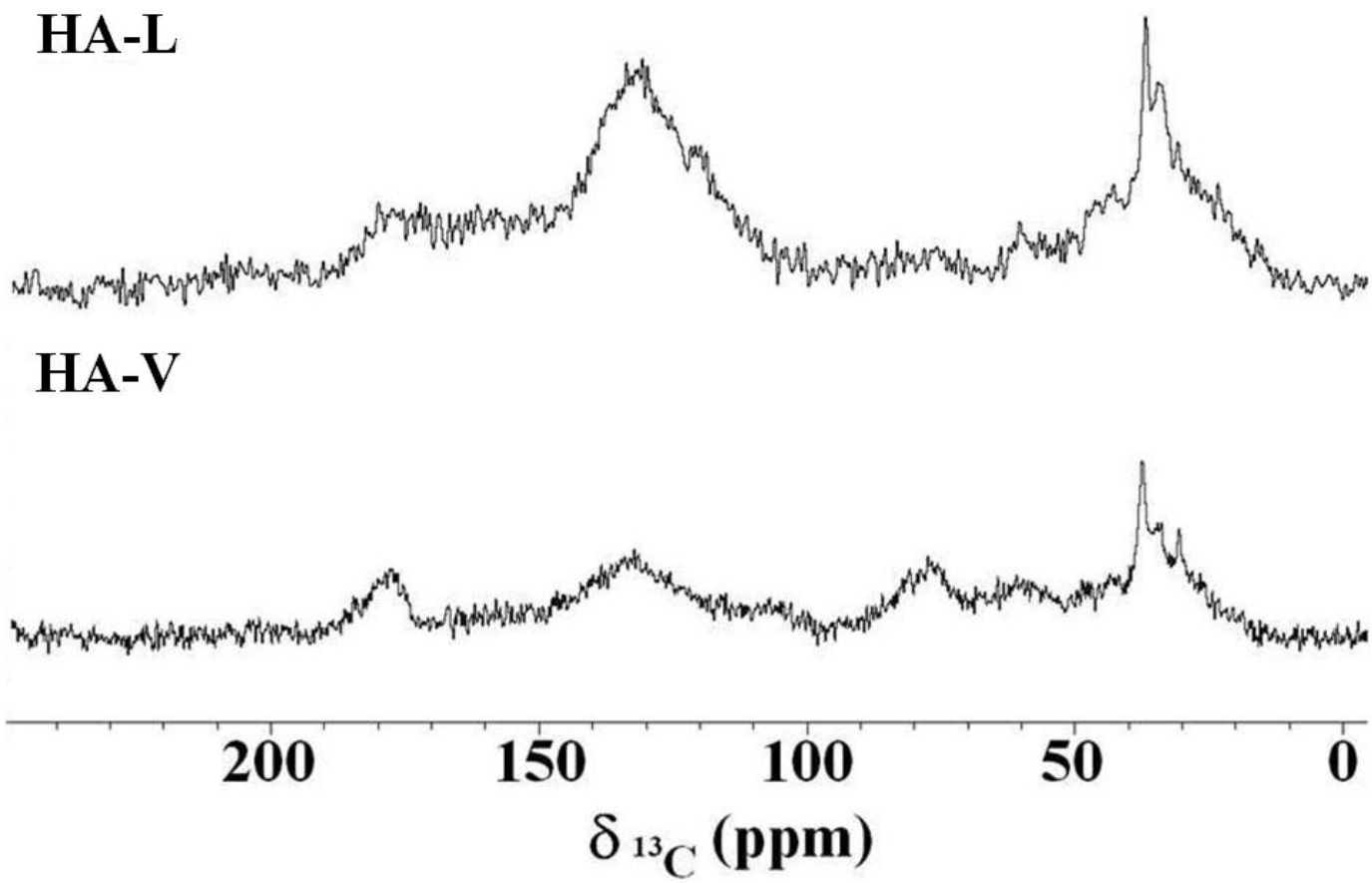

Figure S1. CPMAS ^{13}C-NMR spectra of the humic acids HA-V and HA-L.

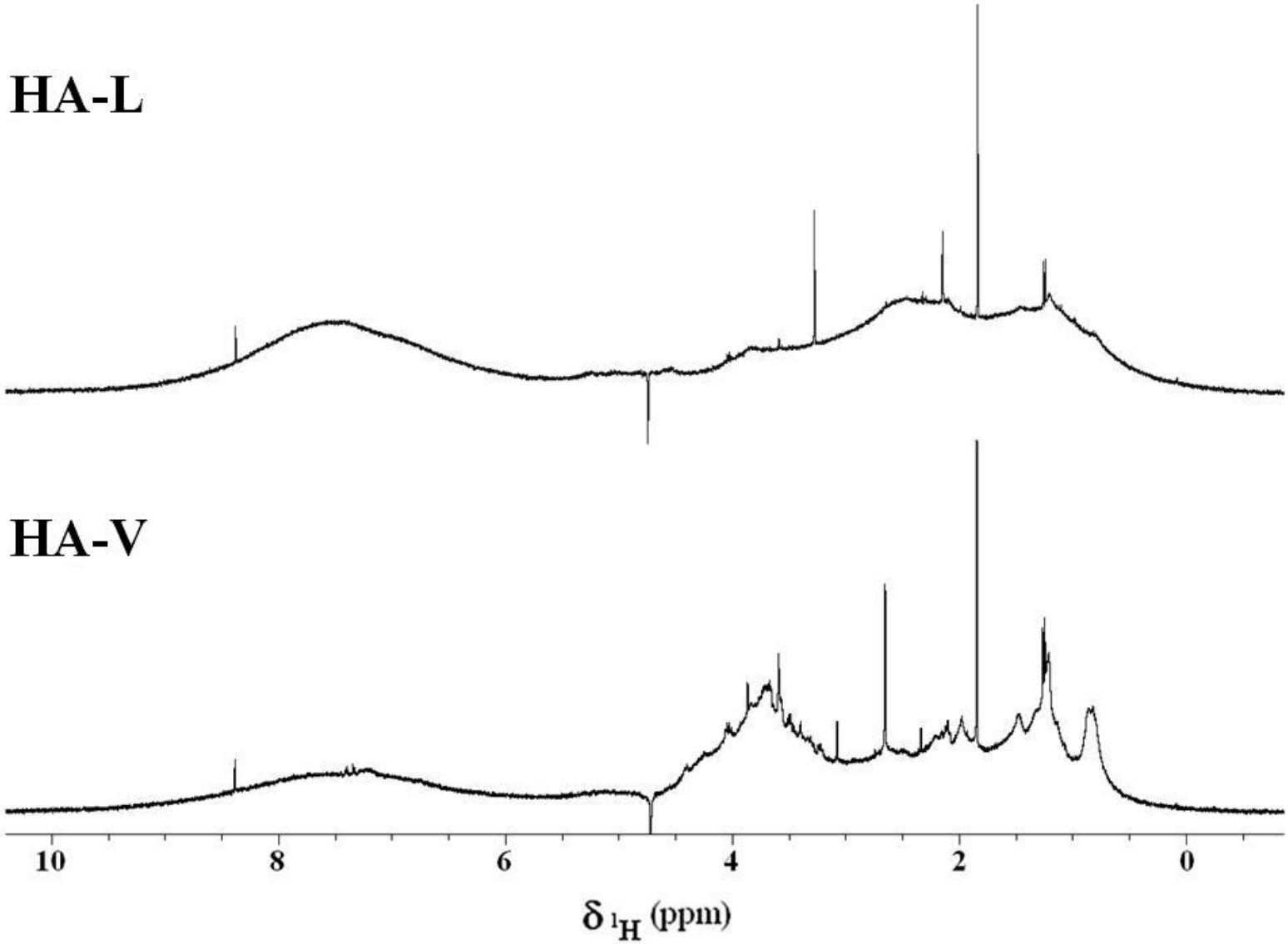

Figure S2. Water-suppressed ^{1}H-NMR spectra of 15 mg ml^{-1} of HA-V and HA-L.

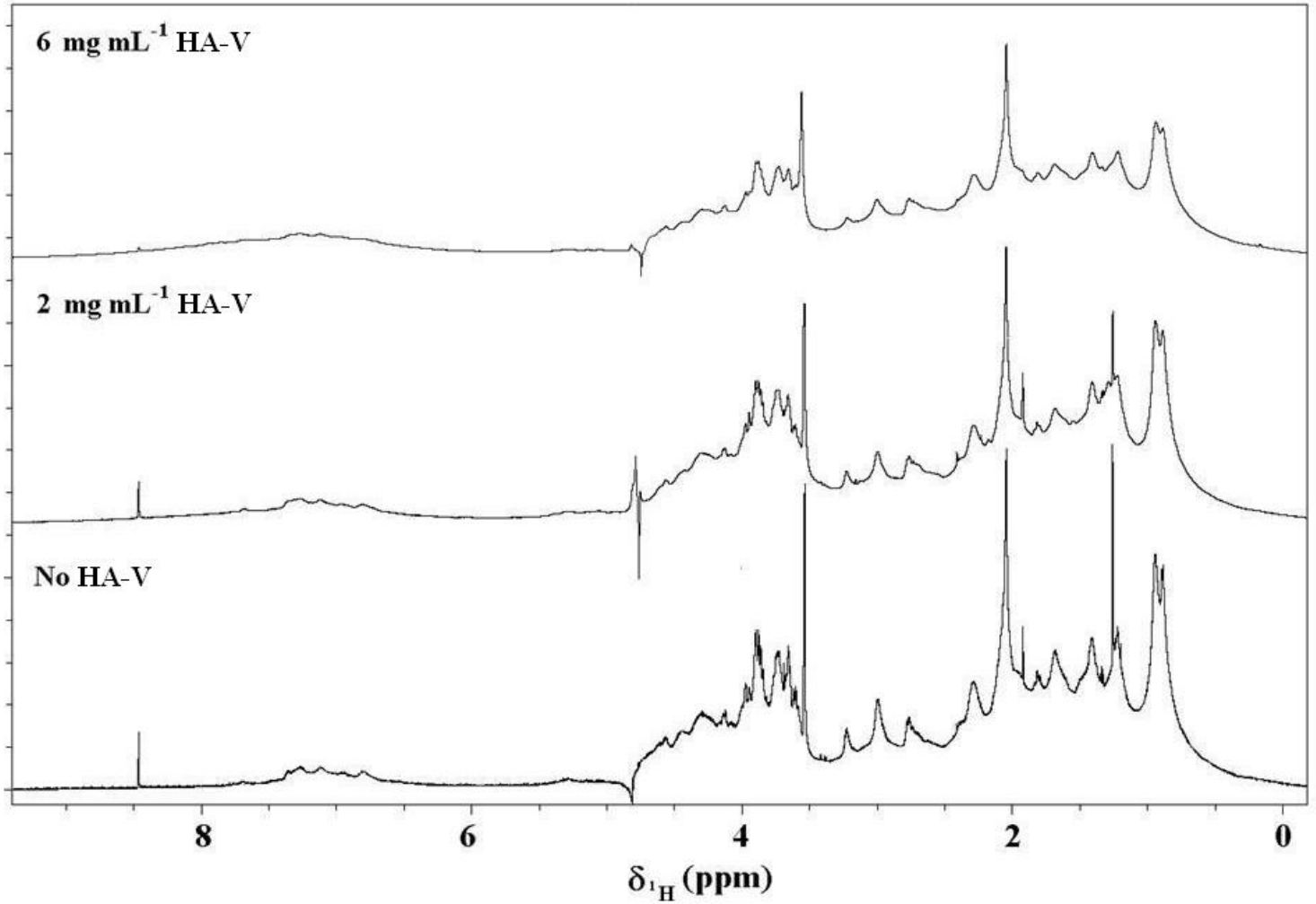

Figure S3. ^{1}H spectra of the AP enzyme solution at pH 10.4 added with increasing aliquots of HA-V.

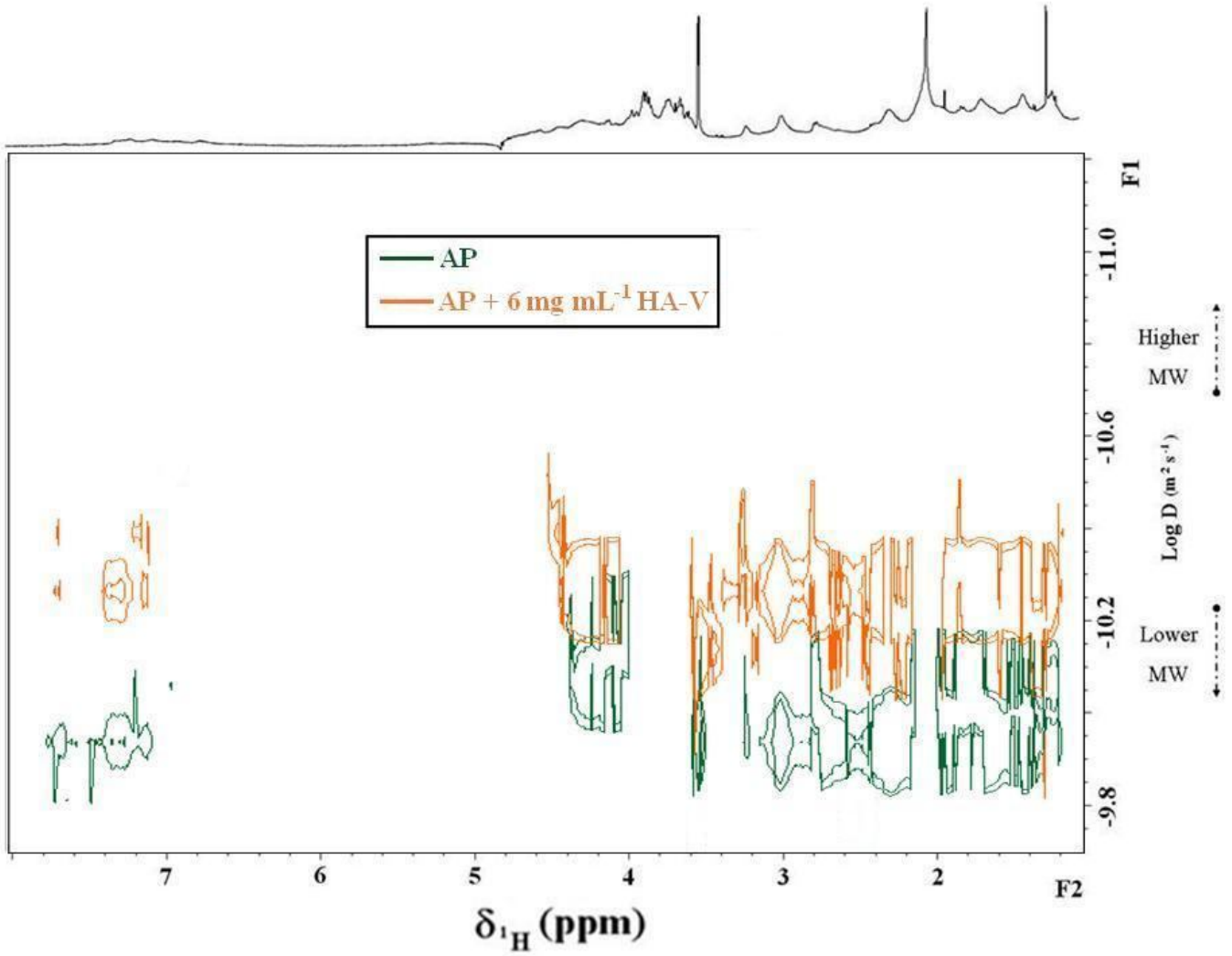

Figure S4. Overlapping of two ^{1}H DOSY spectra of AP. The proton projections of the AP enzyme treated with 0 and 6 mg mL^{-1} of HA-V are shown in green and red, respective

5.

NMR spectroscopy evaluation of the modification of catalytic activity of β-D-Glucosidase following interactions of the enzyme with fulvic acids

Pierluigi Mazzei [a, b] & Alessandro Piccolo[a]*

[a] Centro Interdipartimentale per la Risonanza Magnetica Nucleare (CERMANU), Università di Napoli Federico II, Via Università 100, 80055 Portici, Italy.

[b] Istituto di Metodologie Chimiche, CNR, Via Salaria Km 29.300, 00016 Monterotondo Stazione, Italy.

***Corresponding author**

E-mail: alessandro.piccolo@unina.it, alpiccol@unina.it (A. Piccolo).
Tel.: +39 081 2539160
Centro Interdipartimentale per la Risonanza Magnetica Nucleare (CERMANU), Università di Napoli Federico II, Via Università 100, 80055 Portici (NA), Italy.

To be submitted to "Soil Biology and biochemistry"

Key words: β-D-Glucosidase, Fulvic Acids, NMR, Relaxometry, Enzyme Interactions.

Abstract

The interactions occurring between fulvic acids (FA) and a β-Glucosidase (GLU) enzyme and the inherent modifications of enzymatic activity were investigated here at the pH 5 and 7.2 by ^{1}H NMR spectroscopy. With increasing amounts of FA, the enzyme proton signals were progressively broadened, while the relaxation (T_1 and T_2) and correlation (τ_c) times of GLU decreased and increased, respectively. Both these effects were more relevant for the hydroxy-alkylic and aromatic protons of GLU, thus suggesting that the FA-enzyme associations, which progressively limited GLU tumbling rate, were due to weak interactions, such as H-bonds and dispersive hydrophobic bonds. However, no significant differences were found for the two different pHs. The catalytic activity of β-D-Glucosidase when in weakly-bound complexes with FA was studied by following the NMR signal changes of two substrates, such as *p*-Nitrophenyl-β-D-glucopyranoside (*p*-NPG) and Salicin, and their hydrolysis products. The GLU catalytic activity was substantially slowed down with increasing concentration of FA in solution and the rate reduction was more pronounced for Salicin than for *p*-NPG. The inhibition of the enzymatic activity may be explained with either a partial cover up of the active site of GLU by fulvic molecules or to modifications of the enzyme conformational structure during formation of the humic-enzyme complex. Our results indicate that interactions of FA with GLU, though through weak bonds, are sufficient to partially inhibit its catalytic activity, and suggest that the environmental role of extracellular enzymes may be significantly reduced when coming in contact with natural organic matter.

1. Introduction

Soil enzymes are directly or indirectly involved in the transformation of organic compounds and in the biogeochemical cycle of soil organic matter (Mondini, 2004; Turner *et al*., 2002). Plant and microbes release enzymes in soils, partly as extracellular exo-enzymes, and partly as

cytoplasmic exudates from dead or living cells (Burns, 1982). In particular, the β-Glucosidase (EC 3.2.1.21) enzyme, a widespread soil enzyme, is determinant in the carbon cycle and is closely related to the transformation and accumulation of soil organic matter (Xiao-Chang & Qin, 2006; Busto and Perez-Mateos, 2000). As a member of the glycoside hydrolase family, glucosidase is capable to hydrolyze substrates by cleaving β-1-4-glycosidic linkages (Bock, 1988). The mechanism of enzymatic hydrolysis lies on the action of two carboxyl groups of β-Glucosidase, which concur to break the β-glycosidic bonds (Lawson *et al*. 1998; Rye & Withers, 2000). Thus, β-Glucosidase contributes to degrade β−1-4 glycosylated molecules which are commonly released in soil, such as flavonoid glucosides (Schmidt *et al*., 2011) or cellulosic materials (Saratchandra & Perrott, 1984). Cellulose degradation in soil is a result of the synergistic activity of several enzymes, whose final hydrolysis is completed by β-Glucosidase (Turner *et al*., 2002). In plants, β−Glucosidase is also involved in the degradation of endosperm cell walls during germination, in the formation of intermediates in cell wall lignification, in the activation of defence compounds, and in the synthesis of phytohormones (Schmidt *et al*., 2011).

The interactions of soil enzymes with soil colloids such as clay minerals and humic substances have been repeatedly shown (Burns, 1982, 1996; Stevenson, 1982; Busto & Perez-Mateos, 2000; Nannipieri *et al*., 2002). It has been postulated that the binding of extracellular enzymes to clay or humic matter should make them more resistant to proteolytic degradation and/or to chemical-physical stresses (Nannipieri *et al*., 1996). Moreover, the presence of active enzymes in soil is exploited as an indicator of soil biological quality (Dick, 1997; Turner *et al*., 2002).

Nonetheless, the mechanisms that regulate the formation of humic-enzyme complexes and the effects on the residual catalytic activity of enzymes had not been sufficiently elucidated. This is especially true after the recent innovative understanding of humic substances as supramolecular associations of relatively small and heterogeneous molecules held together in labile conformations by weak dispersive forces (Piccolo, 2001; Piccolo and Spiteller, 2003; Eastman *et al*., 2011). It is

thus likely that the interactions of enzyme with humic matter may be accounted to some of the numerous small molecules which may be detached from the main humic superstructure (Nebbioso and Piccolo, 2011).

The aim of this work was to investigate the nature of interactions occurring between the β-glucosidase enzyme and fulvic acids (FA) and how they affect the catalytic activity of the enzyme. Nuclear Magnetic Resonance (NMR) spectroscopy was used to meet our objectives due to the capacity of this spectroscopy to directly provide reproducible and detailed information on the humic-enzymes interactions at molecular scale and on the changes of substrate concentration during the enzyme catalyzed hydrolysis of the β-glycosidic bond.

2. Materials and Methods

2.1. Fulvic acid. A fulvic acid (FA) was isolated from an Italian Soil (Caserta, IT) classified as Eutric Regosol by standard methods (Smejkalova and Piccolo, 2008a). In the soil alkaline extract, humic acids were separated and removed by a flocculation at pH 1 by 6 M HCl, while FA still soluble in the acidified solution were purified by absorbing on a Amberlite XAD8 resin (Thurman and Malcolm, 1981). After elution by a 1M NaOH solution, and, adjustment of eluates to pH 5, they were dialyzed in Spectrapore 3 tubes against distilled water until chloride-free, and freeze-dried. FA were then redissolved in 0.5M NaOH and passed through a strong cation-exchange resin (Dowex 50) to further eliminate polyvalent metals and freeze-dried again. FA were characterized for their elemental content using a Fisons EA 1108 Elemental Analyzer and the ash content was less than 5%.

2.2. Reagents. The β-D-Glucosidase (GLU) (Grover *et al.*, 1977; Grover and Cushley, 1977) was purchased from Sigma-Aldrich, Italy, as an extract from sweet almonds (2.31 units/ mg). The substrates for enzyme activity were *p*-Nitrophenyl-β-D-glucopyranoside (*p*-NPG, > 98.0 % purity)

and 2-(Hydroxymethyl)phenyl-β-D-glucopyranoside (Salicin, > 99.0 % purity) and were also purchased from Sigma-Aldrich, Italy.

2.3. FA-GLU complex formation. Different amounts of FA (0, 0.1, 0.2, 0.35, 0.5, 0.6, 0.8, 1, 1.5 mg mL^{-1}) were dissolved into two deuterated 0.2 M phosphate buffer solutions (99.8% D_2O/H_2O, ARMAR CHEMICALS) brought to pH 5 and 7.2, and the solutions sonicated for 10 minutes, but not to exceed 30°C. Then, 5 mg of GLU were dissolved into 1 mL of each humic buffer solution, stirred for 10 minutes and left to stabilize for 30 min before NMR measurements.

2.4. Catalytic activity of the FA-GLU complex. Samples to evaluate the catalytic activity of the FA-GLU complex were prepared by dissolving 0.6 mg of GLU in 1 mL of deuterated 0.2 M carbonate buffer solution at pH 5, and already containing 0, 0.03, 0.1 and 0.2 mg mL^{-1} of FA. The solutions were stirred for 10 minutes and left to stabilize for 30 minutes. Then, the enzymatic catalysis was started by adding 10 mg of either *p*-NPG or Salicin. All solutions were transferred into 5 mm NMR tubes for NMR analysis. Each reactions was conducted in duplicate.

2.5. NMR Experiments. A 400 MHz Bruker Avance spectrometer, equipped with a 5 mm Bruker Inverse Broad Band (BBI) probe, working at ^1H frequency of 400.13 MHz, was employed to conduct all liquid-state NMR measurements at a temperature of 298 +/- 1 K. ^1H-NMR spectra were acquired with 2 s of thermal equilibrium delay, 90° pulse length ranging between 9.85 and 13.5 μs, 32768 time domain points and 256 transients.

An inversion recovery pulse sequence, with 20 increments and variable delays from 0.02 to 5 s, was adopted to measure ^1H longitudinal (spin-lattice) relaxation time constants (T_1). The transverse (spin-spin) relaxation time constants (T_2) were measured using a Carr-Purcell-Meiboom-Gill (CPMG) pulse sequence by using 20 increments and 2 (5.6 ms) to 2000 (5600 ms) spin-echo repetitions, with a constant 1.4 ms spin-echo delay. A time domain of 32768 points was set for all

the relaxometric experiments. The correlation times (τ_c) were calculated from T_1 and T_2 as described elsewhere (Carper and Keller, 1997).

The ^{1}H spectral width was 16.66 ppm (6666.2 Hz) and the residual water signal was removed from ^{1}H-NMR spectra by pre-saturation technique. The proton frequency axis was calibrated by associating to 1.1204 ppm the centre of the highest doublet resonating in the region included within the 1.25-1 ppm interval.

A sequence of 12 ^{1}H-NMR acquisitions was launched at 25°C on each FA-GLU solution 11, 13, 15, 23, 30, 38, 45, 53, 65, 78, 90 and 123 min after the start of catalysis or the catalyzed hydrolysis of both *p*-NPG and Salicin substrates as a function of fulvic concentrations (0, 0.03, 0.1 and 0.2 mg mL^{-1}). ^{1}H-NMR spectra were acquired with 2 s of thermal equilibrium delay, an 11 μs 90° pulse length, 32768 time domain points and 32 transients (52 seconds each acquisition). In the case of Salicin, the proton doublets resonating at 5.051 and 5.146, were associated to α anomeric protons of Salicin (S1) and Glucose (P1), respectively. Instead, in the case of *p*-NPG, the doublets resonating at 8.1619 and 8.073 ppm were associated to aromatic *meta* protons of *p*-NPG (S2) and *p*-Nitrophenol (P2), respectively. No zero filling and apodization were applied to free induction decays (FID) excepted for mono-dimensional acquisitions conducted during the catalysis, where 1 Hz multiplication was executed. All spectra were baseline corrected and processed by Bruker Topspin Software (v.1.3), MestReC NMR Processing Software (v. 4.9.9.9) and Origin (v.6.1). Details on the adopted methods for CPMAS ^{13}C-NMR spectroscopy are given in the Supporting Information.

The extent of catalysis was estimated by integrating the areas under the proton signals corresponding to substrates and reaction products (Figures 6 and 7). The relative substrate concentration (%) remaining at different reaction times was calculated by dividing the area of substrate signals by that of products and multiplying by 100.

2.6. Viscosity measurements. Possible artificial modifications of calculated parameters (T_1, T_2 and DOSY self-diffusion constants) by change in viscosity (Smejkalova and Piccolo, 2008 a) was accounted to by measuring solution dynamic viscosity with a Bohlin Advanced Rheometer (Bohlin Instruments Ltd., Gloucestershire, UK), using a coaxial cylinder geometry with a gap size of 150 µm. All measurements were performed in triplicate, at 25ºC, and under a constant shear stress of 0.1 Pa.

3. Results and Discussions

3.1. Evaluation of humic-enzyme complexes

Liquid-state ^{1}H-NMR and solid-state ^{13}C-CPMAS-NMR spectra showed the structural features of the FA used here (Supplementary Figures 1a, 1b). The FA hydrophilic character is reflected by the intense signals in the hydroxy-alkyl and carboxyl regions observed in both ^{1}H and ^{13}C spectra, respectively.

The evidence of the interactions occurring between GLU and FA became evident by observing the ^{1}H-NMR spectra of GLU with increasing FA concentrations at the two pH of 5 and 7.2. Since spectral differences between the two pH conditions were not significantly appreciable, only NMR results for pH 7.2 are shown here. It was observed a progressive signal broadening with increasing FA concentrations in the alkyl, hydroxy-alkyl, and the aromatic regions of proton spectra (Figures 1-3). This effect is attributed to the reduced Brownian motions in the ever larger molecular size of the GLU-FA adduct, that limits the minimization of molecular dipolar couplings. Since the width of NMR signals is inversely proportional to the spin-spin relaxation times, these are progressively and strongly reduced when the molecular mobility is diminished (Bakhmutov, 2004), as in the case of GLU forming non covalent complexes with FA, thus resulting in signal broadening (Smejkalova and Piccolo, 2008 b). The careful purification of the FA used here excludes that the signal broadening effect be attributed to residual paramagnetic metals.

The GLU used here was a homo-dimeric glycoprotein consisting in 2 equal subunits of 65 kDa and had a total molecular weight of 135 kDa (Grover *et al*., 1977). The relatively resolved multiplets of narrow width observed in the ^{1}H spectrum of such a large molecule is explained with the relatively large mobility of branched glyco-peptidic domains in this protein. The enhanced broadening of these multiplets with increasing FA additions (Figure 1) suggests that such branched components became largely involved with hydrophilic FA molecules more than other inner protein domains. However, a progressive saturation of the most accessible GLU domains is indicated by the rapid signals broadening up to 0.35 mg mL^{-1} of FA concentration and the subsequent less pronounced enlargement of enzyme signals when FA reached the concentration of 5 mg mL^{-1} (Figure 1).

Spin-lattice (T_1) and spin-spin (T_2) relaxation times are sensitive NMR parameters to reveal changes in protein flexibility and follow perturbations of the magnetic field on a studied nucleus (Zhang and Forman-Kay, 1995; Tollinger *et al*. 2001; Sapienza and Lee, 2010). The measurements of relaxation times are useful to quantify the overall motion of proteins or parts of proteins when involved in complexes with other molecules (Pickford and Campbell, 2004). A calculation of changes in T_1 and T_2 relaxation times of β–Glucosidase with increasing amount of FA, should further confirm the formation of the non-covalent complexes suggested by signal broadening in ^{1}H-NMR spectra. However, due to severe signal overlapping in proton spectra and lack of previous NMR signal assignment for this specific GLU enzyme, the elaboration of the ^{1}H-NMR spectrum was conducted by associating proton intervals to numbered bucket areas. Thus, the spectrum was divided in 18 discrete regions (1-9 for the alkyl region, 10-15 for the hydroxy-alkyl region; 16-18 for the aromatic region) and relaxation times were calculated by integrating the whole area under each bucket (Figure 4). The same buckets were adopted for both pH 5 and 7.2 treatment, since no evident chemical-shift drifts were detected in the GLU spectrum at different pH conditions. The values for T_1 and T_2 relaxation times at both pH 5 and 7.2, as a function of FA concentration are reported Table 1 and 2, respectively.

A progressive decrease of both relaxation times with increasing FA addition was found in all cases. This confirms the above suggestion that the ever decreasing enzyme mobility following the formation of a FA-GLU complex, must be responsible for the changes in the relaxation properties observed in respect to the free enzyme. In particular, the proton signals included in buckets 4-5, 10, 12, 14, 16-17 showed the largest relative decrease of both T_1 and T_2 at pH 5 (Table 1), thereby suggesting their greatest interaction with FA molecules. In fact, at the largest FA concentration, the T_1 and T_2 relaxation times of GLU measured for these buckets, were generally 40% and 60% smaller than control, respectively. Moreover, the greatest T_2 variation, in respect to the free enzyme, was revealed by the hydroxy-alkyl regions in buckets 10 (75%), 13 (82.9%) and 15 (70.8%). Conversely, the FA additions at pH 7.2 showed a T_1 and T_2 decrease larger than 40% and 60%, respectively, for buckets 10-12 and 15-18 (Table 2). The alkyl GLU domains appeared generally less involved in the humic-enzyme interactions, although some buckets (10, 12, 16 and 17) appeared most affected at either acidic or neutral conditions. Thus, our results suggest which enzyme regions showed the largest affinity to FA as a function of their variation in GLU relaxation times.

Both relaxation times of GLU in solution are dependent on the protein correlation time (τ_C), that is defined as the effective average time needed for a nuclear spin to rotate through one radian (Carper and Keller, 1997) . Therefore, the larger the τ_C values, the slower is the molecular motion (Bakhmutov, 2004). The correlation times have been used as qualitative indexes to indicate the changes in molecular rigidity of host-guest complexes between humic substances and environmental pollutants (Smejkalova and Piccolo, 2008 b; Smejkalova *et al*., 2009).

The addition of progressive amount of FA to the GLU enzyme determined a general increasing trend of τ_C values in all spectral buckets, except for bucket 18 (Table 3 and Figure 5), thus further suggesting a reduced molecular mobility for the FA-GLU complex in respect to the free enzyme. In particular, at both pH 5 and 7.2, the smallest τ_C variation was observed in the alkyl region, whereas the hydroxy-alkyl and aromatic spectral region showed a progressive τ_C

enhancement with increasing FA additions. This further shows a smaller affinity of alkyl than hydroxyl-alkyl components of glucosidase to FA.

The results on GLU signals broadening, relaxation and correlation times indicate that the enzyme-FA interactions were governed by weak bonding forces, to which the GLU hydroxy-alkyl and aromatic protons were mostly responsible. The FA hydrophilic character implies the participation of hydroxyl and carboxyl functional groups in FA to the H-bonds formed with complementary hydroxy-alkylic components in GLU. On the other hand, the involvement of aromatic protons in GLU-FA interactions may be attributed to π–π hydrophobic bonds between the abundant phenolic molecules in FA and the aromatic residues in GLU.

3.2. Catalytic activity of FA-GLU complexes

The extent of residual GLU activity when in the host-guest complex with FA was assessed by following the hydrolysis of two different substrates with NMR spectroscopy. The ^{1}H-NMR spectra of both Salicin and *p*-NPG substrates under catalysis with the FA-GLU complex are reported in Figures 6a and 7a, respectively, as a function of reaction time. The spectra show that the proton signals of substrates (H_{S1} and $H_{S2,}$ respectively) decreased in the course of the enzymatic hydrolysis with increasing time and FA concentration. In fact, the percentage of residual substrate, as measured from proton spectra after 30 min from the start of catalysis, increased progressively with the amount of FA added to GLU, thus suggesting a direct enzyme inhibition due to an increasing formation of host-guest complexes with FA in solution. In fact, both Salicin and *p*-NPG substrates were still present as 70.42% and 58.28% of their initial amount, respectively, at the largest FA concentration in solution (0.2 mg mL^{-1}) after 30 min of reaction time, while their residual amount was only 52.32% and 48.77% with the GLU free enzyme. These findings thus confirm our results shown here and those reported elsewhere (Perez-Mateos, 1991) that soil enzyme may form host-guest complexes with humic matter, and their enzyme catalytic activity may be then significantly reduced.

The sweet almond β-Glucosidase used in this work was assigned to glycosidase Family 1 on the basis of the peptidic sequence obtained from a trapped glycosyl-enzyme intermediate, and the nucleophilic active site was identified with the Ile-Thr-Glu-Asn-Gly peptide group (He and Withers, 1997). Except for Isoleucine, all the aminoacids in such a GLU active site exhibit functional groups, such as –OH for Threonine, –C(O)OH for Glutamate, $–C(O)NH_2$ for Asparagine and $–NH_2$ for Glycine, which may be complementary to the FA oxygen-containing functional groups in the formation of hydrogen bonds. We observed here that the enzymatic catalysis was inhibited by addition of FA to the GLU enzyme solution more for Salicin than for *p*-NPG (Figures 6b and 7b). It may be speculated that the Salicin structure can resemble more than the *p*-NPG structure the fulvic phenolic molecules which may occupy the active site, thus inhibiting the substrate hydrolysis. However, also a partial modification of the conformational structure of the enzyme by the FA molecules may be also the cause of the reduced activity of the FA-GLU complex.

4. CONCLUSIONS

The NMR results indicate that β-D-Glucosidase in aqueous solutions forms host-guest complexes with FA, which are stabilized by non-covalent interactions, such as van der Waals, π–π and H-bonds. The FA-GLU complexes determined the broadening of the GLU signal with increasing FA additions due the progressively limited mobility of the enzyme. The reduction of the translational and rotational motion of the enzyme in the loose newly-formed humic-enzyme complexes were also shown by the changes of relaxation (T_1, T_2) and correlation (τ_C) times, as measured from ^{1}H-NMR spectra for the enzyme progressively added with FA. The values also showed that, at either pH 5 or 7.2, the proton signals in the hydroxy-alkylic and aromatic spectral intervals appeared to be mostly involved in the interactions with FA.

The modification of the enzyme original conformation by complexation with FA had also an impact on the catalysis exerted by the GLU enzyme on the hydrolysis of both *p*-NPP and Salicin

substrates. This reaction was monitored with time by ^{1}H-NMR spectroscopy and it was found that the hydrolytic transformation of substrates was slowed down significantly with increasingly larger FA additions to the enzyme. Moreover, it was observed that the catalytic activity was reduced more for Salicin than for *p*-NPG, and this was attributed to an enhanced competition to the active site by fulvic acid molecules more similar to Salicin than to *p*-NPG. These direct NMR results suggest that extracellular enzymes, which are reputed to play a significant role in the out-of-cell molecular transformations in the environment, may be severely reduced in their activity when interacting with the ubiquitous natural organic matter.

Supplementary data

The Supporting Information contain the description of method adopted for ^{13}C-CPMAS-NMR spectroscopy and the supplementary figures of liquid-state ^{1}H-NMR and ^{13}C-CPMAS-NMR spectra of FA.

References

Bock, K. & Sigurskjold, B. W., 1988. Mechanism and binding specificity of β-glucosidase-catalyzed hydrolysis of cellobiose analogues studied by competition enzyme kinetics monitored by 'H-NMR spectroscopy. European Journal of Biochemistry 178, 711-720.

Bums, R. G., 1982. Enzyme activity in soil: location and a possible role in microbial ecology. Soil Biology & Biochemistry 14, 423-427.

Burns, R. G., 1986. Interactions of enzymes with soil mineral and organic colloids. In: Interactions of Soil Minerals with Natural Organics and Microbes. (eds P. M. Huang & M. Schnitzer), pp. 429-451. Soil Science Society of America, Madison, WI.

Busto, M. D. & Perez-Mateos, M., 2000. Characterization of β-D-glucosidase extracted from soil fractions. European Journal of Soil Science 51, 193-200.

Carper, W. R., Keller, C. E., 1997. Direct Determination of NMR correlation times from spin-lattice and spin-spin relaxation times. Journal of Physical Chemistry A 101, 3246-3250.

Dick, R.P., 1997. Soil enzyme activities as integrative indicators of soil health. In: Pankhurst, C.E., Doube, B.M., Gupta, V.V.S.R. (Eds.), Biological Indicators of Soil Health. CAB International, Wallingford, UK, pp. 121–156.

Eastman, M. A., Brothers, L. A., Nanny, M. A., 2011. ^{2}H NMR Study of Dynamics of Benzene-d6 Interacting with Humic and Fulvic Acids. The journal of physical chemistry A 115, 4359–4372.

Grover, A. K., Macmurchie, D. D., Cushley, R. J., 1977. Studies on almond emulsion beta-D-glucosidase. I. Isolation and characterization of a bifunctional isozyme. Biochimica and Biophysica Acta 482 (1), 98-108.

Grover, A. K., Cushley, R. J., 1977. Studies on almond emulsion beta-D-glucosidase. II. Kinetic evidence for independent glucosidases and galactosidase sites. Biochimica and Biophysica Acta 482 (1), 109-124.

He, S., Withers, S. G., 1997. Assignment of sweet almond β-Glucosidase as a family 1 glycosidase and identification of its active site nucleophile. The journal of Biological Chemistry 272 (40), 24864-24867.

Lawson, S. L., Antony, R., Warren, j., Withers, S. G., 1998. Mechanistic consequences of replacing the active-site nucleophile Glu-358 in Agrobacterium sp. β-glucosidase with a cysteine residue. Biochemistry Journal 330, 203-209.

Legler, G., Harder, A., 1978. Amino acid sequence at the active site of β-glucosidase a from bitter almonds. Biochimica et Biophysica Acta (BBA) – Enzymology 524 (1), 102-108.

Mondini, C., Fornasier, F., Sinicco, T., 2004. Enzymatic activity as a parameter for the characterization of the composting process. Soil Biology & Biochemistry 36, 1587–1594.

Nannipieri, P., Sequi, P., Fusi, P., 1996. Humus and enzyme activity. In: Piccolo, A. (Ed.), Humus Substances in Terrestrial Ecosystems. Elsevier Science B.V., Amsterdam, pp. 293–328.

Nannipieri, P., Kandeler, E., Ruggiero, P., 2002. Enzyme activities and microbiological and biochemical processes in soil. In: Burns, R.G., Dick, R.P. (Eds.), Enzyme in the Environment. Activity, Ecology and Application. Marcel Dekker, Inc., New York, Basel, pp. 1–33.

Nebbioso A., Piccolo, A., 2011. Basis of a Humeomics Science: chemical fractionation and molecular characterization of humic biosuprastructures. Biomacromolecules 12, 1187–1199.

Piccolo, A., 1988. Characteristics of soil humic extracts obtained by some organic and inorganic solvents and purified by HCL-HF treatment. Soil Science 146 (6), 418-426.

Piccolo, A., 2001. The supramolecular structure of humic substances. Soil Science, 166:810–832.

Piccolo, A., Spiteller, M., 2003. Electrospray ionization mass spectrometry of terrestrial humic substances and their size fractions. Anal. Bioanal. Chem. 377, 1047-1059.

Pickford, A. R., Campbell, I. D., 2004. NMR Studies of Modular Protein Structures and Their Interactions. Chemical Reviews 104, 3557-3565.

Rye, C. S., Withers, S. G., 2000. Glycosidase mechanisms. Current Opinion on Chemical Biology 4, 573–580.

Sanchez-Perez, R., Joergensen, K., Motawia, M. S., Dicenta, F. and Moeller, B. L., 2009. Tissue and cellular localization of individual β-glycosidases using a substrate-specific sugar reducing assay. Plant Journal 60, 894–906.

Sapienza, P. J., Lee, A. L., 2010. Using NMR to study fast dynamics in proteins: methods and Applications. Current Opinion in Pharmacology 10, 723–730.

Saratchandra, S. U. & Perrott, K. W., 1984. Assay of b-Glucosidase activity in soils. Soil Science 138, 15-19.

Schmidt, S., Rainieri, S., Witte, S., Matern, U., Martens, S., 2011. Identification of a Saccharomyces cerevisiae Glucosidase That Hydrolyzes Flavonoid Glucosides. Applied and environmental microbiology 77 (5), 1751-1757.

Smejkalova, D., Piccolo, A., 2008a. Aggregation and disaggregation of humic supramolecular assemblies by NMR diffusion ordered spectroscopy (DOSY-NMR). Environmental Science and Technologies 42, 699–706.

Smejkalova, D., Piccolo, A., 2008b. Host-Guest Interactions between 2,4-Dichlorophenol and Humic Substances As Evaluated by ^{1}H NMR Relaxation and Diffusion Ordered Spectroscopy. Environmental Science and Technologies 42, 8440–8445.

Smejkalova, D., Spaccini, R., Fontaine, B., Piccolo, A., 2009. Binding of Phenol and Differently Halogenated Phenols to Dissolved Humic Matter As Measured by NMR Spectroscopy. Environmental Science and Technologies 43, 5377–5382.

Song, G., Novotny, E. H., Simpson, A. J., Clapp, E., Hayes, M. H. B., 2008. Sequential exhaustive extraction of a Mollisol soil, and characterizations of humic components, including humin, by solid and solution state NMR. European Journal of Soil Science 59, 505–516.

Thurman, E., Malcolm, R. L., 1981. Preparative Isolation of Aquatic Humic Substances. Environmental Science and Technologies, 15, 463.

Tollinger, M., Skrynnikov, N. R., Mulder, F. A. A., Forman-Kay, J. D., Kay, L. E., 2001. Slow Dynamics in Folded and Unfolded States of an SH3 Domain. Journal of American Chemistry Society 123, 11341-11352.

Turner B. L., Hopkins, D. W., Haygarth, F. M., Ostle, N., 2002. Glucosidase activity in pasture soils. Applied Soil Ecology 20, 157–162

Vetter, J., 2000. Plant cyanogenic glycosides. Toxicon 38, 11–36.

Witte, E. G., Philipp, H., Vereecken, H., 2002. Study of enzyme-catalysed and noncatalysed interactions between soil humic acid and ^{13}C-labelled 2-aminobenzothiazole using solid-state ^{13}C NMR spectroscopy. Organic Geochemistry 33, 1727–1735.

Xiao-Chang, W. & Qin, L., 2006. Beta-Glucosidase Activity in Paddy Soils of the Taihu Lake Region, China. Pedosphere 16 (1), 118-124.

Zhang, O., Forman-Kay, J. D., 1995. Structural Characterization of Folded and Unfolded States of an SH3 Domain in Equilibrium in Aqueous Buffer. Biochemistry 34, 6784-6794.

Table 1. ^{1}H spin-lattice T_1 (a), spin-spin T_2 (b) relaxation times (s) and standard deviations (%) of enzyme β-D-Glucosidase as a function of FA concentration (mg mL^{-1}) achieved at pH 5.

Bucket Number	FA								
	0	**0.1**	**0.2**	**0.35**	**0.5**	**0.6**	**0.8**	**1**	**1.5**
1	0.736	0.619	0.62	0.513	0.507	0.523	0.504	0.51	0.514
	(0.008)	(0.005)	(0.004)	(0.006)	(0.006)	(0.008)	(0.004)	(0.007)	(0.005)
2	0.676	0.553	0.548	0.455	0.46	0.467	0.455	0.459	0.459
	(0.007)	(0.003)	(0.004)	(0.011)	(0.011)	(0.008)	(0.01)	(0.01)	(0.012)
3	0.832	0.789	0.739	0.584	0.565	0.56	0.568	0.549	0.55
	(0.011)	(0.005)	(0.006)	(0.01)	(0.007)	(0.017)	(0.009)	(0.015)	(0.042)
4	0.612	0.496	0.488	0.407	0.39	0.389	0.362	0.362	0.345
	(0.014)	(0.007)	(0.01)	(0.008)	(0.008)	(0.007)	(0.01)	(0.023)	(0.005)
5	0.636	0.544	0.527	0.432	0.411	0.398	0.382	0.379	0.379
	(0.011)	(0.005)	(0.015)	(0.009)	(0.003)	(0.005)	(0.011)	(0.014)	(0.01)
6	0.623	0.531	0.522	0.425	0.406	0.398	0.389	0.384	0.381
	(0.014)	(0.005)	(0.012)	(0.012)	(0.002)	(0.008)	(0.015)	(0.016)	(0.011)
7	0.664	0.598	0.59	0.514	0.506	0.515	0.5	0.501	0.497
	(0.008)	(0.01)	(0.005)	(0.014)	(0.008)	(0.013)	(0.012)	(0.022)	(0.008)
8	0.733	0.613	0.61	0.533	0.525	0.541	0.521	0.521	0.515
	(0.008)	(0.003)	(0.008)	(0.009)	(0.005)	(0.012)	(0.014)	(0.018)	(0.005)
9	0.601	0.533	0.529	0.486	0.48	0.484	0.453	0.455	0.436
	(0.014)	(0.004)	(0.004)	(0.01)	(0.012)	(0.013)	(0.005)	(0.018)	(0.006)
10	0.757	0.659	0.619	0.475	0.44	0.397	0.379	0.377	0.389
	(0.007)	(0.014)	(0.005)	(0.009)	(0.005)	(0.007)	(0.014)	(0.016)	(0.009)
11	1.553	1.424	1.269	1.241	1.228	1.127	1.128	1.135	1.12
	(0.007)	(0.004)	(0.011)	(0.011)	(0.009)	(0.008)	(0.009)	(0.02)	(0.01)
12	0.751	0.581	0.565	0.493	0.468	0.465	0.402	0.394	0.352
	(0.011)	(0.008)	(0.008)	(0.008)	(0.005)	(0.02)	(0.003)	(0.009)	(0.01)
13	1.211	1.034	0.995	0.98	0.95	0.942	0.847	0.882	0.894
	(0.006)	(0.004)	(0.008)	(0.016)	(0.008)	(0.012)	(0.013)	(0.019)	(0.013)
14	1.35	1.108	1.052	0.901	0.903	0.932	0.809	0.815	0.759
	(0.004)	(0.011)	(0.012)	(0.015)	(0.008)	(0.019)	(0.02)	(0.024)	(0.011)
15	1.201	1.147	1.032	0.875	0.918	0.89	0.854	0.889	0.809
	(0.014)	(0.007)	(0.01)	(0.015)	(0.012)	(0.021)	(0.017)	(0.01)	(0.012)
16	1.571	1.282	1.224	1.18	1.145	1.01	0.852	0.86	0.823
	(0.011)	(0.02)	(0.038)	(0.008)	(0.004)	(0.013)	(0.031)	(0.035)	(0.014)
17	1.392	1.199	1.145	1.02	0.933	0.91	0.85	0.911	0.782
	(0.002)	(0.012)	(0.006)	(0.007)	(0.004)	(0.011)	(0.022)	(0.037)	(0.003)
18	1.625	1.468	1.407	1.38	1.25	1.24	1.23	1.2	1.21
	(0.006)	(0.011)	(0.005)	(0.013)	(0.013)	(0.013)	(0.013)	(0.038)	(0.013)

Table 1. Continued

Bucket Number	FA								
	0	**0.1**	**0.2**	**0.35**	**0.5**	**0.6**	**0.8**	**1**	**1.5**
1	0.073	0.062	0.059	0.056	0.054	0.057	0.053	0.055	0.053
	(0.0042)	(0.0053)	(0.0063)	(0.0063)	(0.0033)	(0.0028)	(0.0041)	(0.003)	(0.0047)
2	0.098	0.094	0.085	0.072	0.077	0.062	0.066	0.069	0.067
	(0.0057)	(0.0041)	(0.0042)	(0.004)	(0.0037)	(0.0059)	(0.0024)	(0.005)	(0.0062)
3	0.093	0.069	0.05	0.057	0.053	0.051	0.048	0.05	0.043
	(0.0085)	(0.0013)	(0.0073)	(0.0047)	(0.0053)	(0.0017)	(0.006)	(0.008)	(0.0081)
4	0.112	0.089	0.068	0.067	0.063	0.057	0.049	0.051	0.043
	(0.0057)	(0.0028)	(0.0027)	(0.0045)	(0.0073)	(0.0089)	(0.0028)	(0.0063)	(0.006)
5	0.092	0.066	0.057	0.05	0.047	0.046	0.04	0.041	0.037
	(0.0071)	(0.0071)	(0.011)	(0.0048)	(0.0063)	(0.0031)	(0.003)	(0.0044)	(0.0088)
6	0.054	0.048	0.047	0.044	0.04	0.042	0.037	0.037	0.031
	(0.0042)	(0.0053)	(0.0038)	(0.0036)	(0.004)	(0.0048)	(0.0015)	(0.0022)	(0.008)
7	0.089	0.07	0.063	0.067	0.066	0.062	0.059	0.062	0.056
	(0.0057)	(0.0033)	(0)	(0.0041)	(0.0037)	(0.0044)	(0.003)	(0.0079)	(0.0025)
8	0.081	0.069	0.063	0.063	0.062	0.06	0.055	0.058	0.053
	(0.0028)	(0.0046)	(0.0069)	(0.0039)	(0.0082)	(0.0063)	(0)	(0.003)	(0.009)
9	0.163	0.118	0.105	0.107	0.102	0.096	0.085	0.084	0.073
	(0.0014)	(0.0079)	(0.0036)	(0.008)	(0.0059)	(0.0066)	(0.001)	(0.005)	(0.0026)
10	0.122	0.108	0.066	0.046	0.043	0.037	0.034	0.037	0.031
	(0.0099)	(0.0086)	(0.0054)	(0.0045)	(0.0028)	(0.0071)	(0.0036)	(0.0043)	(0.0064)
11	0.47	0.358	0.34	0.297	0.287	0.256	0.248	0.242	0.187
	(0.0085)	(0.0044)	(0.0068)	(0.0042)	(0.0049)	(0.0071)	(0.0057)	(0.0063)	(0.009)
12	0.171	0.151	0.139	0.114	0.1	0.096	0.073	0.07	0.056
	(0.0042)	(0.0064)	(0.0085)	(0.0062)	(0.0035)	(0.0034)	(0.0025)	(0.0064)	(0.0076)
13	0.397	0.369	0.256	0.19	0.107	0.093	0.087	0.075	0.068
	(0.0085)	(0.0111)	(0.0061)	(0.0064)	(0.0053)	(0.0057)	(0.0089)	(0.0057)	(0.0071)
14	0.181	0.153	0.149	0.121	0.129	0.089	0.084	0.086	0.088
	(0.0014)	(0.0036)	(0.0051)	(0.0068)	(0.0081)	(0.006)	(0.0028)	(0.0057)	(0.0064)
15	0.243	0.22	0.226	0.168	0.145	0.106	0.089	0.078	0.071
	(0.0085)	(0.0007)	(0.0042)	(0.0064)	(0.0085)	(0.0054)	(0.0074)	(0.0042)	(0.0071)
16	0.135	0.101	0.076	0.048	0.049	0.042	0.04	0.035	0.042
	(0.0085)	(0.0014)	(0.0071)	(0.0061)	(0.0042)	(0.0057)	(0.0064)	(0.0085)	(0.0051)
17	0.184	0.157	0.122	0.085	0.079	0.078	0.065	0.068	0.064
	(0.0028)	(0.0085)	(0.0042)	(0.0057)	(0.003)	(0.0042)	(0.0023)	(0.0057)	(0.0064)
18	0.351	0.348	0.342	0.342	0.341	0.341	0.345	0.349	0.345
	(0.0014)	(0.0071)	(0.0071)	(0.0071)	(0.0089)	(0.0054)	(0.0057)	(0.0028)	(0.0077)

Table 2. ^{1}H spin-lattice T_1 (a), spin-spin T_2 (b) relaxation times (s) and standard deviations (%) of enzyme β-D-Glucosidase as a function of FA concentration (mg mL^{-1}) achieved at pH 7.2.

Bucket Number	FA								
	0	**0.1**	**0.2**	**0.35**	**0.5**	**0.6**	**0.8**	**1**	**1.5**
1	0.54	0.508	0.507	0.48	0.468	0.476	0.464	0.459	0.469
	(0.021)	(0.004)	(0.008)	(0.002)	(0.01)	(0.002)	(0.004)	(0.003)	(0.003)
2	0.493	0.463	0.467	0.448	0.421	0.43	0.432	0.414	0.411
	(0.01)	(0.003)	(0.013)	(0.003)	(0.003)	(0.006)	(0.002)	(0.008)	(0.012)
3	0.832	0.735	0.71	0.709	0.624	0.622	0.599	0.605	0.539
	(0.006)	(0.001)	(0.011)	(0.003)	(0.006)	(0.015)	(0.011)	(0.005)	(0.004)
4	0.435	0.39	0.369	0.36	0.35	0.329	0.341	0.341	0.319
	(0.008)	(0.01)	(0.013)	(0.013)	(0.011)	(0.006)	(0.004)	(0.012)	(0.004)
5	0.494	0.406	0.384	0.336	0.353	0.345	0.346	0.35	0.34
	(0.004)	(0.014)	(0.007)	(0.002)	(0.004)	(0.003)	(0.007)	(0.011)	(0.008)
6	0.423	0.378	0.397	0.351	0.349	0.339	0.347	0.347	0.337
	(0.006)	(0.016)	(0.007)	(0.004)	(0.01)	(0.003)	(0.009)	(0.004)	(0.008)
7	0.524	0.503	0.509	0.461	0.45	0.457	0.453	0.463	0.464
	(0.028)	(0.016)	(0.016)	(0.011)	(0.007)	(0.006)	(0.003)	(0.011)	(0.011)
8	0.506	0.491	0.479	0.455	0.434	0.446	0.451	0.447	0.455
	(0.028)	(0.001)	(0.011)	(0.009)	(0.004)	(0.007)	(0)	(0.013)	(0.016)
9	0.501	0.471	0.456	0.414	0.405	0.389	0.386	0.391	0.382
	(0.007)	(0.003)	(0.008)	(0.01)	(0.007)	(0.007)	(0.007)	(0.014)	(0.014)
10	0.59	0.401	0.366	0.372	0.369	0.36	0.34	0.342	0.35
	(0.021)	(0.014)	(0.007)	(0.028)	(0.011)	(0.016)	(0.011)	(0.003)	(0.017)
11	1.355	1.291	1.135	1.141	1.013	0.884	0.854	0.818	0.76
	(0.014)	(0.023)	(0.007)	(0.014)	(0.004)	(0.016)	(0.006)	(0.014)	(0.014)
12	0.556	0.462	0.407	0.327	0.284	0.284	0.271	0.278	0.272
	(0.014)	(0.024)	(0.01)	(0.006)	(0.006)	(0.004)	(0.004)	(0.014)	(0.01)
13	1.111	0.979	0.915	0.891	0.853	0.759	0.846	0.797	0.768
	(0.017)	(0.014)	(0.006)	(0.012)	(0.006)	(0.003)	(0.013)	(0.008)	(0.007)
14	1.15	0.933	0.812	0.717	0.664	0.65	0.637	0.64	0.661
	(0.003)	(0.01)	(0.013)	(0.004)	(0.005)	(0.017)	(0.008)	(0.01)	(0.012)
15	1.159	0.98	0.821	0.81	0.695	0.726	0.677	0.659	0.662
	(0.01)	(0.023)	(0.004)	(0.016)	(0.004)	(0.006)	(0.006)	(0.017)	(0.018)
16	1.571	1.206	0.94	0.856	0.84	0.74	0.745	0.742	0.74
	(0.03)	(0.014)	(0.013)	(0.008)	(0.007)	(0.011)	(0.01)	(0.011)	(0.006)
17	1.392	0.8	0.8	0.657	0.632	0.604	0.583	0.541	0.512
	(0.028)	(0.017)	(0.003)	(0.021)	(0.013)	(0.009)	(0.018)	(0.016)	(0.017)
18	1.625	1.52	1.38	1.157	1.109	1.025	0.885	0.927	0.794
	(0.016)	(0.021)	(0.014)	(0.003)	(0.012)	(0.006)	(0.009)	(0.022)	(0.009)

Table 2. Continued

Bucket Number	FA								
	0	**0.1**	**0.2**	**0.35**	**0.5**	**0.6**	**0.8**	**1**	**1.5**
1	0.069	0.063	0.058	0.054	0.05	0.053	0.051	0.051	0.049
	(0.0018)	(0.0036)	(0.0024)	(0.0042)	(0.0028)	(0.0017)	(0.0012)	(0.0013)	(0.0011)
2	0.091	0.079	0.078	0.078	0.071	0.063	0.064	0.057	0.05
	(0.0018)	(0.0042)	(0.0015)	(0.0033)	(0.002)	(0.0011)	(0.0021)	(0.0008)	(0.0032)
3	0.089	0.083	0.082	0.08	0.078	0.075	0.073	0.068	0.055
	(0.0012)	(0.0014)	(0.0054)	(0.0015)	(0.001)	(0.001)	(0.0019)	(0.0021)	(0.0017)
4	0.109	0.076	0.056	0.05	0.048	0.045	0.046	0.049	0.044
	(0.0011)	(0.0028)	(0.0017)	(0.0037)	(0.0008)	(0.0019)	(0.0004)	(0.0023)	(0.0023)
5	0.083	0.057	0.046	0.039	0.036	0.036	0.035	0.033	0.032
	(0.0021)	(0.0028)	(0.0021)	(0.0042)	(0.0018)	(0.0005)	(0.0025)	(0.0034)	(0.0022)
6	0.047	0.04	0.033	0.029	0.025	0.026	0.025	0.028	0.028
	(0.0037)	(0.0042)	(0.0042)	(0.0018)	(0.0035)	(0.0002)	(0.0036)	(0.0022)	(0.0023)
7	0.088	0.076	0.067	0.06	0.051	0.052	0.052	0.048	0.047
	(0.0028)	(0.002)	(0.0048)	(0.0028)	(0.0017)	(0.0021)	(0.0008)	(0.0027)	(0.0016)
8	0.078	0.068	0.058	0.051	0.042	0.044	0.041	0.046	0.044
	(0.0042)	(0.004)	(0.003)	(0.0028)	(0.0018)	(0.0014)	(0.0032)	(0.0011)	(0.0003)
9	0.151	0.122	0.097	0.082	0.07	0.07	0.069	0.06	0.057
	(0.0028)	(0.0019)	(0.0038)	(0.0027)	(0.0022)	(0.0036)	(0.0018)	(0.0014)	(0.0024)
10	0.111	0.053	0.034	0.034	0.034	0.033	0.033	0.03	0.027
	(0.0062)	(0.0038)	(0.0014)	(0.0042)	(0.0007)	(0.0016)	(0.0028)	(0.0009)	(0.0024)
11	0.456	0.254	0.272	0.211	0.222	0.145	0.167	0.117	0.104
	(0.0028)	(0.0017)	(0.0034)	(0.0028)	(0.0026)	(0.0004)	(0.0042)	(0.004)	(0.0026)
12	0.166	0.108	0.074	0.056	0.044	0.044	0.041	0.039	0.039
	(0.0042)	(0.0028)	(0.0042)	(0.0028)	(0.0013)	(0.0009)	(0.0033)	(0.0028)	(0.0011)
13	0.118	0.113	0.107	0.105	0.087	0.073	0.07	0.067	0.064
	(0.0042)	(0.0057)	(0.0047)	(0.005)	(0.0005)	(0.0031)	(0.0022)	(0.0038)	(0.0016)
14	0.146	0.111	0.087	0.077	0.066	0.067	0.062	0.062	0.061
	(0.0052)	(0.0022)	(0.0058)	(0.0028)	(0.0026)	(0.0014)	(0.0028)	(0.0025)	(0.002)
15	0.187	0.112	0.088	0.081	0.079	0.075	0.071	0.066	0.066
	(0.0048)	(0.003)	(0.0042)	(0.0041)	(0.0009)	(0.0031)	(0.0035)	(0.0019)	(0.002)
16	0.129	0.084	0.074	0.052	0.049	0.051	0.045	0.041	0.048
	(0.0061)	(0.0025)	(0.0042)	(0.0021)	(0.0014)	(0.0012)	(0.0021)	(0.0035)	(0.0009)
17	0.184	0.103	0.087	0.066	0.053	0.061	0.05	0.053	0.048
	(0.0042)	(0.0027)	(0.0043)	(0.0022)	(0.002)	(0.0013)	(0.0015)	(0.0042)	(0.0013)
18	0.377	0.198	0.164	0.158	0.146	0.126	0.117	0.109	0.107
	(0.0014)	(0.0042)	(0.0014)	(0.0042)	(0.002)	(0.0015)	(0.0014)	(0.0009)	(0.0041)

Table 3. ^{1}H correlation times τ_C (ns) of enzyme β-D-Glucosidase enzyme as a function of pH (5 and 7.2) and FA concentration (mg mL^{-1}).

Bucket Number	FA																	
	pH 5.0									pH 7.2								
	0	0.1	0.2	0.35	0.5	0.6	0.8	1	1.5	0	0.1	0.2	0.35	0.5	0.6	0.8	1	1.5
1	1.33	1.32	1.36	1.25	1.28	1.26	1.29	1.27	1.30	1.15	1.16	1.22	1.24	1.27	1.25	1.25	1.24	1.30
2	1.06	0.95	1.01	1.00	0.96	1.12	1.06	1.03	1.06	0.89	0.95	0.96	0.93	0.96	1.05	1.05	1.09	1.18
3	1.24	1.42	1.64	1.33	1.36	1.39	1.44	1.38	1.50	1.27	1.23	1.22	1.24	1.17	1.19	1.18	1.23	1.30
4	0.90	0.91	1.08	0.97	0.99	1.06	1.11	1.09	1.17	0.70	0.86	1.03	1.09	1.10	1.11	1.11	1.07	1.10
5	1.06	1.18	1.26	1.21	1.23	1.22	1.29	1.27	1.34	0.96	1.08	1.19	1.21	1.31	1.29	1.32	1.36	1.36
6	1.43	1.40	1.40	1.30	1.33	1.29	1.36	1.34	1.47	1.24	1.27	1.46	1.46	1.57	1.52	1.58	1.49	1.47
7	1.11	1.21	1.27	1.13	1.13	1.19	1.20	1.17	1.23	0.95	1.03	1.13	1.14	1.23	1.22	1.23	1.30	1.31
8	1.25	1.23	1.30	1.20	1.20	1.25	1.28	1.25	1.31	1.01	1.10	1.19	1.24	1.34	1.33	1.38	1.30	1.35
9	0.64	0.78	0.84	0.78	0.80	0.84	0.89	0.89	0.96	0.58	0.68	0.80	0.85	0.94	0.91	0.91	1.02	1.04
10	0.99	0.97	1.27	1.34	1.34	1.37	1.41	1.34	1.51	0.88	1.13	1.38	1.39	1.38	1.38	1.34	1.41	1.51
11	0.58	0.69	0.65	0.72	0.74	0.76	0.78	0.80	0.96	0.52	0.85	0.72	0.89	0.78	0.97	0.85	1.07	1.10
12	0.75	0.67	0.71	0.74	0.79	0.82	0.91	0.91	1.00	0.59	0.74	0.90	0.94	1.01	1.01	1.03	1.08	1.07
13	0.54	0.49	0.68	0.86	1.23	1.33	1.30	1.44	1.53	1.28	1.22	1.21	1.21	1.31	1.35	1.46	1.45	1.46
14	1.11	1.10	1.07	1.11	1.07	1.36	1.29	1.28	1.21	1.15	1.20	1.27	1.27	1.32	1.30	1.34	1.34	1.38
15	0.83	0.87	0.78	0.87	1.00	1.20	1.29	1.42	1.42	0.99	1.23	1.27	1.32	1.23	1.29	1.29	1.32	1.33
16	1.43	1.50	1.72	2.31	2.27	2.29	2.22	2.31	2.15	1.47	1.61	1.50	1.75	1.79	1.62	1.75	1.85	1.67
17	1.12	1.13	1.28	1.46	1.45	1.43	1.53	1.55	1.47	1.13	1.14	1.26	1.31	1.45	1.32	1.44	1.33	1.37
18	0.79	0.73	0.71	0.70	0.64	0.64	0.63	0.60	0.62	0.74	1.13	1.20	1.10	1.12	1.17	1.13	1.20	1.11

Table 4
Residual amount of Salicin and *p*-NPG (%) and standard deviations (%) resulting from GLU hydrolysis (25 °C, pH 5) at increasing FA concentrations (mg mL^{-1}) as a function of reaction time (min).

Reaction time	***p*-NPG**				**Salicin**			
	FA							
	0	**0.03**	**0.1**	**0.2**	**0**	**0.03**	**0.1**	**0.2**
11	85.36	87.7	88.62	89.35	93.92	96.4	96.59	96.97
	(0.12)	(0.12)	(0.29)	(0.23)	(0.14)	(0.21)	(0.25)	(0.15)
13	83.48	86	87.32	88.39	91.37	94.32	95.07	95.23
	(0.5)	(0.25)	(0.28)	(0.17)	(0.26)	(0.15)	(0.34)	(0.2)
15	76.48	80.29	82.39	84.42	87.57	91.79	92.56	93.47
	(0.32)	(0.18)	(0.18)	(0.31)	(0.2)	(0.28)	(0.37)	(0.21)
23	64.81	67.75	69.54	73.3	72.04	80.08	82.43	84.08
	(0.3)	(0.25)	(0.37)	(0.16)	(0.25)	(0.27)	(0.26)	(0.11)
30	48.77	50.9	54.11	58.28	52.32	63.69	67.12	70.42
	(0.14)	(0.17)	(0.38)	(0.41)	(0.19)	(0.32)	(0.4)	(0.27)
38	37.74	40.33	42.57	45.74	34.57	46.53	50.77	54.54
	(0.29)	(0.16)	(0.34)	(4.08)	(0.32)	(0.26)	(0.31)	(0.18)
45	29.31	31.9	35.41	38.51	21.71	30.16	36.98	42.07
	(0.43)	(0.29)	(0.2)	(0.38)	(0.29)	(0.22)	(0.41)	(0.26)
53	22.8	26.04	28.4	31.61	14	20.02	24.77	30.39
	(0.45)	(0.18)	(0.26)	(0.2)	(0.21)	(0.3)	(0.36)	(0.11)
65	16.72	20.01	23.43	26.66	6.19	9.57	13.15	19.81
	(0.48)	(0.31)	(0.4)	(0.63)	(0.39)	(0.22)	(0.37)	(0.3)
78	10.81	14.44	18.3	21.09	3.41	6	7.8	13.13
	(0.39)	(0.79)	(0.69)	(0.47)	(0.47)	(0.41)	(0.48)	(0.19)
90	7.12	9.46	13.64	16.72	2.34	5.23	6.83	10.02
	(0.2)	(0.65)	(0.66)	(0.66)	(0.3)	(0.45)	(0.38)	(0.25)
123	4.8	6.41	10.33	14.07	1.7	4.37	5.91	8.48
	(0.21)	(0.72)	(0.5)	(0.62)	(0.36)	(0.52)	(0.51)	(0.24)

Figures

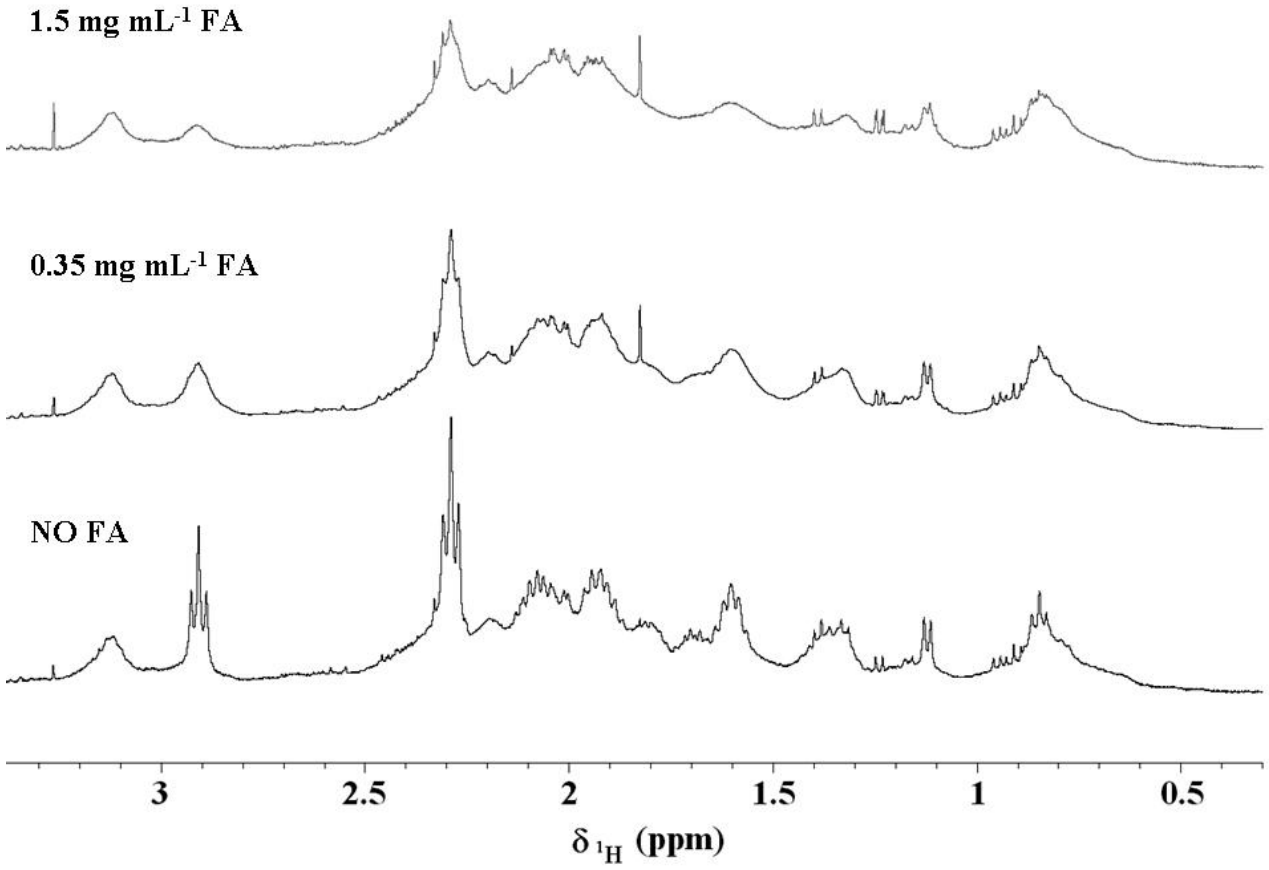

Figure 1. ^{1}H spectra of the 3.4–0.3 ppm interval for the GLU enzyme solution at pH 7.2 with increasing FA concentration.

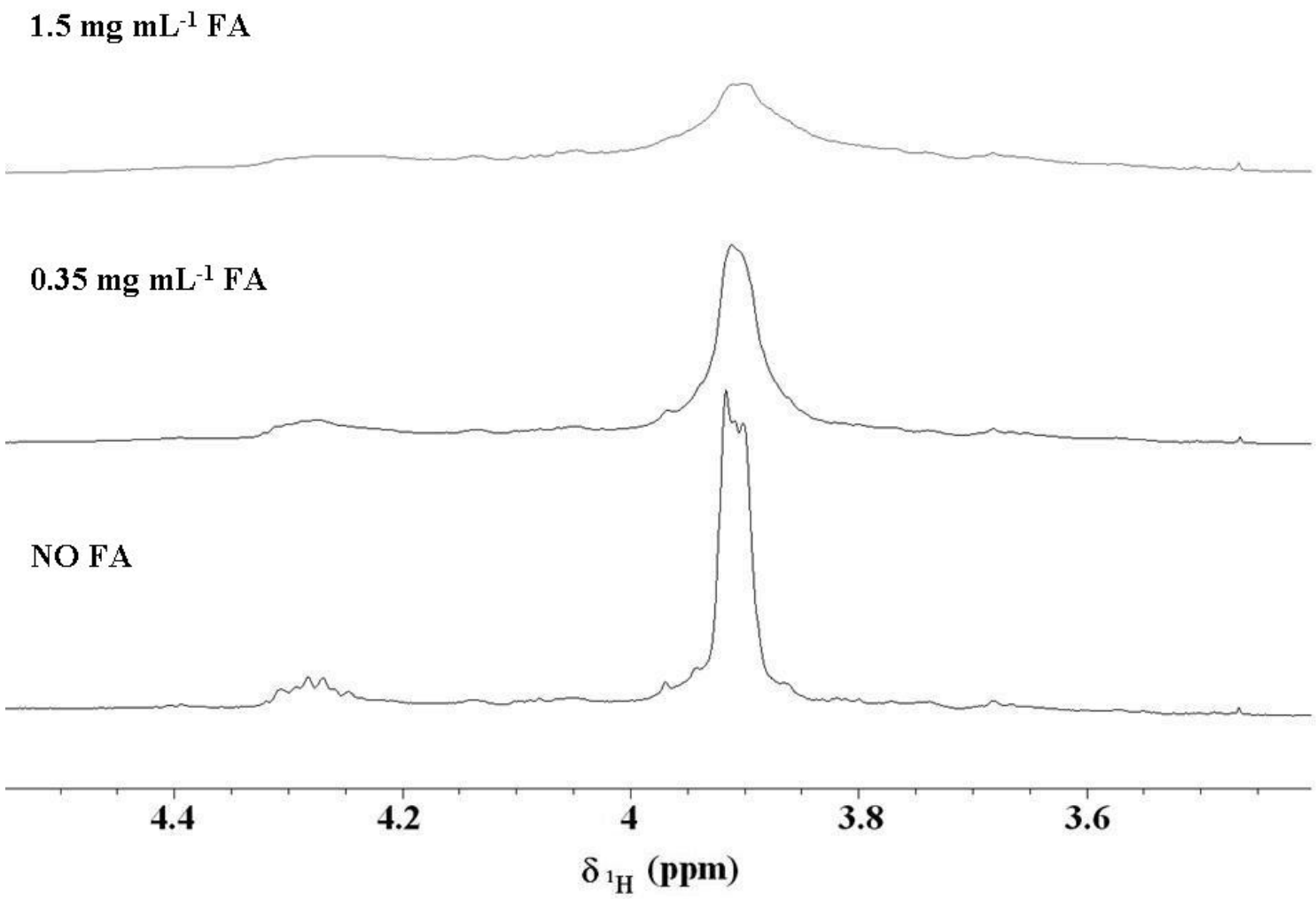

Figure 2. ^{1}H spectra of the 4.5–3.4 ppm interval for the GLU enzyme solution at pH 7.2 with increasing FA concentration.

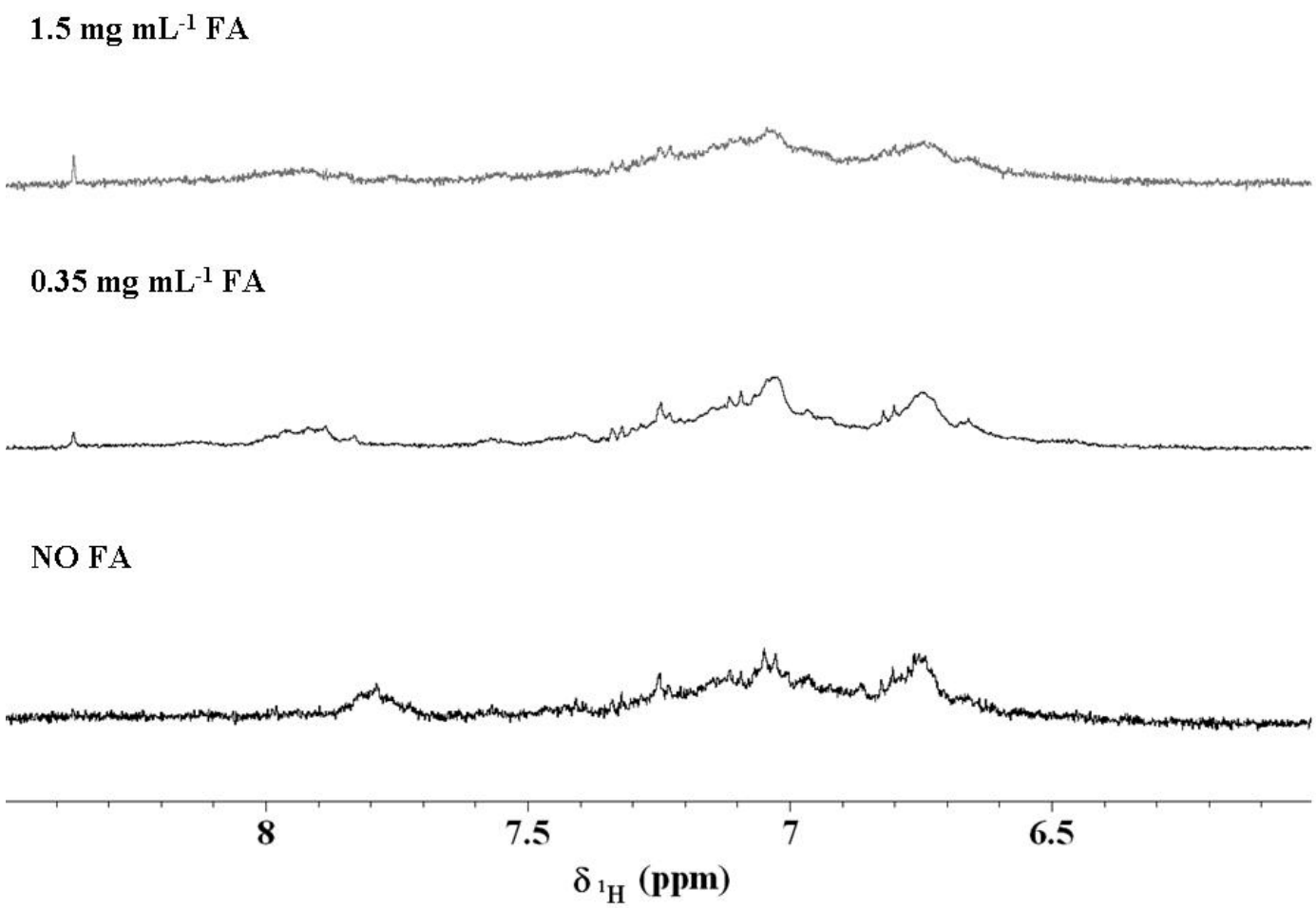

Figure 3. ^{1}H spectra of the 8.5–6 ppm interval for the GLU enzyme solution at pH 7.2 with increasing FA concentration.

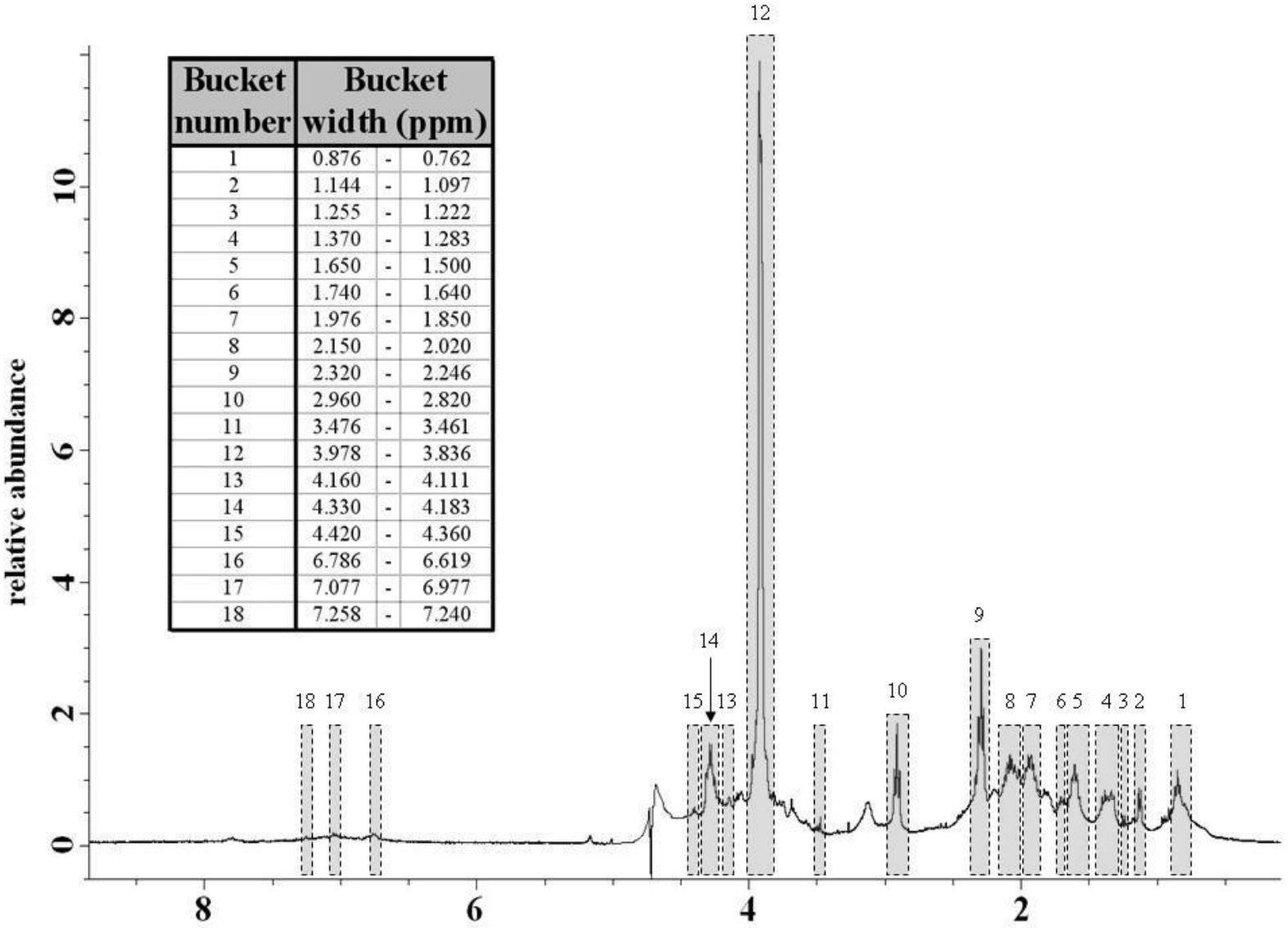

Bucket number	Bucket width (ppm)		
1	0.876	-	0.762
2	1.144	-	1.097
3	1.255	-	1.222
4	1.370	-	1.283
5	1.650	-	1.500
6	1.740	-	1.640
7	1.976	-	1.850
8	2.150	-	2.020
9	2.320	-	2.246
10	2.960	-	2.820
11	3.476	-	3.461
12	3.978	-	3.836
13	4.160	-	4.111
14	4.330	-	4.183
15	4.420	-	4.360
16	6.786	-	6.619
17	7.077	-	6.977
18	7.258	-	7.240

Figure 4. . Bucket partition for the ^{1}H spectrum of β-D-Glucosidase. On the left hand-side of figure, the bucket number and its region limit (ppm) are highlighted.

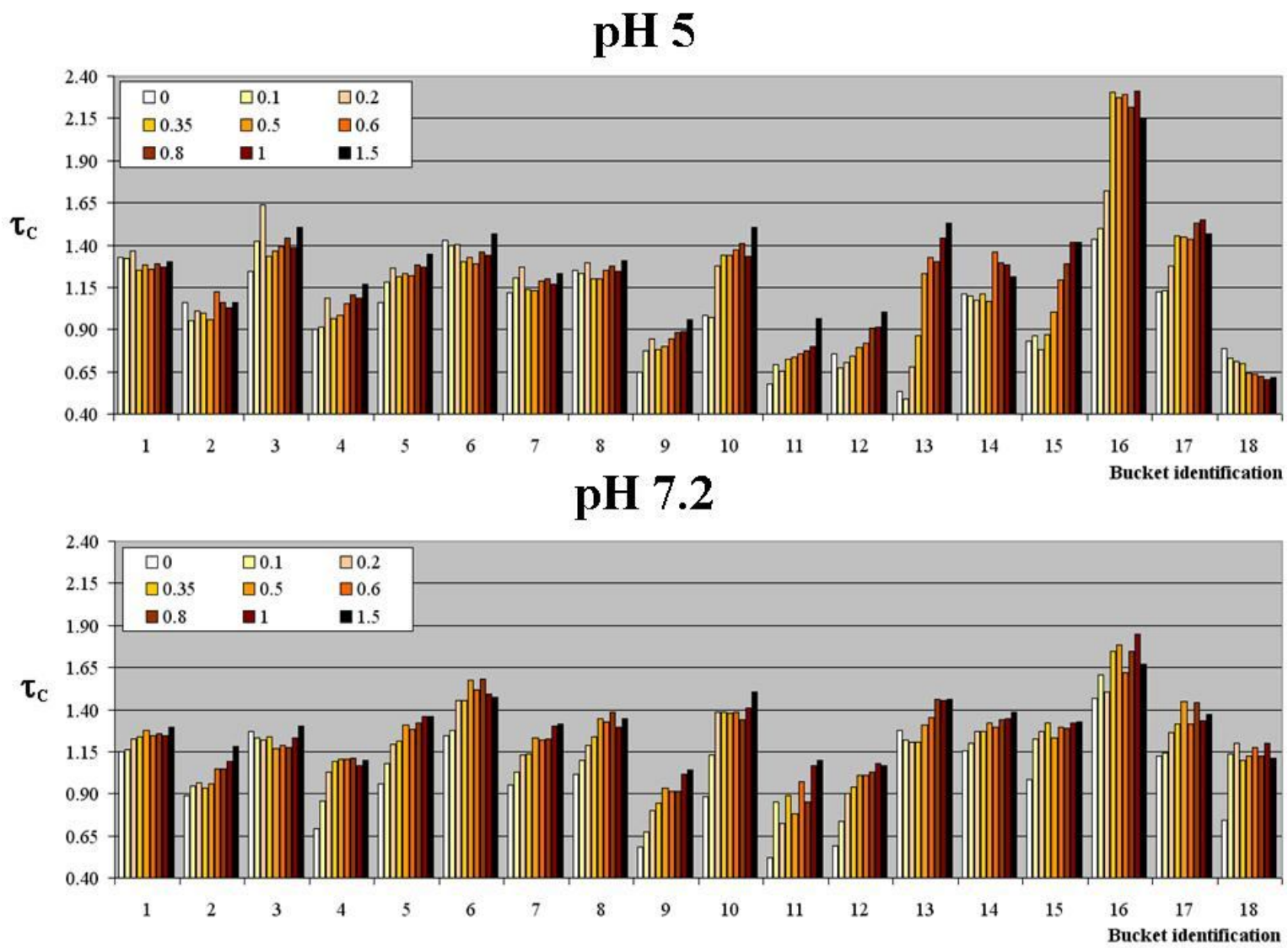

Figure 5. The ^{1}H correlation times (ns) for selected spectral bucket number at pHs 5 and 7.2, as a function of increasing concentration (0, 0.1, 0.2, 0.35, 0.5, 0.6, 0.8, 1, 1.5 mg mL-1) of FA in the GLU solution.

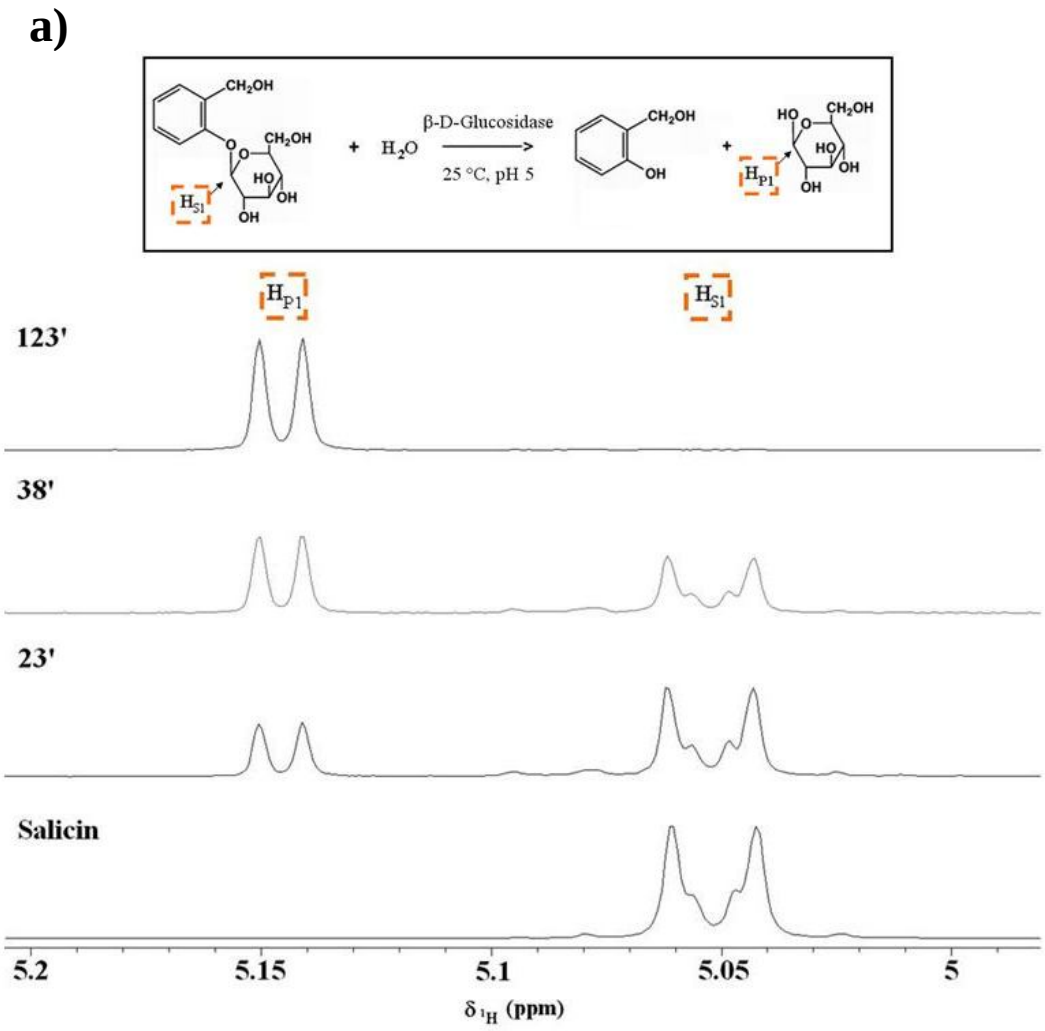

Figure 6. a) ^{1}H spectra of the 5-5.2 ppm interval of Salicin substrate under GLU enzymatic hydrolysis as a function of reaction time (23, 38 and 123 min). **b)** Residual Salicin (%) at different reaction time and FA concentration (mg mL^{-1}).

a)

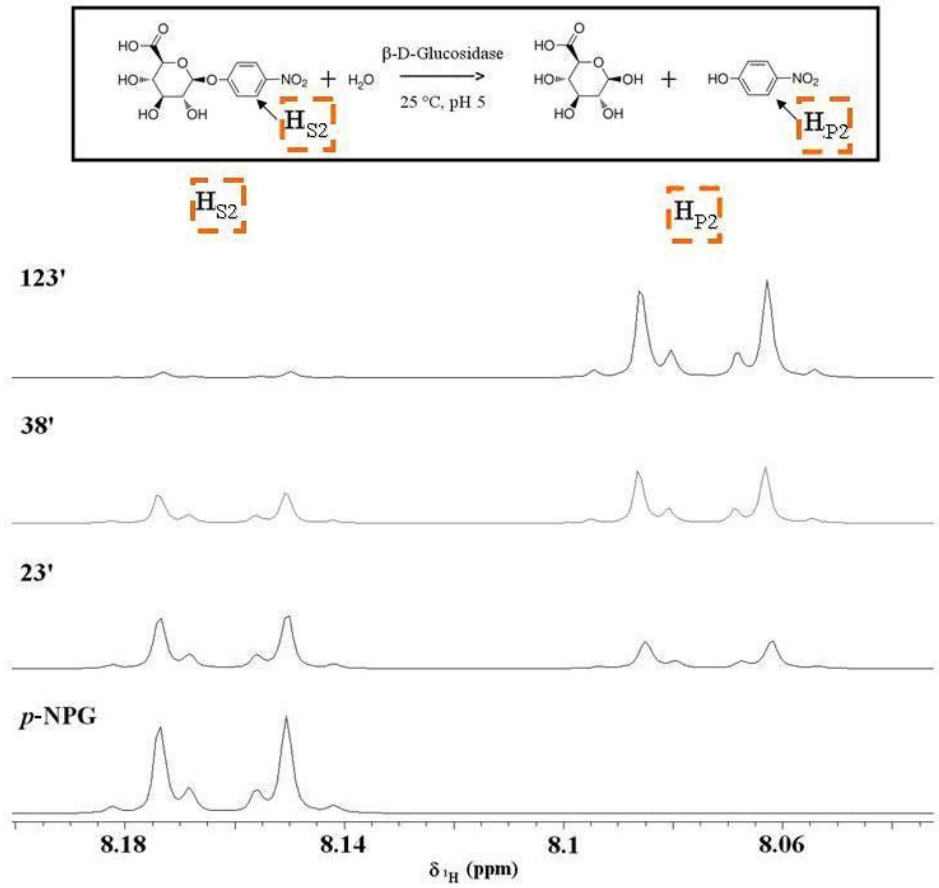

b)

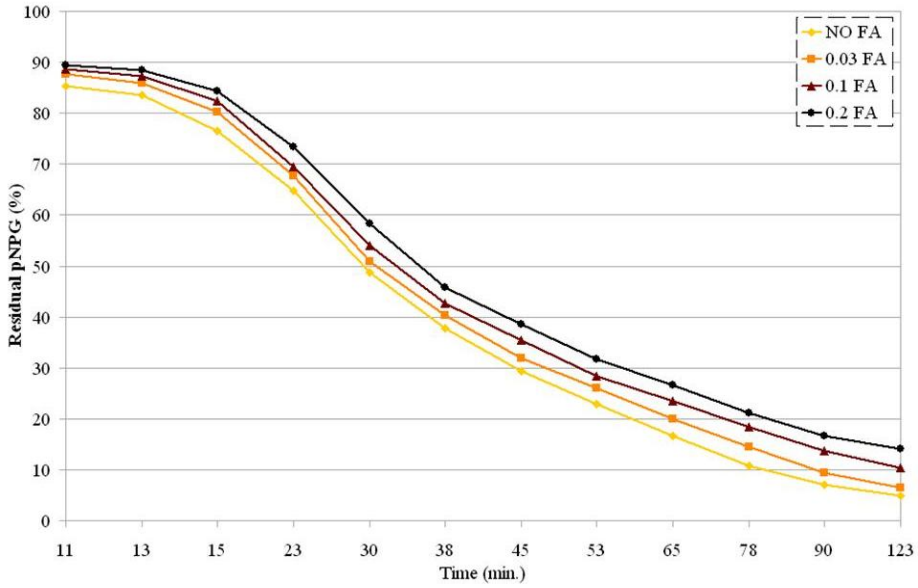

Figure 7. a) ^{1}H spectra of the 8.04-8.20 interval for *p*-NPG under GLU enzymatic hydrolysis as a function of reaction time (23, 38 and 123 min). **b)** Residual *p*-NPG (%) at different reaction time and FA concentration (mg mL^{-1}).

NMR spectroscopy evaluation of the modification of catalytic activity of β-D-Glucosidase following interactions of the enzyme with fulvic acids

Pierluigi Mazzei & Alessandro Piccolo

SUPPORTING INFORMATION

Pages: 2

SUPPORTING MATERIALS AND METHODS

CPMAS ^{13}C-NMR spectroscopy. The cross polarization magic angle spinning (CPMAS) ^{13}C-NMR spectrum of fulvic acids was acquired with a Bruker AVANCE 300, equipped with a 4 mm Wide Bore MAS probe operating at a ^{13}C resonating frequency of 75.475 MHz. Sample (122 mg) was packed in a 4 mm zirconia rotors with Kel-F caps and spun at 13±1 kHz. A ^{1}H ramp sequence was used during a contact time of 1 ms to account for possible inhomogeneity of the Hartmann-Hahn condition.

1500 scans with 1510 data points were collected over an acquisition time of 33.3 ms, and a recycle delay of 2 s. The Bruker Topspin 1.3 software was used to acquire and elaborate the spectra. All the free induction decays (FID) were transformed by applying a 4 k zero filling and a line broadening of 15 Hz.

SUPPORTING FIGURES

One Figure

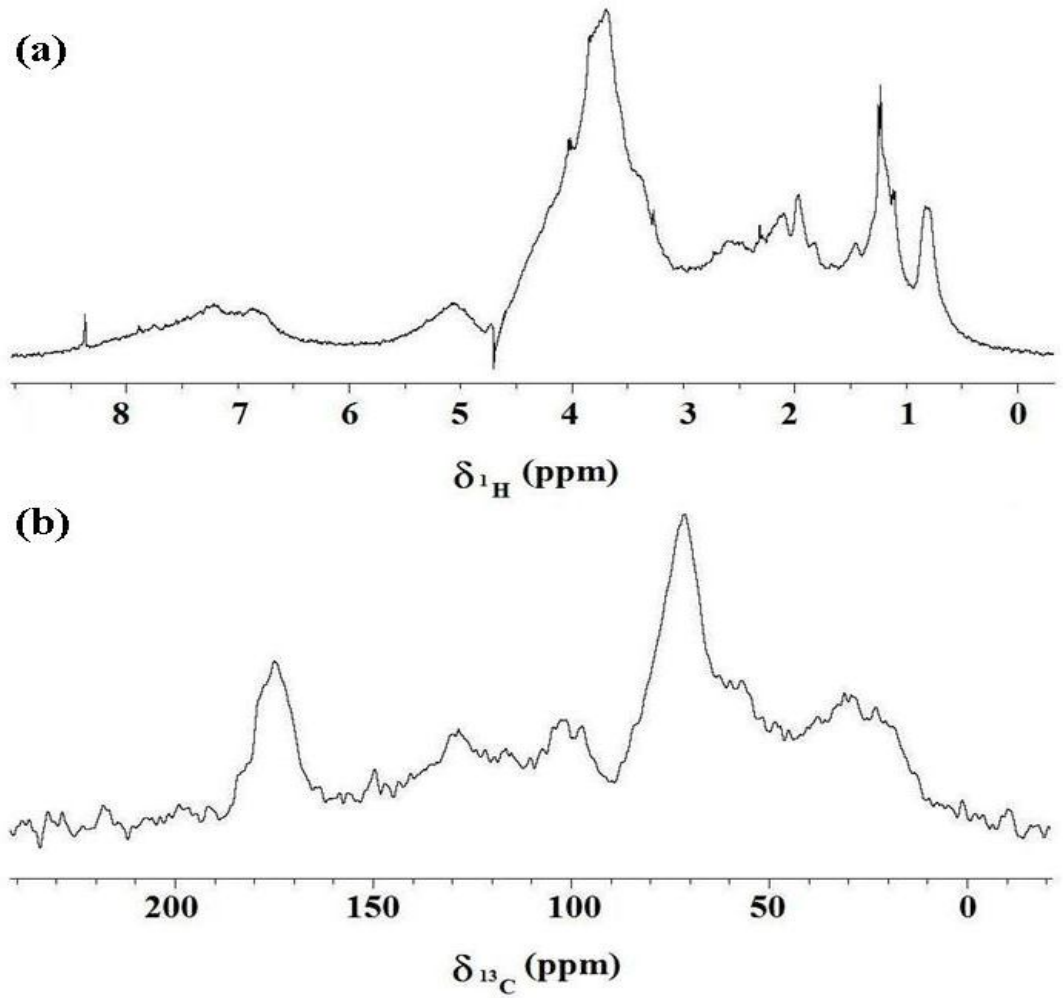

Supplementary Figure 1. ^{1}H liquid-state (a) and ^{13}C CPMAS solid-state (b) NMR spectra of Fulvic acids

6.

Residual catalytic activity of β-D-Glucosidase after immobilization on a humic-clay complex

A preliminary study

6.1. Introduction

The enzymes are present in soil as extracellular exo-enzymes, cytoplasmic exudates, and cell debris, in dead or living cells. A wide range of biotic and abiotic agents (such as the humic substances) can interact with soil enzymes, thus significantly affecting their catalytic activity. Attention is paid here to the β-D-Glucosidase (GLU) enzyme, that plays an important role in the transformation of soil organic matter (see Chapter 5 above).

It has been shown here by ^{1}H-NMR spectroscopy that GLU exhibits a considerable affinity to humic substances and, in particular, with FA, with which a weakly-bound complex is formed at both neutral and slightly acidic conditions. The interactions are attributed to weak bonding forces, including H-bonds. Moreover, it was proved here that the humic-enzyme complex formed in a homogeneous liquid-phase shows a significantly reduced catalytic activity in respect to the free enzyme. This phenomenon was explained with the FA-induced protein conformational modification or obstruction of the enzyme active site. If the formation of humic-enzyme complexes may occur in the soil solution and it accounts for a reduced enzymatic activity in the transformation of dissolved biomolecules, even more important is to verify what would be the residual activity when the enzyme becomes adsorbed on the soil solid phase.

To this aim, a preliminary work is presented here in which an experiment was designed to quantify the catalytic activity exerted in a liquid-solid heterogeneous phase once the

β-D-Glucosidase had been immobilized on a model humic-clay aggregate, represented by an Al-humate-montmorillonite complex (Violante *et al*., 1999).

6.2 Results and discussion

The binding affinity between GLU and the Al-humate-monrtmorillonite (HM) aggregate was calculated on the basis of the results obtained here for the interactions between FA and β-Glucosidase (see Chapter 5). Therefore, the amount of added GLU immobilized on the HM substrate (see Chapter 2 for the adopted experimental procedure) is reported in Table 1 below. The results indicate that about 20% of the added GLU was rather strongly adsorbed on the HM surfaces. In fact, much of the weakly-adsorbed enzyme was removed by the first water washing (55.6 mg per g HM), whereas the remaining part (24.4 mg per g of HM) was removed during the next 3 washing cycles (Table 1).

The residual activity of GLU immobilized on HM was monitored by conducting a heterogeneous catalysis at pH 5 and at 25 °C. The reaction was started by adding 2000 μg mL^{-1} of Salicin substrate and the extent of hydrolysis was quantified by measuring the Salicin concentration as a function of reaction time (Table 2) . At the same time, two different control samples were prepared. The first one was obtained by starting the catalysis in a homogeneous liquid phase (LP), while the second one was set by adding the Salicin to an untreated HM, representing the control sample. The Salicin detection was conducted by an HPLC gradient elution to exclude the overlapping of the Salicin peak (RT = 14.1 ± 0.12 min) on that of the catalytic product, that was 2 hydroxy-methylphenol (RT = 17.3 ± 0.25 min).

Table 2 reports the amount of Salicin measured during the catalysis conducted in both liquid phase (LP) and liquid-solid phase (LSP) as a function of the reaction time. By measuring Salicin concentration in the control sample (data not shown), it was found that only 90.6 % of the added Salicin was detected in solution as a consequence of its adsorption on HM. This is due to the strong

affinity existing between the aromatic Salicin structure and the hydrophobic domains of the HM aggregate.

The extent of hydrolysis observed in LSP was significantly different from that detected in LP (Table 2). In fact, after 20 min (0.33 hours) around 69.6 % of the substrate in the liquid phase was converted in glucose and 2-hydroxy-methyl-phenol, while only the 8.7% of Salicin was hydrolysed in liquid-solid phase. After 1 h, 97.4% and the 23.6% were the residual substrate percentage left in the LSP and LP catalytic systems, respectively. Finally, the substrate was totally degraded (>99 %) within 4 hours (corresponding to an average hydrolysis rate of 25.9 nmoles of Salicin per min, respectively) in the homogeneous liquid phase, whereas a similar extent of hydrolysis was achieved after about two days and 18 h (1.6 nmoles of Salicin per min) in the heterogeneous liquid-solid phase.

These preliminary results showed, first of all, that the β-Glucosidase enzyme was successfully immobilized on a OH-Al-humate-montmorillonite substrate (20 mg per g^{-1} HM). Then, it was verified that when the enzymatic catalysis was conducted in the heterogeneous liquid-solid phase containing the solid GLU-HM adduct, the enzyme adsorption on the humic-clay material strongly affected the catalytic activity of β-Glucosidase, as compared to that exerted in the liquid phase. In fact, the average hydrolysis rate measured for the immobilized enzyme was more then ten times lower than that detected for the free enzyme in the liquid phase.

Tables

Table 1. Concentration of GLU (mg mL^{-1}) detected in the collected supernatants and resulting immobilized enzyme (mg g^{-1} of HM) after consecutive washing cycles (S).

	S1	S2	S3	S4	S5
Removed enzyme	**2.78**	**0.80**	**0.23**	**0.20**	**0**
Total Immobilized enzyme	44.4	28.4	23.9	20.0	20.0

Table 2. Salicin concentration (μg mL^{-1}) resulting after β-D-Glucosidase catalysis (25 °C, pH 5) in homogenous liquid phase (LP) and in heterogeneous liquid-solid phase (LSP) as a function of catalytic reaction time (h).

Reaction time	LP1	LP2	Mean	Standard deviation (%)	LSP1	LSP2	LSP3	Mean	Standard deviation (%)
0.04	1229.5	1215.4	**1222.5**	0.8	1693.3	1695.1	1576.2	**1654.9**	4.1
0.33	555.2	547.7	**551.4**	1.0	1618.8	1585.5	1469.1	**1557.8**	5.0
0.66	195.3	180.3	**187.8**	5.6	1540.8	1480.6	1398.0	**1473.1**	4.9
1	51.5	42.3	**46.9**	13.9	1457.9	1378.1	1315.5	**1383.8**	5.2
2.5	13.3	8.3	**10.8**	32.5	1410.4	1362.2	1263.6	**1345.4**	5.6
4	5.4	3.6	**4.5**	27.9	1367.0	1324.7	1217.7	**1303.1**	5.9
6.5	-	-	-	-	1196.9	1224.5	1118.3	**1179.9**	4.7

7.

Conclusion

This thesis presents the experiments by liquid-state Nuclear Magnetic Resonance (NMR) spectroscopy devoted to reveal the type of interactions established between humic substances and three molecules largely occurring in soil: the herbicide glyphosate and the enzymes β-D-Glucosidase and Alkaline Phosphatase.

It was found that humic substances formed host-guests weakly-bound complexes with all the agro-molecules examined here. Generally, NMR spectra showed an enlargement of resonance signals, that was strictly related to an ever enhancing molecular rigidity due to the increasing content of humic matter in solution. In fact, signal broadening suggests a decreased proton relaxation rate that arises from the development of dipolar interactions increasingly given by the formation of host-guests complexes and the consequent restricted molecular mobility.

In the case of Glyphosate, larger signal variations (broadening and chemical shift) were found for increasing amount of humic matter. However, this phenomenon was larger for the addition of FA than for HA, and, for the pH 5.2 than for pH 7. This implies that the most effective interactions must have been those which were established among the protonated acidic groups of the herbicide and the largely hydrophilic fulvic acid. Both chemical shift drifts of spectral signals and STD experiments showed that protons of the Glyphosate phosphonic group were responsible for the interactions with humic matter.

The molecular spin correlation times (τ_c) were derived by direct NMR measurements of both spin-lattice (T_1) and spin-spin (T_2) relaxation times, which, together with the diffusion coefficients measured by DOSY-NMR spectroscopy, confirmed the occurrence of weakly-bound complexes between humic matter and the studied agro-molecules. In fact, the changes in self-diffusion

coefficients and correlation times appeared consistent and depending on the amount of humic matter added to the agro-molecule solutions. In the case of glyphosate, diffusion measurements showed that the formation of the humic-glyphosate complex was thermodynamically favoured at only pH 5.2 and allowed the calculation of the Gibbs free energies of association.

^{1}H NMR spectra permitted to examine the activity of both soil enzymes in homogeneous liquid phase, as a function of reaction time. In both cases, it was found that the reduction of substrate signal intensity was significantly slowed down when humic molecules adsorption modified the enzymes structure. In fact, the arrangement of enzymes in a non-covalent humic-enzymatic complexes, reduced the enzyme-substrate affinity, thus negatively influencing the catalytic activity.

Moreover, in a preliminary work presented in this thesis, β-Glucosidase was successfully immobilized on OH-Al-humate-montmorillonite. When the enzymatic catalysis reaction was conducted in a heterogeneous phase in the presence of the solid immobilized enzyme, it was observed that the enzyme adsorption on the humic-clay support strongly inhibited the activity of β-Glucosidase, as compared to free enzyme and even to that observed for the host-guest complex in solution.

The results of this thesis seem to contribute to a experimentally-based prediction of the fate and reactivity of agro-molecules when they come in interaction with soluble humic matter. In the case of glyphosate, the findings highlight the importance of weak but spontaneous interactions of this herbicides to the hydrophilic fulvic fraction of soil organic matter resulting in a host-guest association. In the case of the β-D-Glucosidase and Alkaline Phosphatase enzymes, the results suggest, by direct NMR evidence, that extracellular enzymes, which are reputed to play a significant role in the out-of-cell molecular transformations in the environment, may be severely reduced in their activity when interacting with the ubiquitous natural organic matter. These findings indicate that the presumed role of soil enzymes in the transformation and conversion of organic matter in soil must be approached with renewed care.

8.

References

Albers, C. N., Banta, G. T., Hansen, P. E., Jacobsen, O. S., 2009- The influence of organic matter on sorption and fate of glyphosate in soil – Comparing different soils and humic substances. Enc. Pol. 157 (10), 2865-2870.

Andreux, F., 1996. Humus in world soils. In Humic Substances in Terrestrial Ecosystems; Piccolo A.; Ed. Elsevier: Amsterdam.

Baalousha M., Motelica-Heino M., Le Coustumer P. 2006.Conformation and size of humic substances: Effects of major cation concentration and type, pH, salinity, and residence time. Colloids and Surfaces A: Physicochem. Eng. Aspects 272, 48–55.

Bakhmutov, V. I., 2004. Pratical NMR Relaxation for chemists.John Wiley & sons, Ltd.,Chicester, West Sussex, England.

Brand, T., Cabrita, E. J., Berger, S, 2005. Intermolecular interaction as investigated by NOE and diffusion studies. Prog. Nucl. Mag.Reson. Spectrosc. 46, 159–196.

Bentley, R., Haslam, E., 1990. The Shikimate Pathway - A Metabolic Tree with Many Branche. Crit. Rev. Biochem. Mol. Biol. 25, 307–383.

Bock, K. & Sigurskjold, B. W., 1988. Mechanism and binding specificity of β-glucosidase-catalyzed hydrolysis of cellobiose analogues studied by competition enzyme kinetics monitored by ^{1}H NMR spectroscopy. European Journal of Biochemistry 178, 711-720.

Borggaard, O. K., Gimsing, A. L., 2008. Fate of glyphosate in soil and the possibility of leaching to ground and surface waters: a review. Pest. Manag. Sci. 64, 441-456.

Bortiatynski, J. M., Hatcher P. G., Minard, R. D., 1997. The development of ^{13}C labeling and ^{13}C NMR spectroscopy techniques to study the interaction of pollutants with humic substances. In Nuclear Magnetic Resonance Spectroscopy in Environmental Chemistry; Nanny, M. A., Minear, R. A., Leenheer, J. A., Eds.; Oxford University Press: New York.

Bridges, E. M., Mukhopadhyay, S. S., 2003. Processes of soil formation. In handbook of processes and modelling in the soil-plant system. Benbi, D. K., Nieder, R. Eds. Food product press, The Haworth reference press New York.

Bums, R. G., 1982. Enzyme activity in soil: location and a possible role in microbial ecology. Soil Biology & Biochemistry 14, 423-427.

Burns, R. G., 1986. Interactions of enzymes with soil mineral and organic colloids. In: Interactions of Soil Minerals with Natural Organics and Microbes. (eds P. M. Huang & M. Schnitzer), pp. 429-451. Soil Science Society of America, Madison, WI.

Busse, M. D., Ratcliff, A. W., Shestak, C. J., Powers, R. F., 2001. Glyphosate toxicity and the effects of long-term vegetation control on soil microbial communities. Soil Biol. Biochem. 33, 1777-1789.

Busto, M. D. & Perez-Mateos, M., 2000. Characterization of β-D-glucosidase extracted from soil fractions. European Journal of Soil Science 51, 193-200.

Cantor, C. R., Schimmel, P. R., 1980. Biophysical chemistry. Part II: Techniques for the study of biological structure and function. Freeman, New York.

Carper, W. R., Keller, C. E., 1997. Direct Determination of NMR correlation times from spin-lattice and spin-spin relaxation times. Journal of Physical Chemistry A 101, 3246-3250.

Cartigny, B., Azaroual, N., Imbenotte, M., Mathieu, D., Vermeersch, G., Goulle´ , J. P., Lhermitte, M., 2004. Determination of glyphosate in biological fluids by ^{1}H and ^{31}P NMR spectroscopy. Forensic Sci. Int. 143, 141–145.

Ceccanti, B., Doni, S., Macci, C., Cercignani, G., Masciandaro, G., 2008. Characterization of stable humic–enzyme complexes of different soil ecosystems through analytical isoelectric focussing technique (IEF). Soil Biology & Biochemistry 40, 2174–2177.

Chamignon, C., Haroune, N., Forano, C., Delort, A.M., Besse-Hoggan, P., Combourieu, B., 2008. Mobility of organic pollutants in soil components. What role can magic angle spinning NMR play? Eur. J. Soil Sci. 59, 572–583.

Chapman, S., Cowling, T. G., 1990. The mathematical theory of non-uniform gases: an account of the kinetic theory of viscosity, thermal conduction, and diffusion in gases. Chapter 6. Elementary theories of the transport phenomena. (3th Ed.). Cambridge, pp. 97-108.

Cobas, J. C., Groves, P., Martín-Pastor, M., De Capua, A., 2005. New applications, processing methods and pulse sequences using diffusion NMR. Curr. Anal. Chem 1, 289–305.

Cohen, Y., Avram, L., Frish, L., 2005.Diffusion NMR spectroscopy. Angew. Chem., Int. Ed. 44, 520–554.

Colombo, S. D. M., Masini, J. C., 2011. Developing a fluorimetric sequential injection methodology to study adsorption/ desorption of glyphosate on soil and sediment samples. Microchem. J. 98, 260–266.

Cozzolino, A., Conte, P., Piccolo, A., 2001. Conformational changes of humic substances induced in some hydroxy-, keto-, and sulfonic acids. Soil. Biol. Biochem. 33, 563-571.

Dick, R.P., 1997. Soil enzyme activities as integrative indicators of soil health. In: Pankhurst, C.E., Doube, B.M., Gupta, V.V.S.R. (Eds.), Biological Indicators of Soil Health. CAB International, Wallingford, UK, pp. 121–156.

Dick, W. A., Cheng, L., Wang, P., 2000. Soil acid and alkaline phosphatase activity as pH adjustment indicators. Soil Biology & Biochemistry 32, 1915–1919.ù

Dixon, A. M., Mai, A. M., Larive, C. K., 1999. NMR investigation of the interactions between 4′-fluoro-1′-acetonaphtone and the Suwanee river fulvic acid. Environ. Sci. Technol. 33, 958–964.

Eastman, M. A., Brothers, L. A., Nanny, M. A., 2011. ^{2}H NMR Study of Dynamics of Benzene-D6 Interacting with Humic and Fulvic Acids. The journal of physical chemistry A 115, 4359–4372.

Eriksson, H. J. C., Somsen, G. W., Hinrichs, W. L. J., Frijlink, H. W., De Jong, G. J., 2001. Characterization of human placental alkaline phosphatase by activity and protein assays, capillary electrophoresis and matrix assisted laser desorption / ionization time-of-flight mass spectrometry. Journal of Chromatography B, 755, 311–319.

Fomba, K. W., Galvosas, P., Roland, U., Kaerger, J., Kopinke, F. D., 2011. Mobile Aliphatic Domains in Humic Substances and Their Impact on Contaminant Mobility within the Matrix. Environmental Science and Technologies 45, 5164–5169.

Ganin, E. V., Vang, V. D., 2003. Host-Guest Complexes. Selective Reaction of Crown Ether Hosts with Triphenylmethane Derivatives. Russian Journal of General Chemistry 73 (8), 1320-1321.

Ge, X., D'Avignon, D.A., Ackermana, J. J. H., Sammons, R. D., 2010. Rapid vacuolar sequestration: the horseweed glyphosate resistance mechanism. Pest. Manag. Sci. 66, 345–348.

George, T . S., Turner, B. L., Gregory, P. J., Cade-menun, B. J., Richardson, A. E., 2006. Depletion of organic phosphorus from Oxisols in relation to phosphatase activities in the rhizosphere. European Journal of Soil Science 57, 47–57.

Ghosh, K., and Schnitzer, M., 1980. Macromolecular structures of humic substances. Soil Sci. 129, 266-276.

Grover, A. K., Macmurchie, D. D., Cushley, R. J., 1977. Studies on almond emulsion beta-D-glucosidase. I. Isolation and characterization of a bifunctional isozyme. Biochimica and Biophysica Acta 482 (1), 98-108.

Grover, A. K., Cushley, R. J., 1977. Studies on almond emulsion beta-D-glucosidase. II. Kinetic evidence for independent glucosidases and galactosidase sites. Biochimica and Biophysica Acta 482 (1), 109-124.

Hao, C., Morse, D., Morra, F., Zhao, X., Yang, P., Nunn, B., 2011. Direct aqueous determination of glyphosate and related compounds by liquid chromatography/tandem mass spectrometry using reversed-phase and weak anion-exchange mixed-mode column. J. Chromatography A. 1218, 5638– 5643.

Hayes, M. H. B., Swift, R. S., 1978. The chemistry of soil organic colloids. In: The chemistry of soil constituents. Greenland & Hayes ed., pp. 179-320.

Hayes, W. J., Wayland, J., Laws, E. R., 1991. Handbook of pesticide Toxicology. Vol 3; San Diego, California, pp. 1339–1340.

He, S., Withers, S. G., 1997. Assignment of sweet almond β-Glucosidase as a family 1 glycosidase and identification of its active site nucleophile. The journal of Biological Chemistry 272 (40), 24864-24867.

Holtz, K. M., Kantrowitz, E. R., 1999. The mechanism of the alkaline phosphatase reaction: insights from NMR, crystallography and site-specific mutagenesis. FEBS Letters 462, 7-11.

Houk, K. N., Leach, A. G., Kim, S. P., Zhang, X. 2003. Thermodynamic Organic Complexes. Binding Affinities of Host–Guest, Protein–Ligand, and Protein–Transition-State Complexes. Angew. Chem. Int. 42, 4872 – 4897.

Hu, Y. S., Zhao, Y. Q., Sorohan, B., 2011. Removal of glyphosate from aqueous environment by adsorption using water industrial residual. Desalination 271, 150-156.

Iakimenko, O., Otabbong, E., Sadovnikova, L., Persson, J., Nilsson, I., Orlov, D., Ammosova, Y., 1996. Dynamic transformation of sewage sludge and farmyard manure components. 1. Content of humic substances and mineralisation of organic carbon and nitrogen in incubated soils. Agriculture, Ecosystems and Environment 58, 121-126.

Kim, E. E., Harold, W. W., 1991. Reaction mechanism of alkaline phosphatase based on crustal structures. Journal of Molecular Biology 218, 449-464.

Langmuir, I., 1916. The constitution and fundamental properties of solids and liquids. part I. Solids. J. Am. Chem. Soc. 38, 2221-2295.

Lawson, S. L., Antony, R., Warren, j., Withers, S. G., 1998. Mechanistic consequences of replacing the active-site nucleophile Glu-358 in Agrobacterium sp. β-glucosidase with a cysteine residue. Biochemistry Journal 330, 203-209.

Le Du, M. H., Stigbrand, T., Taussigi, M. J., Ménez, A., Stura, E. A., 2001. Crystal Structure of Alkaline Phosphatase from Human Placenta at 1.8 Å Resolution. Implication for a substrate. 276 (12), 9158–9165.

Legler, G., Harder, A., 1978. Amino acid sequence at the active site of β-glucosidase a from bitter almonds. Biochimica et Biophysica Acta (BBA) – Enzymology 524 (1), 102-108.

Lipok, J., Owsiak, T., Młynarz, P., Forlani, G., Kafarski, P., 2011. Phosphorus NMR as a tool to study mineralization of Organophosphonates - The ability of Spirulina spp. to degrade glyphosate. Enzyme Microb. Tech. 41, 286–291.

Llinas, P., Stura, E. A., Ménez, A., Kiss, Z., Stigbrand, T., Millàn, J. L., Le Du, M. H. 2005. Structural Studies of Human Placental Alkaline Phosphatase in Complex with Functional Ligands. Journal of Molecular Biology 350, 441–451.

Longstaffe, J. G., Simpson, A. J., 2011. Understanding solution-state noncovalent interactions between xenobiotics and natural organic matter using $^{19}F/^{1}H$ heteronuclear saturation transfer difference nuclear magnetic resonance spectroscopy. Environmental Toxicology and Chemistry 30 (8), 1745–1753.

Mamy, L., Barriuso, E., Benoit, G., 2005. Environmental fate of herbicides trifluralin, metazachlor, metamitron and sulcotrione compared with that of glyphosate, a substitute broad spectrum herbicide for different glyphosate-resistant crops. Pest. Manag. Sci. 61, 905-916.

Mayer, M., Meyer, B., 1999. Characterization of Ligand Binding by Saturation Transfer Difference NMR Spectroscopy. Angew. Chem. Int. Ed. 38 (12), 1784-1788.

Meyer, B., Peters, T., 2003. NMR Spectroscopy Techniques for Screening and Identifying Ligand Binding to Protein Receptors. Angew. Chem. Int. Ed. 42 (8), 864-890.

Mondini, C., Fornasier, F., Sinicco, T., 2004. Enzymatic activity as a parameter for the characterization of the composting process. Soil Biology & Biochemistry 36, 1587–1594.

Nannipieri, P., Sequi, P., Fusi, P., 1996. Humus and enzyme activity. In: Piccolo, A. (Ed.), Humus Substances in Terrestrial Ecosystems. Elsevier Science B.V., Amsterdam, pp. 293–328.

Nannipieri, P., Kandeler, E., Ruggiero, P., 2002. Enzyme activities and microbiological and biochemical processes in soil. In: Burns, R.G., Dick, R.P. (Eds.), Enzyme in the Environment. Activity, Ecology and Application. Marcel Dekker, Inc., New York, Basel, pp. 1–33.

Nanny, M. A. 1999. Deuterium NMR characterization of noncovalent interactions between monoaromatic compounds and fulvic acids. Org. Geochem. 30, 901–909.

Nanny, M. A., Bortiatynski, M., Hatcher, P. G., 1997. Noncovalent interactions between acenaphtenone and dissolved fulvic acid as determined by 13CNMRT1 relaxation measurements. Environ. Sci. Technol. 31, 530–534.

Nardi, S., Sessi, E., Pizzeghello, D., Sturaro, A., Rella, R., Parvoli, G., 2002. Biological activity of soil organic matter mobilised by root exudates. Chemosphere 46, 1075–1081.

Nebbioso, A., Piccolo, A., 2011. Basis of a Humeomics Science: chemical fractionation and molecular characterization of humic biosuprastructures. Biomacromolecules 12, 1187–1199.

Nelson, D.L., Cox, M. M., 2004. Enzymes In: Lehninger – Principles of biuochemistry 4th Edition. pp. 191-225.

Oades, J. M, 1984. Soil organic matter and structural stability, mechanisms and implication for management. Plant soil 76, 319-337.

Olander, L. P., Vitousek, P. M., 2000. Regulation of soil phosphatase and chitinase activity by N and P availability. Biogeochemistry 49, 175–190.

Peuravuori, J. 2005. NMR spectroscopy study of freshwater humic material in light of supramolecular assembly. Environ. Sci. Technol., 39, 5541-5549.

Piccolo, A., 1988. Characteristics of soil humic extracts obtained by some organic and inorganic solvents and purified by HCL-HF treatment. Soil Science 146, 418-426.

Piccolo, A., Celano, G., 1993. Modification of infrared spectra of the herbicide glyphosate induced by pH variation. J. Environ. Sci. Health B28 (4), 447-457.

Piccolo, A., Celano, G., Arienzo, M., Mirabella, A, 1994. Adsorption and desorption of Glyphosate in some European soils. J. Environ. Sci Heal B. B29 (6), 1105-1115.

Piccolo, A., Celano, G., 1994. Hydrogen bonding interactions of the herbicide Glyphosate with water soluble humic substances. Environ. Toxicol. Chem. 13, 1737-1741.

Piccolo, A., Celano, G., Conte, P., 1996. Adsorption of Glyphosate by Humic Substances. J. Agric. Food Chem. 44, 2442-2446.

Piccolo, A., Conte, P., Cozzolino, A., 1999. Effects of mineral and monocarboxylic acids on the molecular association of dissolved humic substances. European Journal of Soil Science 50, 687-694 .

Piccolo, A., 2001. The supramolecular structure of humic substances. Soil Science, 166:810–832.

Piccolo, A., Conte, P., Cozzolino, P., 2001. Chromatographic and spectrophotometric properties of dissolved humic substances compared with macromolecular polymers. Soil Science 166, 174-185.

Piccolo, A., 2002. The Supramolecular structure of humic substances. A novel understanding of humus chemistry and implications in soil Science. Adv. Agron. 75, 57-134.

Piccolo, A., Spiteller, M., 2003. Electrospray ionization mass spectrometry of terrestrial humic substances and their size fractions. Anal. Bioanal. Chem. 377, 1047-1059.

Piccolo, A., Conte, P., Cozzolino, A., Spaccini. R. 2003. in: D.K. Benbi and R. Nieder (Eds.), Handbook of processes and modelling in soil-plant system. Haworth Press, New York, 2003, pp. 83-120.

Piccolo, A., Spiteller, M., Nebbioso, A., 2010. Effects of sample properties and mass spectroscopic parameters on electrospray ionization mass spectra of size-fractions from a soil humic acid. Analytical and Bioanalytical Chemistry 397, 3071-3078.

Pickford, A. R., Campbell, I. D., 2004. NMR Studies of Modular Protein Structures and Their Interactions. Chemical Reviews 104, 3557-3565.

Pilar, M. C., Ortega, N., Perez-Mateos, M., Busto, M. D., 2003. Kinetic behaviour and stability of escherichia coli ATCC27257 alkaline phosphatase immobilised in soil humates. Journal of the Science of Food and Agriculture 83, 232–239.

Perez-Mateos, M., Busto, M. D., Rad, J. C., 1991. Stability and Properties of Alkaline Phosphate Immobilized by a Rendzina Soil. Journal of the Science of Food and Agriculture 55, 229-240.

Price, K. E., Lucas, L. H., Larive, C. K., 2004. Analytical applications of NMR diffusion measurements. Anal. Bioanal. Chem. 378, 1405–1407.

Quiquampoix, H., Servagent-Noinville, S., Baron, M., 2002. Enzyme adsorption on soil mineral surfaces and consequences for the catalytic activity. In: Burns RG, Dick RP (eds) Enzymes in the environment. Marcel Dekker, New York, pp 285–306.

Richardson, A. E., George, T. S., Hens, M., Simpson, R. J., 2005. Utilization of soil organic phosphorus by higher plants. In: Organic Phosphorus in the Environment (eds B.L. Turner, E. Frossard & D. Baldwin). CABI Publishing, Wallingford, pp. 165–184.

Ranieri-Raggi, M., Ronca, F., Sabbatini A., Raggi, A., 1995. Regulation of skeletal-muscle AMP deaminase: involvement of histidine residues in the pH-dependent inhibition of the rabbit enzyme by ATP. Biochem. J. 309, 845-852.

Ritter, P., 1998. Gli Enzimi. In: Fondamenti di Biochimica, Zanichelli, pp. 98-116.

Rye, C. S., Withers, S. G., 2000. Glycosidase mechanisms. Current Opinion on Chemical Biology 4, 573–580.

Sanchez-Perez, R., Joergensen, K., Motawia, M. S., Dicenta, F. and Moeller, B. L., 2009. Tissue and cellular localization of individual β-glycosidases using a substrate-specific sugar reducing assay. Plant Journal 60, 894–906.

Sapienza, P. J., Lee, A. L., 2010. Using NMR to study fast dynamics in proteins: methods and Applications. Current Opinion in Pharmacology 10, 723–730.

Saratchandra, S. U. & Perrott, K. W., 1984. Assay of b-Glucosidase activity in soils. Soil Science 138, 15-19.

Sarkar, J.M., Leonowicz, A., Bollag, J.M. 1989. Immobilization of enzymes on clays and soils. Soil Biol Biochem 21, 223–230.

Schimel, J.P. , Bennett , J. , 2004. Nitrogen mineralization: challenges of a changing paradigm. Ecology 85, 591–602.

Schmidt, S., Rainieri, S., Witte, S., Matern, U., Martens, S., 2011. Identification of a Saccharomyces cerevisiae Glucosidase That Hydrolyzes Flavonoid Glucosides. Applied and environmental microbiology 77 (5), 1751-1757.

Schonbrunn, E., Eschenburg, S., Shuttleworth, W. A., Schloss, J. V., Amrheini, N., Evans, J. N. S., Kabsch, W., 2001. Interaction of the herbicide glyphosate with its target enzyme 5-enolpyruvylshikimate 3-phosphate synthase in atomic detail. PNAS 98 (4), 1376–1380.

Shirzadi, A., Simpson, M. J., Xu, Y., 2008. Simpson A.J. Application of Saturation Transfer Double Difference NMR to Elucidate the Mechanistic Interactions of Pesticides with Humic Acid. Environ. Sci. Technol. 42, 1084–1090.

Simpson, A. J., 2002. Determining the molecular weight, aggregation, structures and interactions of natural organic matter using diffusion ordered spectroscopy. Magn. Reson. Chem. 40, S72-S82.

Sinsabaugh, R.L., Moorhead, D.L., 1994. Resource allocation to extracellular enzyme production: a model for nitrogen and phosphorus control of litter decomposition. Soil Biol Biochem 26, 1305–1311.

Smejkalova, D., Piccolo, A., 2008 a. Aggregation and disaggregation of humic supramolecular assemblies by NMR diffusion ordered spectroscopy (DOSY-NMR). Environmental Science and Technologies 42, 699–706.

Smejkalova, D., Piccolo, A., 2008 b. Host-Guest Interactions between 2,4-Dichlorophenol and Humic Substances As Evaluated by ^{1}H NMR Relaxation and Diffusion Ordered Spectroscopy. Environmental Science and Technologies 42, 8440–8445.

Smejkalova, D., Spaccini, R., Fontaine, B., Piccolo, A., 2009. Binding of Phenol and Differently Halogenated Phenols to Dissolved Humic Matter As Measured by NMR Spectroscopy. Environmental Science and Technologies 43, 5377–5382.

Smeulders, D. E., Wilson, M. A., Kannangara, G. S. K., 2001. Host–guest interactions in humic materials. Organic Geochemistry 32, 1357–1371.

Song, G., Novotny, E. H., Simpson, A. J., Clapp, E., Hayes, M. H. B., 2008. Sequential exhaustive extraction of a Mollisol soil, and characterizations of humic components, including humin, by solid and solution state NMR. European Journal of Soil Science 59, 505–516.

Steinrücken, H. C., Amrhein, N, 1980. The herbicide glyphosate is a potent inhibitor of 5-enolpyruvylshikimic acid-3-phosphate synthase. Biochem. Biophys. Res. Commun. 94 (4), 1207-1212.

Stenson, A. C., Landing, W. M., Marshall, A. G., Cooper, W. T., 2002. Ionization and fragmentation of humic substances in electrospray ionization fourier transform-ion cyclotron resonance mass spectrometry. Anal. Chem. 74, 4397–4409.

Stenson, A.C., Marshall, A.G., Cooper, W.T., 2003. Exact masses and chemical formulas of individual Suwannee river fulvic acids from ultrahigh resolution electrospray ionization Fourier Transform Ion Cyclotron Resonance mass spectra. Anal. Chem. 75, 1275–1284.

Stevenson, F. J., 1982. Humus Chemistry: Genesis, composition, reactions. John Wiley & Sons, New York.

Stevenson, F.J., 1994. Humus chemistry, 2nd edn. Wiley, New York.

Sun, Y., Wang, C., Wen, Q., Wang, G., Wang, H., Qu, Q., Hu, X, 2010. Determination of Glyphosate and Aminomethylphosphonic Acid in Water by LC Using a New Labeling Reagent, 4-Methoxybenzenesulfonyl Fluoride. Chromatographia 72, 679–686.

Tan, K. H., 1994. Environmental Soil Science; Marcel Dekker, New York.

Tan, K. H., 1998. Principles of soil chemistry; 3rd Ed.; Marcel Dekker, New York.

Tan, W. F., Norde, W., Koopal, L. K., 2011. Humic substance charge determination by titration with a flexible cationic polyelectrolyte. Geochimica et Cosmochimica Acta 75, 5749–5761.

Tarafdar, J. C., Claassen, N., 1988. Organic phosphorus compounds as a phosphorus source for higher plants through the activity of phosphatases produced by plant roots and microorganisms. Biology and Fertility of Soils 5 (4), 308-312.

Thibodeau, E. A., Bowen, W. H., Marquis, R. E, 1985. pH-Dependent Fluoride Inhibition of Peroxidase Activity. J Dent Res 64 (10), 1211-1213.

Thurman, E., Malcolm, R. L., 1981. Preparative Isolation of Aquatic Humic Substances. Environmental Science and Technologies, 15, 463.

Tietjen, T., Wetzel, R. G., 2003. Extracellular enzyme-clay mineral complexes: Enzyme adsorption, alteration of enzyme activity, and protection from photodegradation. Aquatic Ecology 37, 331–339.

Tisdall, J. M., 2003. Formation of soil aggregates and accumulation of soil organic matter. In Structure and organic matter storage in agricultural soils. Carter, M. R., Stewart, B. A., Eds, CRC press: Boca Raton (FL).

Tollinger, M., Skrynnikov, N. R., Mulder, F. A. A., Forman-Kay, J. D., Kay, L. E., 2001. Slow Dynamics in Folded and Unfolded States of an SH3 Domain. Journal of American Chemistry Society 123, 11341-11352.

Tomaszewski, J. E., Schwarzenbach, R. P., Sander, M., 2011. Protein Encapsulation by Humic Substances. Environmental Science and Technologies 45, 6003–6010.

Turner B. L., Hopkins, D. W., Haygarth, F. M., Ostle, N., 2002. Glucosidase activity in pasture soils. Applied Soil Ecology 20, 157–162.

Vereecken, H., 2005. Mobility and leaching of glyphosate: a review. Pest. Manag. Sci. 61, 1139–1151.

Vetter, J., 2000. Plant cyanogenic glycosides. Toxicon 38, 11–36.

Viel, S., Mannina, L., Segre, A., 2002. Detection of a π-π complex by diffusion-order spectroscopy (DOSY). Tetrahedron Lett. 43, 2515–2519.

Violante, A., Arienzo, M., Sannino, F., Colombo, C., Piccolo, A., Gianfreda, L., 1999. Formation and characterization of OH-Al-humate-montmorillonite complexes. Organic Geochemistry 30, 461-468.

Wimmer, R., Aachmann, F. L., Larsen, K. L., Petersen, S. B., 2002. NMR diffusion as a novel tool for measuring the association constant between cyclodextrin and guest molecules. Carbohyd. Res. 337, 841–849.

Witte, E. G., Philipp, H., Vereecken, H., 2002. Study of enzyme-catalysed and noncatalysed interactions between soil humic acid and ^{13}C-labelled 2-aminobenzothiazole using solid-state ^{13}C NMR spectroscopy. Organic Geochemistry 33, 1727–1735.

Wrobel, K., Sadi, B. B. M., Wrobel, K., Castello, J. R., Caruso, J. A., 2003. Effect of metal ions on the molecular weight distribution of humic substances derived from municipal compost; ultrafiltration and size exclusion chromatography with spectrophotometric and inductively coupled plasma-MS detection. Anal. Chem. 75, 761-767.

Xiao-Chang, W. & Qin, L., 2006. Beta-Glucosidase Activity in Paddy Soils of the Taihu Lake Region, China. Pedosphere 16 (1), 118-124.

Zelenkova, N. F., Vinokurova, N. G., Leontievskii, A. A., 2010. Determination of Amine-Containing Phosphonic Acids and Amino Acids as Dansyl Derivatives. J. Anal. Chem. 65 (11), 1143-1147.

Zhang, O., Forman-Kay, J. D., 1995. Structural Characterization of Folded and Unfolded States of an SH3 Domain in Equilibrium in Aqueous Buffer. Biochemistry 34, 6784-6794.

Zhang, Y. , Du, J., Zhang, F., Yu, Y., Zhang, J., 2011. Chemical characterization of humic substances isolated from mangrove swamp sediments: The Qinglan area of Hainan Island, China. Estuarine, Coastal and Shelf Science 93, 220-227.

9.

Appendix 1

Analytica Chimica Acta 673 (2010) 167–172

Contents lists available at ScienceDirect

Analytica Chimica Acta

journal homepage: www.elsevier.com/locate/aca

NMR spectroscopy evaluation of direct relationship between soils and molecular composition of red wines from Aglianico grapes

Pierluigi Mazzei[a,b], Nicola Francesca[c], Giancarlo Moschetti[c], Alessandro Piccolo[a,*]

[a] Centro Interdipartimentale per la Risonanza Magnetica Nucleare (CERMANU), Universita 'di Napoli Federico II, Via Universita' 100, 80055 Portici, Italy
[b] Istituto di Metodologie Chimiche, CNR, Via Salaria Km 29.300, 00016 Monterotondo Stazione, Italy
[c] Dipartimento di Scienze Entomologiche, Fitopatologiche, Microbiologiche Agrarie e Zootecniche, Università di Palermo, Viale delle Scienze, 90128 Palermo, Italy

ARTICLE INFO

Article history:
Received 11 March 2010
Received in revised form 25 May 2010
Accepted 2 June 2010
Available online 9 June 2010

Keywords:
Nuclear Magnetic Resonance
Aglianico red wines
Multivariate statistical analysis
Terroir

ABSTRACT

^{1}H NMR spectroscopy was employed to investigate the molecular quality of Aglianico red wines from the Campania region of Italy. The wines were obtained from three different Aglianico vineyards characterized by different microclimatic and pedological properties. In order to reach an objective evaluation of "terroir" influence on wine quality, grapes were subjected to the same winemaking procedures. The careful subtraction of water and ethanol signals from NMR spectra allowed to statistically recognize the metabolites to be employed in multivariate statistical methods: Principal Component Analysis (PCA), Discriminant Analysis (DA) and Hierarchical Clustering Analysis (HCA). The three wines were differentiated from each other by six metabolites: α-hydroxyisobutyrate, lactic acid, succinic acid, glycerol, α-fructose and β-D-glucuronic acid. All multivariate analyses confirmed that the differentiation among the wines were related to micro-climate, and carbonate, clay, and organic matter content of soils. Additionally, the wine discrimination ability of NMR spectroscopy combined with chemometric methods, was proved when commercial Aglianico wines, deriving from different soils, were shown to be statistically different from the studied wines. Our findings indicate that multivariate statistical elaboration of NMR spectra of wines is a fast and accurate method to evaluate the molecular quality of wines, underlining the objective relation with *terroir*.

1. Introduction

Red wine is a complex molecular mixture resulting from fermentation of juice of *Vitis Vinifera* must [1]. The flavours and chemical composition of wine are usually related to the general environmental conditions insisting on vineyards from which wine is produced [2] Many geographical factors such as climate, soil geology and composition, wild yeasts [3,4] and lactic acid bacteria [5], are able to synergistically influence wine molecular characteristics [6]. The relationship between wine quality and its specific site of production is commonly described by the French term "*terroir*" [7].

The analytical methods most used to investigate correlation between chemical composition of red wines and environmental factors related to winemaking are: High Performance Liquid Chromatography (HPLC) [8], Gas Chromatography–Mass Spectrometry (GC–MS) [9], Fourier Transform Ion Cyclotron Resonance Mass Spectrometry (FT-ICR-MS) [10,11], High Performance Ion Exclusion Chromatography (HPICE) [12], and Nuclear Magnetic Resonance Spectrometry (NMR), used both with classical [12–14] and Site Natural Isotopic Fractionation (SNIF) NMR techniques [15].

Although NMR has poor sensitivity, liquid state NMR can rapidly provide spectra with highly reproduciblity describing the main molecular profile of wines without laborious sample pretreatments. Moreover, it has been shown [8,13,16] that NMR results, elaborated by multivariate statistical methods, can be used to identify and classify metabolites, common to many wines. The simplification of a multidimensional dataset obtained by liquid state ^{1}H NMR spectra, was successfully achieved with a number of multivariate statistical techniques, such as Principal Component Analysis (PCA), Discriminant Analysis (DA) and Hierarchical Clustering Analysis (HCA).

Recently, the combination of NMR spectroscopy with multivariate analysis has shown its high potential in wine quality assessment. Kosir et al. [15] attempted to classify Slovenian wines according to both geographical origins and beet sugar enrichment, by coupling the SNIF-NMR with some multivariate statistical methods. However, they were not able to significantly differentiate the wines produced in two adjacent Slovenian regions [15]. Brescia et al. [6], using the classical NMR spectroscopy with statistical analy-

* Corresponding author at: Centro Interdipartimentale per la Risonanza Magnetica Nucleare (CERMANU), Universita 'di Napoli Federico II, Via Universita' 100, 80055 Portici (NA), Italy. Tel.: +39 081 788 5236; fax: +39 081 775 5130.
E-mail addresses: Alessandro.piccolo@unina.it, alpiccol@unina.it (A. Piccolo).

0003-2670/$ – see front matter © 2010 Elsevier B.V. All rights reserved.
doi:10.1016/j.aca.2010.06.003

sis, were able to classify red wines produced in near by provinces of Apulia (Italy), but failed to distinguish wines obtained from different grape varieties [12]. Later, with a similar approach, they discriminated Apulian from Slovenian red wines confirming the efficacy of this method in assessing the geographical origin of wines [16]. Moreover, wines of Montepulciano d'Abruzzo (Italy) were satisfactorily depending on production years, yeast strains, and winemaking processes [8]. The applicability of a polyphasic approach was further confirmed when wines deriving from different cultivars, as grown on three different soils, were discriminated [7].

The aim of this work was to combine NMR spectroscopy with multivariate analysis in order to correlate wine quality to soil locations from which the cultivar originated. In order to reach an objective classification of the wine *terroir*, the grape variety "Aglianico", an ancient autoctonous cultivar of Campania (Italy), was collected from three near by soils with distinct pedological properties, and subjected to the same winemaking process. The wine samples were analyzed by ^{1}H NMR spectroscopy and spectral data elaborated by PCA, DA and HCA statistical methods.

2. Experimental

2.1. Vineyards, soil sites and wine details

The vineyards under study are located in Taurasi (Avellino, Campania, Italy) (41°00′35.39″N/14°57′34.29″E), but grown in three different soil sites: Case D'Alto [C], Coste Morante [S] and Macchia dei Goti [M]. The vineyards of "Aglianico di Taurasi" were planted in the same year (1982), on the same rootstock (1103 Paulsen) within a spurred cordon culture system. The plant density was 2000 stumps per hectare.

Soil C (41°00′11.05″N/14°58′19.00″E) is located 400 m above sea level and developed from volcanic ashes and pomices on cinereous platforms. The soil is deep, mildly coarse textured, well drained and rich in nitrogen (N) and organic carbon (C). Soil S (41°01′18.38″N/14°56′50.51″E) is situated 325 m above sea level. It is clayey and calcareous, slightly alkaline, with discrete exchangeable potassium and good C/N ratio. Soil M (40°59′54.63″N/14°57′42.81″E) is located 340 m above sea level, and is calcareous clayey and rich in exchangeable calcium and potassium.

Samples from the C, S and M vineyard soils were collected in 2005. Soil samples were air-dried, sieved on 2 mm sieves, and analyzed for organic carbon, total nitrogen, C/N ratio, available phosphorous (P_2O_5), electrical conductivity, cation exchange capacity (CEC), pH and total carbonates, as by the Official Italian Analytical Methods for Soil [17].

The 2005 vintage grapes were manually harvested from these vineyards and subjected to the same winemaking process as that carried out at the winery "Azienda Agricola Contrade di Taurasi di Enza Lonardo" located in Taurasi. Briefly, five quintals of harvested grapes were de-stemmed and crushed. Then, the three musts (about 3 hL) were transferred in different sanitised steel tanks, with the same inner volume (10 hL). The musts were treated with $K_2S_2O_5$ (60 mg kg^{-1} of grapes). Fermentations took place at 28 °C with indigenous yeast and caps were submerged twice a day. Macerations of pomaces lasted 12 days. The musts were pressed (about 8 bar) to obtain finished wines. About seven months after the end of malo-lactic fermentation, the wines were sieved through a rotary drum filter and finally bottled on December 2006.

A total number of 16 wine bottles were used for NMR analysis: five from Case d'Alto (C), six from Coste Morante (S), and five from Macchia dei Goti (M). Two more wine samples (F) were obtained from bottles of another Aglianico red wine commercially sold as "Fidelis 2005", and originated from the Taburno area (Benevento, Italy) at a distance of about 40 km from Taurasi.

2.2. NMR experiments

Wine samples were used immediately after bottle uncorking and prepared by mixing 0.25 mL of wine with 0.75 mL of a deuterated water (99.8% D_2O/H_2O, Armar Chemicals) solution containing 2% (v/v) formic acid (98–100% RG, Merck Chemicals) as internal standard. Before analysis, each sample was stirred in a vortex, and transferred into a stoppered NMR tube (5 mm, 7″, 507-HP-7, NORELL) and the remaining void volume gently degassed by a N_2 flux.

A 400 MHz Bruker Avance spectrometer, equipped with a 5 mm BBI Bruker probe and working at the ^{1}H frequency of 400.13 MHz, was employed to conduct all liquid state NMR measurements at a temperature of 298 ± 1 K. Mono-dimensional ^{1}H spectra were acquired with 2 s of thermal equilibrium delay, a 90° pulse length ranging between 8.21 and 8.86 μs, 200 transients, 32,768 time domain points, and 11.9692 ppm (4.7893 kHz) as spectral width. The free induction decay (FID) was multiplied by an exponential factor corresponding to 0.5 Hz. An excitation sculpting (*ZGESGP*) [18] and a modified T1 inversion-recovery (*mT1IR*) multi-suppression pulse sequences were both applied to suppress residual water signal and ethanol multiplets.

For excitation sculpting experiments, a specific shape pulse was built by modifying the basic shape pulse *SQUA100.1000* reported in the Bruker Topspin database. The most efficient signals multi-suppression occurred when the shape pulse length (P12) and power (SP1) were adequately calibrated. These parameters were optimized, respectively, at 7000 μs for all samples, and from 40.01 to 41.4 dB, depending strictly on sample. The T1 inversion-recovery sequence was adjusted to provide simultaneous suppression of both water and ethanol signals by, respectively, water pre-saturation and selection of appropriate inversion-recovery time-length.

Structural identification of wine metabolites was achieved by 2D NMR experiments: homo-nuclear ^{1}H–^{1}H COSY (COrrelation SpectroscopY) and TOCSY (Total COrrelation SpectroscopY), and hetero-nuclear ^{1}H–^{13}C HSQC (Hetero-nuclear Single-Quantum Correlation). In both 2D homo-nuclear experiments excitation sculpting was applied by employing two Bruker pulse sequences *COSYDFESGPPH* and *MLEVESGPPH* respectively. 2D spectra were acquired with 96 total transients, a time domain of 2k points (F2) and 256 experiments (F1), 16 dummy scans, and 11.9692 ppm as spectral width. Moreover, TOCSY experiments were conducted with a mixing time of 80 ms and trim pulse length of 2500 ms. The hetero-nuclear HSQC experiments were acquired with 80 total transients, 16 dummy scans, 0.5 ms of trim pulse length, a time domain of 2k points and 256 experiments, and 300 ppm (120.039 kHz) as ^{13}C spectral width. A baseline correction was applied to all mono- and bi-dimensional spectra and the proton frequency axis was calibrated by associating the formic acid signal at 8.226 ppm [19]. Spectra were processed by using both Bruker Topspin Software (v.1.3) and MestReC NMR Processing Software (v.4.9.9.9).

2.3. Multivariate data analyses

Statistical data elaboration was achieved by the XLStat software v.7.5.2 (Addinsoft). A number (119) of ^{1}H NMR variable buckets were screened, each bucket width being adequately chosen to include individual peaks or distinct multiplets, when possible. These buckets were equally adopted for all spectra. Prior to multivariate analysis, each spectrum was normalized by dividing the single bucket area by the sum of each signal integrated area. The

Table 1
^{1}H chemical shift and assignment of signals which mostly differentiated wine samples.

Peak identifier	Buckets interval (ppm)	Assignments	δ (ppm)	Multiplicity and group
1	1.299–1.248	α-Hydroxyisobutyrate	1.267	s, CH_3
2	1.438–1.373	Lactic acid	1.410	d, 7 β-CH_3
3	2.688–2.638	Succinic acid	2.665	s, CH_3
4	3.577–3.510	Glycerol	3.542	q, CH_2
5	3.782–3.743	α-Fructose	3.766	t, C2H, ring
6	4.624–4.586	β-D-Glucuronic acid	4.605	d, C1H, ring

s: singlet; d: doublet; t: triplet; q: quartet.

normalized values were further mean centred for PCA (Principal Component Analysis) and DA (Discriminant Analysis). The validation of the DA method validation consisted in building a validation set, achieved by dividing all samples in a training set and in a test set. The former set employed a discriminant model formed by 10 of the 16 samples, whereas the latter set was used to test the model and comprised 6 of the remaining samples. A similar partition, containing 37.5% of samples in the test set, allowed a sufficient number of samples in the training set as well as a representative number of samples in the test set [16]. This validation was repeated 5 times by changing, each time randomly, the samples included in the training and test set.

A HCA (Hierarchical Component Analysis) was developed by applying a hierarchical ascendant cluster analysis. By this technique, the extent of similarity among samples was measured by Euclidean distances, while cluster aggregation was based on the average linkage method [20].

3. Results and discussion

The ^{1}H NMR spectra of red wines (Supplementary Fig. S1a) showed that most intense signals were those of ethanol (a triplet at 1.204 ppm and a quartet at 3.674 ppm) and water (a singlet at 4.804 ppm). These signals interfere with spectral elucidation since their large intensities not only depress other meaningful signals but also overlap other molecular peaks resonating at near by frequencies. Excitation sculpting (*ZGESGP*) and a modified T1 inversion-recovery (*mT1IR*) pulse sequences were applied to suppress these interfering water and ethanol signals.

The *mT1IR* pulse sequence is related to ^{1}H spin–lattice relaxation times of all visible signals and showed that spins of ethanol signals relaxed almost completely before all other molecular spins began to significantly return to equilibrium. In fact, it was observed that application of a 3 s delay between initial 180° and second 90° hard pulse, efficiently suppressed the ethanol multiplets and acetic acid singlet at 2.09 ppm [13,21], while it allowed recovering all other signals without significant intensity loss. In addition, this pulse sequence included a water signal pre-saturation, that resulted in a concomitant removal of both undesired water and ethanol signals (Supplementary Fig. S1c). Even though both excitation sculpting and modified T1 inversion-recovery techniques were efficient in suppressing the interfering signals, the *mT1IR* pulse sequence was more successful in showing a cleaner ^{1}H spectrum of red wine (see comparison in Supplementary Fig. S1b and c). Consequently, the *mT1IR* sequence was applied to all mono-dimensional spectra of wine samples. Moreover, *mT1IR* spectra of wine samples from the same soil did not show significant differences, whereas variations were noticeable in wines from different soils. Therefore, these spectra could be integrated to evaluate, in details, the effect of soil site on wines molecular composition. An example of selected buckets with variable amplitudes within the 4.55–1.15 ppm spectral region is shown in Fig. 1.

A preliminary Analysis of Variance (ANOVA) was applied to a data matrix constituted by 119 variables and 16 samples. It was observed that only 6 out of the 119 employed variables contributed to wine differentiation within a 95% confidence interval (Fisher test) [22]. The buckets capable of statistical differentiation is indicated by arrows in Fig. 1, while precise bucket intervals with structural assignment of related compound variables are reported in Table 1. These compounds were α-hydroxyisobutyrate [13], lactic acid, succinic acid, glycerol, α-fructose, and β-D-glucuronic acid [13,23]. A spectral expansion for these metabolites is reported in Supplementary Fig. S2. Molecular attribution to signals in respective buckets was achieved by combining spectral interpretation of mono- and double-dimensional experiments (Supplementary Figs. 3–5). Signals identification was further supported by molecular attribution reported in literature for wine ^{1}H NMR spectra [13,14,16,21,24]. Most of the above compounds are mainly of microbial origin: lactic acid is the metabolic product of malo-lactic fermentation performed by malo-lactic bacteria (MLB) [25]; succinic acid is the major organic acid produced by yeast metabolism [26]; glycerol is the final product of glyceropiruvic fermentation by yeast and its formation accompanies ethanol production in sugar fermentation [27]. Although fructose is not a product of microbial origin, its concentration, related to glucose content, may influence yeast fermentation, the glycerol concentration depending on glucose/fructose content in must [28]. Moreover, the composition of yeasts wild strains and MLB were found slightly different in the three musts and related wines (data not shown).

The multivariate Principal Component Analysis (PCA) calculates linear combinations of a starting set of variables on the basis of their maximum variance [16]. It reduces the dimensions multiplicity of the original data matrix, while retaining the maximum amount of variability, as well as the original information contained in the data set [29]. PCA decomposes a data matrix with m rows (wine samples) and n columns (NMR spectral areas) into the product obtained by

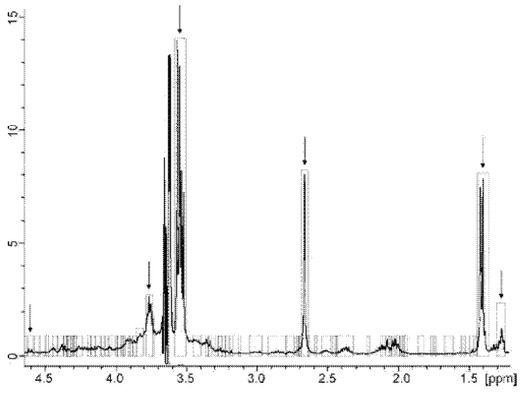

Fig. 1. ^{1}H spectrum of M1 sample. The superimposed rectangles contain the selected buckets within the 4.55–1.15 ppm region, which were equally employed to integrate all wine spectra. Arrows indicate peaks which statistically contributed to discriminate among C, S and M wine samples [Case d'Alto (C), Coste Morante (S) and Macchia dei Goti (M)].

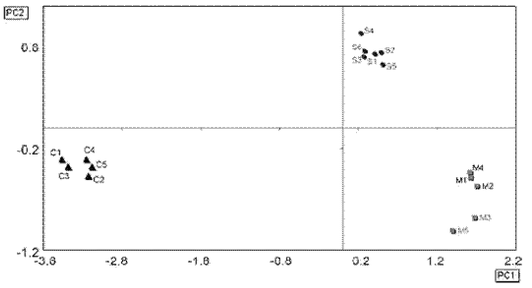

Fig. 2. Scatter-plot of the scores generated from the two principal components, PC1 and PC2, obtained using analytical data from ^{1}H NMR red wine spectra.

multiplying a matrix of scores (m rows for wine samples and $P<n$ columns for Principal Components, PCs), with a matrix of loadings ($P<m$ rows for PCs and n columns for NMR spectral areas). Each combination of two resulting PCs, creates a bi-dimensional space, constituted by PCs as axis. Loading vectors are associated to each of such factorial planes, correlated to the original variables, and orientated toward the direction in which the maximum variance of variables is expressed. This representation projects the original observations in a new reference system, whose coordinates are regulated by the variance, and provides a final bi-dimensional score-plot, that may be interpreted with loading-plot information [30]. This means that score-plots can indirectly highlight possible differences or similarities among samples, while loading-plots reveal the responsible spectral components (variables).

The PCA analysis was conducted on a data matrix containing only the six variables capable of sample differentiation (Table 1) [20]. In PCA, the first two Principal Components explained 86.0 and 11.2% of total variance, respectively (Fig. 2). The three different wine samples were projected to three separated score-plot regions, whose differences resulted statistically significant ($p<0.0001$) by the Barlett's sphericity test [31]. In fact, it was found (Fig. 2) that PCA well discriminated the C wine from S and M along the PC1 direction, being the former positioned in the negative PC1 score. On the other hand, M and S wines were mutually well separated along the PC2 axis. Furthermore, this PCA distribution showed that wine replicates deriving from the same soils were associated with close score-plot domains, while groupings of wine replicates were spatially well separated according to soil differences (Fig. 2). This finding testified that the molecular characteristics of the three wines were sufficiently varied to show PCA distinctions.

The three variables which mostly contributed to differences by PC1 were provided by lactic acid (74.0%), α-fructose (12.7%), and glycerol (12.2%) (Table 2). The PCA linear orientations of variance vectors for these variables are shown in the loading-plot (Fig. 3), that correlates score-plot domains with variables. The large distance among coordinate values along PC1 between the C and the S and M domains (Supplementary Table S1) may then be attributed

Table 2
Principal Component Analysis eigenvalues and variable contributions (%).

Eigenvalues and variables	PC1	PC2
Eigenvalue	3.472	0.453
Variance (%)	85.967	11.220
Cumulate variance (%)	85.967	97.187
β-D-Glucuronic acid	0.033	1.334
α-Fructose	12.732	5.224
Glycerol	12.203	9.228
Succinic acid	0.464	76.362
Lactic acid	74.025	0.020
α-Hydroxyisobutyrate	0.543	7.831

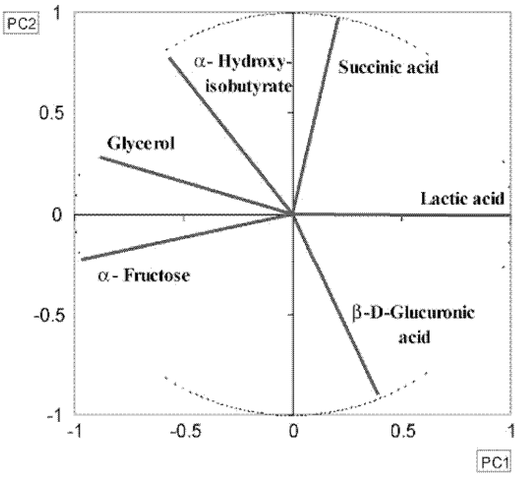

Fig. 3. Loading-plot of the variables associated with the first two principal components of PCA, calculated using analytical data.

to larger lactic acid in S and M wines than in C wine. Such score-plot distinction is additionally provided by the greater content of α-fructose and glycerol found for C than for S and M wines. However, the more positive PC1 scoring for M than for S wines is explained by a greater glycerol content in the latter. As for PC2, the main difference among samples was provided by succinic acid (76.362%), whose content was largest in S wine. Moreover, M samples showed both greater and smaller content of β-D-glucuronic acid and α-hydroxyisobutyrate, respectively, than C and S samples. It is furthermore noted that within the M statistical domain, M3 and M5 samples showed more negative PC2 scorings than the remaining M samples, due to concomitant larger β-D-glucuronic and lower glycerol amounts.

The Discriminant Analysis (DA) is a supervised statistical method to classify samples. DA extracts discriminant functions from a data matrix composed by independent variables in order to maximize inter-class variance and minimize intra-class variance. This criterium can be supported by a validation test in order to verify the statistical confidence with which the a priori classification of some observations (test set) coincides with the a posteriori DA prediction as elaborated by information provided by the remaining samples (training set). One of the five applied discriminant models, which were obtained by a validation test is shown (Supplementary Fig. 6). In this model, C3, C4, S3, S6, M3 and M5 samples were used as test-set samples. Since PCA indicated that M3 and M5 samples were slightly differentiated from other M samples, and may thus be hardly recognized by DA, we chose M3 and M5 samples as M unknown objects to verify the reliability of DA analysis. This DA exercise proved that all wine observations were correctly associated to respective group with 100% of success (observation coordinates and square distances for this model are reported in Supplementary Table S2). Moreover, in all five developed discriminant models, each wine sample was correctly associated to the respective group with 100% of success and a significance of 0.05.

The observed PCA differentiation among wine samples is reflected by different soil properties. In fact, while S and M soils are definitely carbonatic soils, as shown by pH value and total carbonates content, the volcanic C soil is less carbonatic (Table 3). Moreover, the S and M soils have a larger clay character and a greater organic carbon and total nitrogen content than the C soil. The diverse soil properties were confirmed by PCA differentiation

Table 3
Properties of soils under vineyards.

Properties	C	S	M
Gross sand (%)	43.8	13.8	16.7
Fine sand (%)	41.6	33.1	34.7
Silt (%)	12.1	22.8	21
Clay (%)	2.5	30.3	27.6
Organic carbon ($g\,kg^{-1}$)	27.1	13.5	12.2
N total ($g\,kg^{-1}$)	2.45	1.28	1.05
C/N	11.1	10.6	11.6
P_2O_5 ($mg\,kg^{-1}$)	24.3	43.6	16.9
Electric conductivity ($dS\,m^{-1}$)	0.099	0.145	0.126
C.E.C. (mequiv./100 g)	26.3	29.3	24.4
pH (H_2O)	6.58	8.15	8.26
Total carbonates ($g\,kg^{-1}$)	10.5	60.6	109

among wine samples and this suggested that soil characteristics had a bearing on the molecular quality of wines obtained from the soils.

The PCA was modified (PCAe) by adding to the data matrix two more samples of a commercial Aglianico wine (F) from Campania region (supplementary Table S3). Since PCA score-plots arrange similar samples in near by zones, while placing dissimilar samples in distant zones, addition of different unrelated samples to the dataset would presumably project their scoring in a distinct domain of the score-plot. Fig. 4 shows the new PCAe score-plot where the separation between F (negative scoring on both principal functions) and previous C, S, and M samples is significant. Such separation of F samples was attributed to much lower content of glycerol and succinic acid for PC2, and to both smaller and larger amount of lactic acid and α-fructose, respectively, in PC1, than for C, S, and M samples (Fig. 4).

HCA is an unsupervised method that recognizes and distributes data grouping, according to their affinity, in clusters of progressive dissimilarity, as described in a dendrogram. It is assumed that the closer the objects in a space defined by variables, the more similar are their properties. HCA was thus conducted to verify the classification of C, S and M wines according to their mutual dissimilarity and their relation to F wines. The resulting dendrogram and main descriptive values are shown in Fig. 5 (relative matrix with quantitative dissimilarities in Supplementary Table S4). Knot 35 in the dendrogram shows that the most dissimilar clusters are those

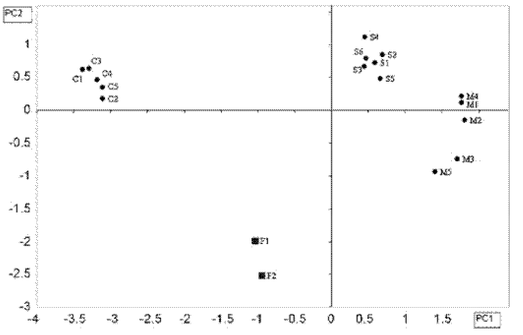

Fig. 4. Scatter-plot of PCAe. The scores generated from the two principal components, PC1 and PC2, obtained using analytical data from ^{1}H NMR red wine spectra. F is two samples of an Aglianico different from C, S, and M. The PC1 and PC2 explained, respectively, 70.48% and 23.068% of the total variance.

between F wines and the rest of Aglianico samples. This indicates that this HCA approach visibly discriminates wines of different origin and quality. Furthermore, knot 34 reveals that the C cluster is recognized by HCA as different from the macro-cluster containing S and M wines. This is in accordance with results from both the PCA score-plot and its relation to soil properties. HCA provides further insight by closely classifying M and S clusters (knot 33) and confirming PCA results, which indicated that M3 and M5 were slightly different, within the M cluster, from M1, M2 and M4 samples.

4. Conclusions

The study shows that ^{1}H NMR spectroscopy combined with multivariate statistical analyses can rapidly and efficiently discriminate three red wines derived from the same Aglianico grape variety grown on different soils. Multi-suppression of both water and ethanol signals in wine samples, by a specifically modified inversion-recovery pulse technique, offered highly reproducible NMR spectra without overlapping of meaningful peaks. Although this approach also removed the acetic acid signal, the discrimination among the wines were anyhow assured.

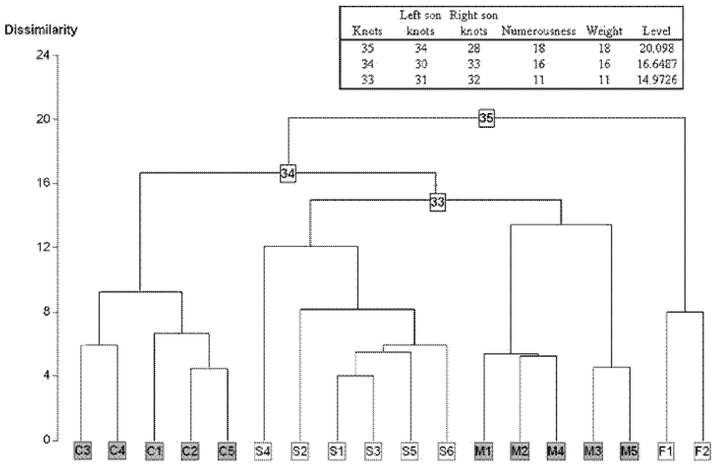

Fig. 5. Dendrogram of red wines obtained using analytical data. Euclidean distance was employed to find the dissimilarity among the samples, and the average correlation as aggregation method.

Despite the wines were produced employing the same grape variety and the same winemaking procedures, the PCA elaboration of their ^{1}H NMR spectra was able to significantly recognize dissimilarities among their molecular properties, as shown by the content of lactic acid, α-fructose, glycerol, succinic acid, β-D-glucuronic acid and α-hydroxyisobutyrate. Statistical variables of PCA were also employed to perform a discriminant analysis, whose five validation tests provided a 100% correct prediction of differences among wines.

Since the diversity of the three wines could be only reconciled to differences in soils, these results suggest that bio-pedo-climatic factors determined the ultimate wine quality. However, some metabolites (lactic and succinic acid, and glycerol) may have derived from must and wine microbial activity, thus suggesting that indigenous yeasts and MLB may also contribute to the expression of terroir. Multivariate statistical analysis of ^{1}H NMR spectra indicated a marked difference between one of the Aglianico wines and the other two. Since the vineyards from which the wines originated were closely located (lower than 3 km apart), wine quality appears to be conditioned less by macro-climate than by micro-climate and intrinsic soil properties, which in turn influence the must microflora. In fact, the differentiated wine originated from a soil of higher altitude than for the other two wines, with consequent differences in temperature and humidity. Moreover, soil characteristics, such as texture and carbonate as well as organic carbon content, varied between one soil and the other two ones. The peculiarity of this one different soil is reflected by PCA, DA and HCA results from ^{1}H NMR spectra of wines, thereby sustaining the assumption that soil physical and chemical properties are able to determine the overall wine quality.

A further evidence of the efficacy of combining careful NMR spectroscopy with multivariate statistics to assess wine quality and its *terroir*, was shown by comparing results of the three wines under study with those of a commercially available Aglianico wine from another soil site. Both ^{1}H NMR spectroscopy and multivariate elaboration clearly indicated that the latter wine had a significant different quality than the formers. Thus, the findings of this work are promising in indicating ^{1}H NMR spectroscopy as a rapid and objectively sound technique for a geographical identification of wine quality.

Acknowledgements

We thank Alessandro Lonardo, owner of "Azienda Agricola Contrade di Taurasi" (Taurasi, AV, Italy). We are grateful to Maurizio De Simone for his oenological support in the cellar.

Appendix A. Supplementary data

Supplementary data associated with this article can be found, in the online version, at doi:10.1016/j.aca.2010.06.003.

References

[1] A. Ramos, H. Santos, in: G.A. Webb (Ed.), Annual Reports on NMR Spectroscopy, vol. 37, Academic Press, New York, 1998, pp. 179–199.
[2] G.V. Jones, M.A. White, O.R. Cooper, K. Storchmann, Clim. Change 73 (2005) 319–343.
[3] N. Francesca, M. Chiurazzi, R. Romano, M. Aponte, L. Settanni, G. Moschetti, World J. Microbiol. Biotechnol. 26 (2010) 337–351.
[4] E. Nikolaou, E.H. Soufleros, E. Bouloumpasi, N. Tzanetakis, Food Microbiol. 23 (2006) 205–211.
[5] E. Boido, K. Medina, L. Farina, F. Carrau, G. Versini, E. Dellacassa, J. Agric. Food Chem. 57 (2009) 3278–6271.
[6] G.V. Jones, in: R.W. Macqueen, L.D. Meinert (Eds.), Geoscience Canada Reprint Series Number 9, Geological Association of Canada, Newfoundland, 2006, pp. 1–14.
[7] G.E. Pereira, J.P. Gaudillere, C.V. Leeuwen, G. Hilbert, M. Maucourt, C. Deborde, A. Moing, D. Rolin, VI International Terroir Congress, Montpellier, 2006.
[8] M. Giaccio, A. Del Signore, J. Sci. Food Agric. 84 (2004) 164–172.
[9] M. Ugliano, L. Moio, J. Sci. Food Agric. 86 (2006) 2468–2476.
[10] R.D. Gougeon, M. Lucio, M. Frommberger, D. Peyron, D. Chassagne, H. Alexandre, F. Feuillat, A. Voilley, P. Cayot, I. Gebefugi, N. Hertkorn, P. Schmitt-kopplin, PNAS 106 (2009) 9174–9179.
[11] A. Cuadros-Inostroza, P. Giavalisco, J. Hummel, A. Eckardt, L. Willmitzer, H. Pena-cortes, Anal. Chem. 82 (2010) 3573–3580.
[12] M.A. Brescia, V. Caldarola, A. De Giglio, D. Benedetti, F.P. Panizzi, A. Sacco, Anal. Chim. Acta 458 (2002) 177–186.
[13] Y.Y. Du, G.Y. Bai, X. Zhang, M.L. Liu, Chin. J. Chem. 25 (2007) 930–936.
[14] S. Clark, N.W. Barnett, M. Adams, I.B. Cook, G.A. Dyson, G. Johnston, Anal. Chim. Acta 563 (2006) 339–345.
[15] I.J. Kosir, M. Kocjancic, N. Ogrinc, J. Kidric, Anal. Chim. Acta 429 (2001) 195–206.
[16] M.A. Brescia, I.J. Kosir, V. Caldarola, J. Kidric, A. Sacco, J. Agric. Food Chem. 51 (2003) 21–26.
[17] Ministerial Decree of Italian Republic, Decreto Ministeriale delle Politiche Agricole e Forestali del 13 Settembre 1999, Published on Official Gazette n° 248, 21st October 1999.
[18] T. Parella, P. Adell, F. Sanchez-Ferrando, A. Virgili, Magn. Reson. Chem. 36 (1998) 245–249.
[19] L.A. Cardoza, B.J. Cutak, J. Ketter, C.K. Larive, J. Chromatogr. A 1022 (2004) 131–137.
[20] R. Todeschini, Introduzione alla Chemiometria, EdiSES s.r.l., Naples, 1998, pp. 37–79.
[21] E.F. Boffo, L.A. Tavares, M.M.C. Ferreira, A.G. Ferreira, Food Sci. Technol. 42 (2009) 1455–1460.
[22] P. Dagnelie, Théorie et méthodes statistiques, vol. 2, Les Presses Agronomiques de Gembloux, Gembloux, 1986.
[23] A. Caridi, Int. J. Food Microbiol. 120 (2007) 167–172.
[24] I.J. Kosir, J. Kidric, Anal. Chim. Acta 458 (2002) 77–84.
[25] C. Davis, D. Wibowo, R.E. Eschenbruch, T.H. Lee, G.H. Fleet, Am. J. Enol. Vitic. 36 (1985) 290–301.
[26] T. Magarifuchi, K. Goto, Y. Iimura, M. Tadenuma, G. Tamura, J. Ferment. Bioeng. 80 (1995) 335–361.
[27] M.J. Taherzadeh, L. Adler, G. Liden, Enzyme Microb. Technol. 31 (2002) 53–66.
[28] S.K. Yalcin, Z.Y. Ozbas, World J. Microbiol. Biotechnol. 21 (2005) 1303–1310.
[29] D. Smejkalova, R. Spaccini, A. Piccolo, Eur. J. Soil Sci. 59 (2008) 496–504.
[30] R.G. Brereton, in: J. Wiley, sons (Eds.), Chemometrics—Data analysis for the Laboratory and Chemical Plant, Wiley, England, 2003, pp. 184–249.
[31] W.R. Dillon, M. Goldstein, Multivariate Analysis. Methods and Applications, John Wiley & Sons, New York, 1984, pp. 44–47.

10.

Appendix 2

ENVIRONMENTAL Science & Technology

ARTICLE

pubs.acs.org/est

Carbon Sequestration in Soil by in Situ Catalyzed Photo-Oxidative Polymerization of Soil Organic Matter

Alessandro Piccolo,[†,*] Riccardo Spaccini,[†] Antonio Nebbioso,[†] and Pierluigi Mazzei[†,‡]

[†]Dipartimento di Scienze del Suolo, della Pianta, dell'Ambiente e delle Produzioni Animali, Università di Napoli Federico II, Via Università 100, 80055 Portici, Italy

[‡]Istituto di Metodologie Chimiche, CNR, Via Salaria Km 29.300, 00016 Monterotondo Stazione, Italy

ABSTRACT: Here we describe an innovative mechanism for carbon sequestration in soil by in situ photopolymerization of soil organic matter under biomimetic catalysis. Three different Mediterranean soils were added with a synthetic water-soluble iron-porphyrin, irradiated by solar light, and subjected first to 5 days incubation and, then, 15, and 30 wetting and drying (w/d) cycles. The *in situ* catalyst-assisted photopolymerization of soil organic carbon (SOC) increased water stability of soil aggregates both after 5 days incubation and 15 w/d cycles, but not after 30 w/d cycles. Particle-size distribution of all treated soils confirmed the induced soil physical improvement, by showing a concomitant lower yield of the clay-sized fraction and larger yields of either coarse sand- or fine sand-size fractions, depending on soil texture, though only after 5 days incubation. The gain in soil physical quality was reflected by the shift of OC content from small to large soil aggregates, thereby suggesting that photopolymerization stabilized OC by both chemical and physical processes. A further evidence of the carbon sequestration capacity of the photocatalytic treatment was provided by the significant reduction of CO_2 respired by all soils after both incubation and w/d cycles. Our findings suggest that "green" catalytic technologies may potentially be the bases for future practices to increase soil carbon stabilization and mitigate CO_2 emissions from arable soils.

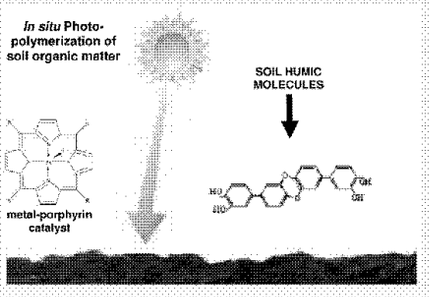

■ INTRODUCTION

Agricultural lands under food and bioenergy crops, managed grass and permanent crops including agro-forestry, occupy about 40−50% of the Earth's land surface, and accounted for an estimated emission of 5.1−6.1 $GtCO_2$-eq/yr (10−12% of total global anthropogenic emissions of GHGs).[1] However, actual measures to mitigate GHGs emission from agricultural soils are limited to improved cropland practices such as crop rotation, nutrient management, tillage/residue management, agroforestry, and return to natural vegetation.[2] These practices are not only far from substantially reducing GHGs emissions from soils or permanently stabilizing soil organic matter (SOM),[3−5] but are also predicted to hardly match more than a maximum of 25% of the GHGs reductions required by the Kyoto Protocol within 2050.[6] Despite the knowledge that GHGs release from soil largely derives from biochemical transformations of plant litter and SOM,[7−9] no new and much wished biotechnological measures are adopted so far to augment mitigation.[1]

The humified organic matter in soil (70−80% of SOM)[10] represents the most persistent pool in OC accumulation with mean residence time of several hundreds of years,[11] and, thus, the principal potential C sink in the biosphere, whose advanced comprehension may help to mitigate CO_2 emissions from soil.[12] Soil humus is composed by the hydrophobic and heterogeneous aliphatic and aromatic molecules progressively surviving the microbial transformation of dead biological tissues.[13] Recent scientific evidence shed new light on the chemical nature of humus by describing humic molecules as heterogeneous but relatively small in mass (≤1000 Da),[14,15] rather than the previously assumed macropolymers.[16] Humic molecules were shown to be tightly associated in supramolecular structures, which are prevalently stabilized by noncovalent hydrophobic bonds.[13]

Based on this new understanding, we reasoned that small aromatic humic molecules could be covalently linked to each other by oxidative coupling reactions under appropriate catalysis, thereby enhancing their molecular size and complexity. We have already shown that larger and more chemically stable humic molecules were obtained by treating solutions of humus extracts in oxidative (H_2O_2) conditions, with a phenoloxidase enzyme, such as peroxidase,[17] or a biomimetic catalyst, such as a water-soluble iron-porphyrin.[18] Both the enzymatic and biomimetic catalysts accelerate the oxidative coupling of phenols via a free-radical mechanism.[19] Moreover, we found that the biomimetic catalysis increased the molecular dimension of humic molecules in solution simply by photo-oxidation under solar radiation, without the need of an additional oxidant.[20] By applying photo-oxidative catalyzed conditions on lignin-derived phenolic monomers (similar to those found in soil humus), we proved the

Received: May 9, 2011
Accepted: June 29, 2011
Revised: June 24, 2011
Published: June 29, 2011

rapid formation of new intermolecular C—C and C—O—C bonds leading to several identified (up to tetramers) and unidentified oligomers.[21−23]

The catalyzed photo-oxidative formation of covalent bonds among phenolic molecules in situ in soil is expected to chemically stabilize SOM by increasing the content of chemical energy in soil humic structures. The induced greater stabilization of soil humus would have the consequence to enhance the metabolic threshold required by soil microorganisms to mineralize SOM, thus resulting in soil carbon sequestration and reduction of CO_2 emission from soil. Moreover, increasing the mass of humus molecules would facilitate soil particles association into larger soil aggregates and thus improving soil physical quality.[24−26] The positive effect of the photopolymerization process was already hinted by a preliminary work, in which the catalyst was used on a microcosm controlled experiment, and determined a reduced respiration from one bare soil.[27]

Here, we aimed to verify on three different Mediterranean soils whether the new approach based on a catalyst-assisted photopolymerization reaction may stabilize in situ soil organic carbon against microbial mineralization. The persistence of the effect on SOC was studied by subjecting the soils added with the biomimetic iron-porphyrin catalyst subjected to subsequent severe disaggregating processes such as 15 and 30 wetting and drying cycles. SOM stabilization was evaluated by assessing soil physical quality, distribution of organic carbon in soil particle sizes and soil respiration.

■ MATERIALS AND METHODS

Soil Samples and Characterization. Soil samples were collected from the surface layers (0−30 cm) of three agricultural plots from south-central Italy: 1. Porrara (Avellino), 2, Colombaia (Caserta), 3. Itri (Latina). Samples were air-dried, sieved through a 4.75 mm sieve, and used for characterization and incubation experiments. Soil texture was measured by the pipet method. Total organic carbon (TOC) was determined by the standard Walkley−Black titration method. Clay mineralogy was determined on oriented samples by X-ray diffraction (XRD) using a Rigaku Geigerflex D/MaxB diffractometer with Fe-filtered CoKα-radiation generated at 40 kV and 30 mA.

Biomimetic Catalyst. The preparation procedure of the *meso*-tetra-(2,6-dichloro-3-sulfonatophenyl)porphyrinate of Fe(III) [Fe(TDCPPS)Cl], have been previously described.[18] Briefly, a *meso*-Tetra(2,6-dichlorophenyl)porphyrin (H_2TDCPP) was first synthesized and then treated for 12 h under argon atmosphere with a 100 mL of a water solution containing 100 mg of Fe(II)SO_4. The solution was then filtered and purified through a cationic exchange resin Dowex 50W X8−100 (50−100 mesh), previously conditioned with a 10% HCl solution. The column was eluted with water and the recovered material dried upon vacuum. The final Fe(TDCPPS)Cl product, was recrystallized in methanol-acetone in order to purify the sample from residual salts.

Photopolymerization Experiments. For each replicate (n = 3), 60 g of air-dried soil sample was placed on a Petri dish (12 cm diameter) and soil moisture was kept at 40% of water holding capacity (WHC) by adding X mL of water (X = 20, 17, 10 mL, for Porrara, Colombaia and Itri soil, respectively) in order to obtain a control series. The polymerized series were similarly prepared (n = 3) and added with 0.24 μmol of synthetic water-soluble Fe-(TDCPPS)Cl dissolved in the X mL of water pertaining to WHC of each soil. After preparation, both control and polymerized series were left under natural solar radiation throughout the following treatments: (i) covered with a Petri dish and incubated for 5 days; (ii) submitted to 15 wetting/drying (w/d) cycles; (iii) submitted to 30 w/d cycles. During w/d cycles, samples were uncovered after a 5 day incubation and distilled water was added, whenever samples became dry (approximately once a week), to re-establish WHC.

Soil Aggregate Stability. Separation of water-stable aggregates was done by a wet sieving method.[28] An air-dried subsample (30 g) was placed on the top sieve of a set of three nested sieves (1.0, 0.50, and 0.25 mm). The sample was gently rewetted and then submerged into 2 cm of distilled water for 30 min. After this time, the sieves were manually oscillated (up and down 4 cm) for 30 times during 1 min. Recovered aggregate fractions were oven−dried at 60 °C, weighed, and stored at room conditions.

The mean weight diameter index in water (MWDw), used for the determination of aggregate stability, was calculated according to the following equation:

$$\mathrm{MWDw} = \sum_{i=1}^{n} X_i W_i$$

where X_i is the mean diameter of each aggregate fraction and W_i is the proportion of the total sample weight occurring in the ith fraction.

The amount of OC (%) in each aggregate fraction was normalized to the weight of each fraction: OC content in fraction (g kg^{-1}) × mass of recovered fraction (g kg^{-1})/total OC recovered (g kg^{-1}).

Particle-Size Fractionation. All samples were fractionated by applying low-energy sonication, followed by sieving and centrifugation separations as previously described.[29] Since the dispersion efficiency is significantly affected by the output of the sonication energy, the applied energetic was calibrated.[30] In brief, 9 g of air-dried subsample (<2 mm) were dispersed in 60 mL of distilled water using a probe-type ultrasonic disaggregator (Sonicator Ultrasonic liquid processor, Misonix Incorporated) applying an energy of 267 J·mL^{-1}. To avoid reduction in cavitation, the temperature of soil suspension was kept below 35 °C.[30] Coarse sand (2000−200 μm) and fine sand (200−63 μm) were separated by manual wet sieving with about 250 mL of cooled distilled water, while silt (63−2 μm), and clay (<2 μm) fractions were separated by centrifugation at 1000 and 5000 rpm, respectively. The separated fractions were oven−-dried at 60 °C and stored at room conditions.

Soil Respiration. Soil respiration was evaluated by a dynamic absorption method. Briefly, 9 g of air-dried and rewetted soil sample (<2 mm) were placed on a airtight soil respiration flask in which a CO_2-free air was continuously fluxed by a peristaltic pump. The CO_2 emitted from soil was then captured in a trap containing a 0.01 M NaOH solution. The amount of CO_2 absorbed in this solution was determined after 27 days by back-titration with 0.01 M HCl after addition of 7 mL of 0.5 M $BaCl_2$. The ambient CO_2 concentration was determined by inserting blank samples (i.e.: no soil) into the respiration system.

Statistical Analysis. A coupled two-tailed Student's t test was used to compare values obtained for control and treatments, and difference was considered to be significant at the level of $P \leq 0.05$. All values are based on triplicate samples from which the mean and the standard error of the mean (s.e.m) were calculated.

Table 1. Properties of Soils (mean ± s.e.m)

property	Porrara	Colombaia	Itri
coarse sand (g kg^{-1})	119 ± 6	180 ± 7	80 ± 3
fine sand (g kg^{-1})	237 ± 10	230 ± 9	440 ± 11
silt (g kg^{-1})	227 ± 8	350 ± 7	380 ± 10
clay (g kg^{-1})	417 ± 12	240 ± 5	100 ± 4
organic C (g C kg^{-1})	9.1 ± 0.4	13.1 ± 0.9	4.0 ± 0.2
pH-H_2O	8.3 ± 0.1	8.2 ± 0.1	8.4 ± 0.1
minerals[a]	C+++, F++, I++, K++, M++, Q+++, S+++	C+++, F+++, I++, K++, M++	D+++, F+, LCK+

[a] *C* = calcite, *D* = dolomite, *F* = feldspar, *I* = Illite, *K* = kaolinite, LCK = low crystalline kaolinite, *M* = mica, *Q* = quartz, *S* = smectite; +++ = predominant, ++ = present, + = traces.

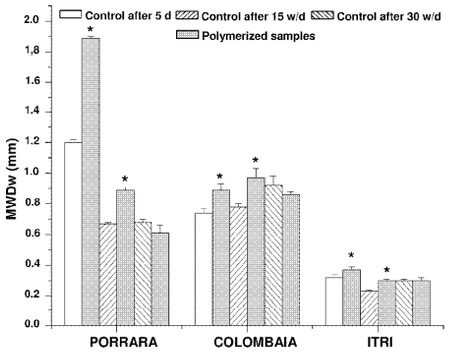

Figure 1. Mean weight diameter in water (MWDw) for the three soils, Porrara, Colombaia, Itri, before and after the photopolymerization treatment for a 5 day incubation, and 15 and 30 wetting and drying cycles (w/d). Error bars indicate standard error (n = 3). The asterisks denote significant differences between control and treatment at the level of $P \leq 0.05$.

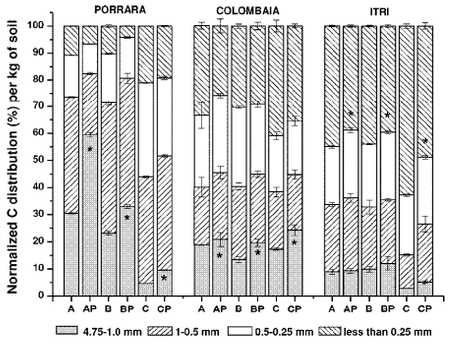

Figure 2. Percent distribution of organic carbon in different fractions of water-stable aggregates for the three soils, Porrara, Colombaia, Itri, before and after photopolymerization treatment for 5 days incubation, and 15 and 30 wetting and drying cycles (w/d). *A* = control soil after 5 days incubation; AP = photopolymerized soil after 5 days incubation; *B* = control soil after 15 w/d cycles; BP = photopolymerized soil after 15 w/d cycles; *C* = control soil after 30 w/d cycles; CP = photopolymerized soil after 15 w/d cycles. Error bars indicate standard error (n = 3). The asterisks denote significant differences between control and treatment at the level of $P \leq 0.05$.

■ RESULTS AND DISCUSSION

While the pH and mineralogy of the selected agricultural soils indicate their similar calcareous origin, large variations were noted in both textural and organic carbon properties (Table 1). The textural composition of soils affected the values of the mean-weight diameter of soil aggregates in water (MWDw), an index of aggregate stability.[28] This was large in the control sample of the most clayey and well structured Porrara soil, while progressively decreased with increase of sand content in Colombaia and Itri soil.

The catalyst-assisted photopolymerization treatment significantly increased the MWDw over control values for all the three soils after a 5 day incubation (Figure 1). Again, it was the originally well-structured Porrara soil that showed the most dramatic increase. The gain in aggregate stability indicates that the photopolymerization treatment was effective in increasing the molecular mass and cross-linking of soil humic molecules, thereby promoting a tighter association among soil particles and formation of larger water-stable aggregates. The persistence of the aggregating effect induced by the SOM photopolymerization in all samples is suggested by MWDw values, which remained larger than the respective control samples even after the soils had been subjected to 15 w/d cycles (Figure 1). The beneficial effects of the catalyzed photopolymerization were lost for all soils after 30 w/d cycles, whereby the MWDw values were no longer different from the relative control.

The molecular modification of SOM following the photopolymerization treatment was reflected by the percent distribution of OC in the separated water-stable aggregates (Figure 2). After only 5 days of incubation, a significant decrease of OC in small-sized aggregates (<0.25 mm) was noted for all three soils, whereas OC significantly increased in the largest macro-aggregates (4.75−1.0 mm) only by the most clayey Porrara soil. The OC accumulation in the largest aggregates increased also with w/d cycles, becoming significant over control after 15 and 30 cycles for the silty Colombaia soil, and after 30 cycles for the sandy and least stable Itri soil.

These results suggest that the catalytic photopolymerization of SOM was effective in forming macro-aggregates at the expenses of microaggregates, thereby improving the soil physical quality. Moreover, the process of SOM photopolymerization not only remained active within the period of the w/d experiments and progressively increased the mass of humic molecules, but also enabled a greater OC content into larger aggregates, due to aggregation of stabilized microaggregates. This implies that, despite the generalized loss of physical stability under the severe

Table 2. Percent (mean ± s.e.m.) of Yield and Content of Total Organic Carbon (TOC) for Particle-Size Fractions (μm) in Soils, Following 5 Day Incubation, And 15 and 30 Wetting and Drying Cycles (w/d). [a]

	coarse sand 2000−200	fine sand 200−63	silt 63−2	clay <2	toc[b]
		PORRARA			
		5 Day Incubation			
A	18.7 ± 1.2b	20.3 ± 2.2a	43.7 ± 2.2a	17.3 ± 1.9a	0.84a
AP	22.0 ± 2.0a	22.2 ± 2.7a	42.4 ± 2.1a	13.3 ± 0.3b	0.80a
		15 w/d Cycles			
A	14.8 ± 0.7a	12.3 ± 0.9a	51.7 ± 1.5a	21.2 ± 1.3a	0.78b
AP	15.4 ± 1.5a	12.9 ± 1.1a	50.4 ± 3.6a	21.4 ± 2.9a	0.83a
		30 w/d Cycles			
A	14.4 ± 0.8a	12.0 ± 1.0a	52.3 ± 1.3a	21.3 ± 1.4a	0.70b
AP	15.0 ± 1.3a	12.7 ± 1.2a	50.2 ± 2.2a	22.1 ± 1.7a	0.81a
		COLOMBAIA			
		5 Day Incubation			
A	27.3 ± 2.6a	17.6 ± 1.2b	47.8 ± 1.1a	7.3 ± 0.4a	1.43a
AP	27.6 ± 2.6a	19.7 ± 0.4a	46.8 ± 1.9a	5.9 ± 0.3b	1.40a
		15 w/d Cycles			
A	26.4 ± 2.1a	17.8 ± 0.8a	47.8 ± 2.2a	8.0 ± 0.5a	1.08b
AP	27.3 ± 1.9a	19.1 ± 1.1a	45.5 ± 3.2a	8.2 ± 0.3a	1.23a
		30 w/d Cycles			
A	26.2 ± 1.8a	18.0 ± 0.7a	47.6 ± 2.0a	8.2 ± 0.4a	0.92b
AP	27.4 ± 2.0a	19.2 ± 1.2a	45.0 ± 2.3a	8.5 ± 0.2a	1.15a
		ITRI			
		5 Day Incubation			
A	12.4 ± 0.8a	71.4 ± 0.5a	11.0 ± 0.9a	5.3 ± 0.1a	0.43a
AP	12.7 ± 1.7a	72.2 ± 0.4b	11.0 ± 1.1a	4.2 ± 0.1b	0.42a
		15 w/d Cycles			
A	10.3 ± 1.5a	70.2 ± 0.7a	13.8 ± 1.6a	5.7 ± 0.7a	0.42a
AP	10.4 ± 1.4a	71.4 ± 1.1a	13.8 ± 1.9a	4.4 ± 0.4b	0.41a
		30 w/d Cycles			
A	10.2 ± 1.1a	70.1 ± 0.7a	13.7 ± 1.0a	5.9 ± 0.8a	0.40a
AP	10.3 ± 1.0a	71.5 ± 0.9a	13.6 ± 1.6a	4.6 ± 0.3b	0.40a

[a] Different letter in columns indicate statistical difference ($P \leq 0.05$) between control soil (A) and treated soil (AP). [b] s.e.m. = ± 0.1% ($n = 3$).

degradation induced by w/d cycles (Figure 1), the soil particles aggregated by the photopolymerized SOM were able to resist excessive slacking in water and OC redistribution into small-sized aggregates, as it was instead observed for control samples.

The effects of the SOM photopolymerization treatment were also observed when a distribution of soil particle-size fractions was obtained by sonication (Table 2). The 5 day incubation provided a statistically significant difference in particle-size distribution between control and treated samples for all three soils. While the yield of the clay-size (<2 μm) fraction decreased, that of the coarse sand-size (2000−200 μm) increased concomitantly for the most clayey Porrara soil. For the increasingly sandy soils of Colombaia and Itri, the noted significant decrease in yield of the clay-size (<2 μm) fraction was compensated by an increase of the fine sand-size (200−63 μm) fraction. However, the 15 and 30 w/d cycles canceled the differences in yield distribution of particle-sizes noted after the 5 day incubation for both Porrara and Colombaia soils. For the treated Itri soil, the yield reduction in clay-size (<2 μm) was still appreciated after 15 and 30 w/d cycles, although, possibly because of the applied sonication energy, the yield increase of the fine sand-size (200−63 μm) fraction was no longer statistically different from control (Table 2).

Moreover, the catalyzed photo-oxidative stabilization of soil particle-sizes was also reflected by the sum of OC in particle-size fractions (Table 2). While the 5 day incubation did not show a statistical difference between control and treated samples for all soils, the 15 and 30 w/d cycles showed a significant increase of particle-size TOC in treated samples of the most clayey and OC-rich Porrara and Colombaia soils. This suggests that the induced mass increase of humic molecules and consequent physical stabilization of soil samples were able to promote both a chemical and physical sequestration of SOM, that was not reverted even by the continuous and harsh w/d soil disrupting cycles.

A stronger chemical and physical stabilization of OC after the catalytic photopolymerization of soils can be also inferred by the amount of CO_2 respired by soil samples (Figure 3). The microbial mineralization of SOM was significantly inhibited in

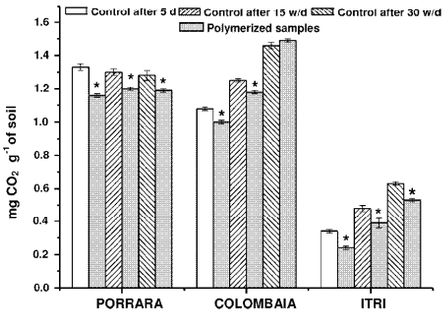

Figure 3. Soil respiration (mg $CO_2.g^{-1}$ of soil) from the three soils, Porrara, Colombaia, Itri, before and after photopolymerization treatment for 5 day incubation, and 15 and 30 wetting and drying cycles (w/d). Error bars indicate standard error ($n = 3$). The asterisks denote significant differences between control and treatment at the level of $P \leq 0.05$.

the photopolymerized samples, as compared to control, for all soils after 5 day incubation and even 15 w/d cycles. The reduction of CO_2 emission was significant for Porrara and Itri soils also after 30 w/d cycles, whereas no significant difference was noted for this treatment for the Colombaia soil. The CO_2 respiration behavior of Porrara and Itri soils confirmed that the catalytic photopolymerization had strongly stabilized their SOM, thereby inhibiting microbial mineralization of OC.

The different result for the Colombaia soil after 30 w/d cycles may be attributed to its relatively large amount of OC (Table 1) and specific humic molecules. Although the phenolic components of this soil must have been photopolymerized as shown by the increased OC content in larger aggregates even after 30 w/d cycles (Figure 2), other unreacted humic molecules (presumably medium or long-chain alkyls)[31] may have been released from clay-humic aggregates, made fragile by the repeated w/d cycles, and microbially mineralized as in control. Nevertheless, the OC stabilization obtained in soil samples of Porrara, Colombaia, and Itri mitigated the CO_2 emission by, respectively, 12.8, 7.4, and 29.4% after a 5 day incubation, 8.3, 5.6, 18.7% after 15 w/d cycles, and 7.0, −2.0, 15.9% after 30 w/d cycles (Figure 3). Such mitigation corresponded to 0.34, 0.16, and 0.20 Tons of CO_2. Ha^{-1} for Porrara, Colombaia, and Itri soils, respectively, after 5 days of incubation, and still to 0.18 and 0.20 Tons of $CO_2.Ha^{-1}$ for Porrara and Itri soils, respectively, even after the severe disaggregation of 30 w/d cycles.

The implications of this work are 2-fold. First, only one addition (corresponding to 10 $kg.Ha^{-1}$) of a water-soluble biomimetic catalyst for the in situ photopolymerization of SOM reduced CO_2 emissions from soils to a larger extent than that uncertainly estimated with mathematical models from European agricultural soils.[32] This is to be attributed to the increased intermolecular covalent bonds established among SOM components, resulting into a greater energy requirement for microorganisms to mineralize OM. The soil humic molecules most susceptible to a catalyst-assisted photopolymerization are the phenols derived from the microbial degradation of lignin. Since these phenols are also rapidly mineralized in soil,[33] their photo-oxidative coupling catalyzed by iron-porphyrin provides a means to sequester their carbon in soil.

Second, the cross-coupling of soil phenolic molecules by the photocatalytic oxidation improved soil physical quality by enhancing the stability of soil microaggregates and promoting their aggregation into larger sizes. In fact, the resulting more hydrophobic polyphenols were more easily adsorbed on solid soil surfaces than single phenols, thus favoring interparticle aggregation and their stabilization into macro-aggregates. These combined effects produced a chemical and physical sequestration of SOM, and both contributed to mitigate CO_2 emission from soils. The innovative catalytic technology described here may be potentially employed to control SOM dynamics, as well as physical quality, in agricultural soils.

■ AUTHOR INFORMATION

Corresponding Author

*Phone: +39 0812539160; e-mail: alessandro.piccolo@unina.it.

■ ACKNOWLEDGMENT

This work was supported by the Assessorato alla Ricerca Scientifica of the Regione Campania, Italy and by the National FISR project n. 248-MESCOSAGR.

■ REFERENCES

(1) Smith, P., Martino, D., Cai, Z., Gwary, D., Janzen, H. et al. . In *Agriculture, Climate Change 2007: Mitigation. Contribution of Working Group III to the Fourth Assessment Report of the Intergovernmental Panel on Climate Change*; Metz, B et al. , Eds.; Cambridge University Press: New York, 2007, pp 497−540.

(2) Conant, R. T.; Easter, M.; Paustian, K.; Swan, A.; Williams, S. Impacts of periodic tillage on soil C stocks: A synthesis. *Soil Tillage Res.* **2007**, *95*, 1-10.

(3) Schlesinger, W. H. Carbon sequestration in soils: some cautions amidst optimism. *Agric., Ecosyst. Environ.* **2000**, *82*, 121-127.

(4) Schlesinger, W. H.; Lichter, J. Limited carbon storage in soil and litter of experimental forest plots under increased atmospheric CO_2. *Nature* **2001**, *411*, 466-469.

(5) Six, J.; Ogle, S. M.; Breidt, F. J.; Conant, R. T.; Mosier, A. R.; Paustian, K. The potential to mitigate global warming with no-tillage management is only realized when practised in the long term. *Global Change Biol.* **2004**, *10*, 155-160.

(6) Read, D.; May, R. The role of land carbon sinks in mitigating global climate change. *Policy Document 10/01, Royal Society* **2001**, 27.

(7) Smith, P. In *The Global Carbon Cycle. Integrating Humans, Climate, And the Natural World*; Field, C. B., Raupach, M. R., Eds.; Island Press: Washington DC, 2004, pp 479−491.

(8) Janzen, H. H. Carbon cycling in earth systems-a soil science perspective. *Agric., Ecosyst. Environ.* **2004**, *104*, 399-417.

(9) Fontaine, S.; Barot, S.; Barre, P.; Bdioui, N.; Mary, B.; Rumpel, C. Stability of organic carbon in deep soil layers controlled by fresh carbon supply. *Nature* **2007**, *450*, 277-280.

(10) Stevenson, F. J. *Humus Chemistry: Genesis, Composition, Reaction*; Wiley: New York, 1994.

(11) Andreux, F. In *Humic Substances in Terrestrial Ecosystems*; Piccolo, A., Ed.; Elsevier: Amsterdam, 1996, pp 45−100.

(12) Paustian, K.; Andren, O.; Janzen, H. H.; Lal, R.; Smith, P.; Tian, G.; Tiessen, H.; Van Noordwijk, M.; Woomer, P. L. Agricultural soils as a sink to mitigate CO_2 emissions. *Soil Use Manage.* **1997**, *13*, 230-244.

(13) Piccolo, A. The supramolecular structure of humic substances. A novel understanding of humus chemistry and implications in soil Science. *Adv. Agron.* **2002**, *75*, 57-134.

(14) Piccolo, A.; Spiteller, M. Electrospray ionization mass spectrometry of terrestrial humic substances and their size-fractions. *Anal. Bioanal. Chem.* **2003**, *377*, 1047-1059.

(15) Piccolo, A.; Spiteller, M.; Nebbioso, A. Effects of sample properties and mass spectroscopic parameters on electrospray ionization mass spectra of size-fractions from a soil humic acid. *Anal. Bioanal. Chem.* **2010**, *397*, 3071–3078.

(16) Piccolo, A.; Conte, P.; Cozzolino, A. Chromatographic and spectrophotometric properties of dissolved humic substances compared with macromolecular polymers. *Soil Sci.* **2001**, *166*, 174–185.

(17) Cozzolino, A.; Piccolo, A. Polymerization of dissolved humic substances catalyzed by peroxidase. Effects of pH and humic composition. *Org. Geochem.* **2002**, *33*, 281–294.

(18) Piccolo, A.; Conte, P.; Tagliatesta, P. Increased conformational rigidity of humic substances by oxidative biomimetic catalysis. *Biomacromolecules* **2005**, *6*, 351–358.

(19) Shaik, S.; Hirao, H.; Kumar, D. Reactivity of high-valent iron–oxo species in enzymes and synthetic reagents: a tale of many states. *Acc. Chem. Res.* **2007**, *40*, 532–542.

(20) Smejkalova, D.; Piccolo, A. Enhanced molecular dimension of a humic acid induced by photo oxidation catalyzed by biomimetic metalporphyrins. *Biomacromolecules* **2005**, *6*, 2120–2125.

(21) Smejkalova, D.; Piccolo, A. Rates of oxidative coupling of humic phenolic monomers catalyzed by a biomimetic iron-porphyrin. *Environ. Sci. Technol.* **2006**, *40*, 1644–1649.

(22) Smejkalova, D.; Piccolo, A.; Spiteller, M. Oligomerization of humic phenolic monomers by oxidative coupling under biomimetic catalysis. *Environ. Sci. Technol.* **2006**, *40*, 6955–6962.

(23) Smejkalova, D.; Conte, P.; Piccolo, A. Structural characterization of isomeric dimers from the oxidative oligomerization of catechol with a biomimetic catalyst. *Biomacromolecules* **2007**, *8*, 737–743.

(24) Tisdall, J. M.; Oades, J. M. Organic matter and water-stable aggregates in soils. *J. Soil Sci.* **1982**, *33*, 141–163.

(25) Piccolo, A.; Mbagwu, J. S. C. Role of hydrophobic components of soil organic matter on the stability of soil aggregates. *Soil Sci. Soc. Am. J.* **1999**, *63*, 1801–1810.

(26) Baldock, J. A.; Skjemstad, J. O. Role of the matrix and minerals in protecting natural organic materials against biological attack. *Org. Geochem.* **2000**, *31*, 697–710.

(27) Gelsomino, A.; Tortorella, D.; Cianci, V.; Petrovicova, B.; Sorgona, A.; Piccolo, A.; Abenovoli, M. R. Effects of a biomimetic iron-porphyrin on soil respiration and maize root morphology as by a microcosm experiment. *J. Plant Nutr. Soil Sci.* **2010**, *173*, 399–406.

(28) Kemper, D. W.; Rosenau, R. C. In *Methods of Soil Analysis*; Part, I; Klute, A., Ed.; ASA and SSSA, 1986, pp 425—442.

(29) Stemmer, M.; Gerzabek, M. H.; Kandeler, E. Organic matter and enzyme activity in particle size fractions of soils obtained after low-energy sonication. *Soil Biol. Biochem.* **1998**, *30*, 9–17.

(30) Roscoe, R.; Buurman, P.; Velthorst, E. J.; Vasconcellos, C. A. Soil organic matter dynamics in density and particle size fractions as revealed by the $^{13}C/^{12}C$ isotopic ratio in a Cerrado's oxisol. *Geoderma* **2001**, *104*, 185–202.

(31) Nebbioso, A.; Piccolo, A. Basis of a Humeomics science: chemical fractionation and molecular characterization of humic biosuprastructures. *Biomacromolecules* **2011**, *12*, 1187–1199.

(32) Freibauer, A.; Rounsevell, M.; Smith, P.; Verhagen, A. Carbon sequestration in the agricultural soils of Europe. *Geoderma* **2004**, *122*, 1–23.

(33) Dungait, J. A. J.; Bol, R.; Lopez-Capel, E.; Bull, I. D.; Chadwick, D.; Amelung, W.; Granger, S. J.; Manning, D. A. C.; Evershed, R. P. Applications of stable isotope ratio mass spectrometry in cattle dung carbon cycling studies. *Rapid Commun. Mass Spectrom.* **2010**, *24*, 495–500.